GIA NEWS FROM RESEARCH

RUBIES FROM THE MONTEPUEZ AREA (MOZAMBIQUE)

Vincent Pardieu, Supharart Sangsawong, Jonathan Muyal, Boris Chauviré, Laurent Massi, and Nicholas Sturman.

Figure 1: Hexagonal tabular, silky ruby crystal from the Ruby from Montepuez mining area (Mozambique). Photo: V. Pardieu © GIA.

Table of Contents

OBJECTIVES

The first objective of this study is to complete the work begun in previous GIA publications on the new deposits in northern Mozambique that began to dominate the ruby trade within months of their discovery in May 2009.

This new publication will focus on the study of the samples collected during the different field expeditions to northern Mozambique in 2009 and 2012.

This new study will permit the reader to:

1) Obtain a better understanding of the complex geological conditions of the ruby deposit located near Montepuez based on data observed/obtained by the GIA team while visiting the deposit for the second time in September 2012.

2) Discover some fascinating in-depth studies of four GIA reference samples, selected from hundreds of reference specimens collected on site in Mozambique.

3) Enjoy a very rich inclusion study revealing, via 69 high-resolution photos, the fascinating internal world of these exotic rubies.

ABSTRACT:

Rubies from Montepuez in northern Mozambique are particularly interesting as this new material rapidly dominated the ruby trade in Thailand, the world's major ruby trading center, since the discovery of the deposit during the spring of 2009.

This new material is quite different from rubies traditionally encountered in the market such as the marble type rubies, known for their strong fluorescent aspect related to their low iron content, like those from Mogok or Mong Hsu in Myanmar (Burma) or basalt related rubies, known for their low fluorescence due to higher iron content, from Thailand or Cambodia.

Indeed the new deposit in Montepuez is not marble or basalt related but instead is an amphibole related deposit similar to the ruby deposits near Winza (Tanzania), M'Sawize (Mozambique) and probably the deposit near Didy (Madagascar), three other ruby deposits discovered fairly recently in Africa.

Amphibole type rubies usually have higher iron content than those commonly found in marble related deposits but also usually exhibit lower iron content compared to those from basalt related deposits. It is interesting to note that these non-classic (i.e. amphibole type) metamorphic stones fill the gap, in relation to chemistry and appearance, between the highly fluorescent marble type rubies and the weakly fluorescent basalt related rubies familiar to the trade.

For gemologists willing to find out where the gems they are studying come from, the fact that the rubies from Montepuez are coming from an amphibole related deposit is fascinating as the combination of the inclusion scene, the chemical fingerprint and the spectra associated with these stones will usually enable them to differentiate these gems quite easily from their cousins mined from marble or basalt related deposits.
The data presented here, using GIA reference samples, should be very helpful in this regard.

INTRODUCTION:

Corundum has been known from Mozambique since the Portuguese colonial times (Afonso and Marques 1998; Lächelt 2004). However very little information has been published about rubies or sapphires from Mozambique in the gemological literature until 2009, when a very short note was released (Koivula and Kammerling 1991). The reason was that the production was very limited and most of the stones produced were cabochon quality at best.

Nevertheless, since the end of 2008 the gem markets in Bangkok and other places have seen a tremendous increase in rubies coming out of Mozambique, in fact to such an extent that Mozambique rubies soon started to dominate the market in Thailand.

To this day rubies and sapphires in northern Mozambique have recently been mined from 4 different deposits, 3 of them (M'sawize, Ruombeze and Ngauma) located in Niassa Province and one (near Montepuez town) located in the Cabo Delgado Province.

Most of the stones seen between the summer of 2008 and May 2009 came from the M'Sawize area in the Niassa Province. The material was commonly heavily fractured and was mainly used as the source material for lead glass treatment, but many stones seen in the GIA Laboratories in Bangkok, New York and Carlsbad were fine enough to be faceted and used in jewelry without any treatment. A preliminary study on rubies reportedly from the Niassa Province was released on GIA websites by GIA gemologists on March 22nd 2009 (Pardieu et al. 2009a).

During the summer of 2009, a new material mined near the town of Montepuez appeared in the market (McClure 2009) and started to dominate it . Three field expeditions to Mozambique took place at the end of 2009 resulting in the visit to the two main ruby deposits near M'sawize village in the Niassa Province and Montepuez town in the Cabo Delgado Province. An expedition report was subsequently released on GIA websites on December 23nd 2009 (Pardieu et al. 2009b; Pardieu et al. 2009c).

By 2010, material from the Montepuez area was clearly dominating the market in Thailand, not only as unheated or lead glass filled material, but also as flux healed rubies (Pardieu et al. 2010). On the official papers the area was under the control of Mwiriti, a local Mozambican company with no previous experience in gem mining. However, most, if not all the production reaching the markets, was coming from thousands of artisanal miners (called "garimpeiros" locally in this former Portuguese colony) who invaded the Mwiriti concession in order to search for rubies and sell them to the Tanzanian, West African, Thai and Sri Lankan gem merchants waiting nearby.

In June 2011 Mwiriti announced that they had entered into a partnership with Gemfields, a British gem mining company known for its emerald and amethyst mining activities in Zambia. The new company that resulted from this partnership was called: "Ruby from Montepuez Mining" or "MRM" of which Gemfields has a 75% holding and Mwiriti Ltd., 25%.

During the summer of 2012, one year after the Montepuez deposit was acquired by Gemfields, the GIA laboratory conducted another field expedition to northern Mozambique, with the support of Gemfields and MRM, in order to collect additional samples at the source. An update about ruby mining near Montepuez was subsequently published in Gems & Gemology (Pardieu and Chauviré 2012) and "Le Regne Mineral" (Pardieu and Chauviré 2013).

LOCATION AND ACCESS:

Unlike the other deposits near M'sawize and Ruombeze that are very remote and located inside (M'sawize) or near (Ruombeze) the Niassa National Reserve, the ruby mining area located near Montepuez town can easily be accessed in less than 3 hours by road from Pemba, the administrative capital of the Cabo Delgado Province (see Figure 2). It is very convenient as the 204 kilometer long road linking Montepuez to Pemba, its port and its international airport was recently renovated and is currently one of the best in the country. The existing good quality infrastructure in the Pemba and Montepuez regions is expected to improve further over the coming years owing to some significant agriculture and gold mining projects that are ongoing in the area, as well as to the existence of the ruby deposits. Furthermore, huge natural gas deposits have recently been discovered off-shore from Pemba, and are currently being developed by the Italian energy company ENI and the American petroleum company Anadarko.

The ruby deposit itself is located mainly south of Namanhumbire village about 30km east of Montepuez town on the way to Pemba (see Figure 3). By the end of September 2012 the extent of the known ruby and sapphire (mainly pink) deposits in the region were composed of several spots located on a rather narrow band about 40 to 50 kilometers in length from Namahaca in the north west to the Nacaca area in the south east (see Figure 3 and Figure 4).

Figure 2: Google Earth map showing the location of the different ruby and sapphire deposits in northern Mozambique and southern Tanzania.

Figure 3: Detailed Google Earth map of the ruby rich region between Pemba and Montepuez showing the known ruby deposits located more or less along a line extending from Namahaca to Nacaca areas.

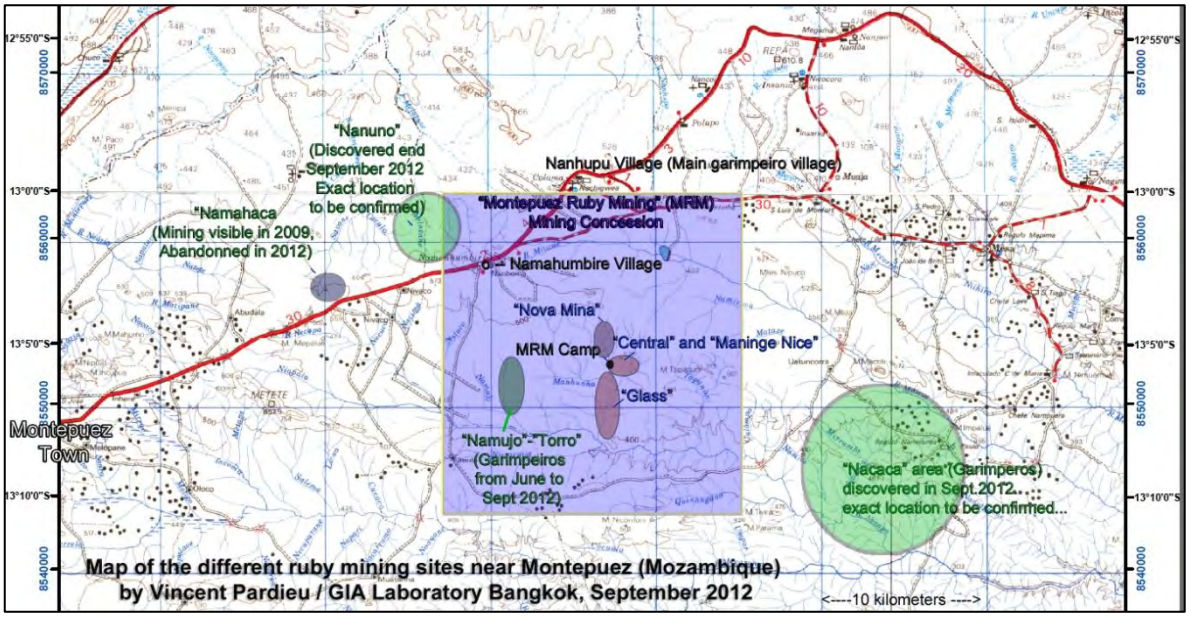

Figure 4: Detailed map of the ruby producing area near Montepuez town showing the extent of the ruby mining concession (central square) owned by Ruby from Montepuez Mining (MRM) in September 2012 in relation to the known existing ruby producing areas in the region.

GEOLOGY OF THE RUBY FROM MONTEPUEZ PRODUCTION AREA:

North Mozambique mainly consists of the southern part of the Mozambique Belt. This belt experienced a lot of tectonic and metamorphic events like the assembly and dispersal of Rodinia and Gondwana supercontinent (Muhongo et al. 2001a; Melezhik et al. 2008). These rocks are emplaced thanks to two distinct tectonic events; the Mozambican Orogeny (between 1100 and 580 My) and East African Orogeny (between 800 and 650 My) which led to the formation of current India, Africa, Madagascar and Sri Lanka (Meert and Van Der Voo 1997; Melezhik at al. 2008). The southern part of the Mozambique Belt (which constitutes northern Mozambique) is composed by medium to high grade metamorphic rocks and their protolites are aged between 1150 and 950 My (Kröner and Stern 2004; Macey et al. 2010). This part is divided into different units separated by complex boundaries, mainly thrust faults (see figure 5). Eastern units overlap central and eastern parts of northern Mozambique. These rocks underwent strong deformation and metamorphism; the peak of metamorphism aged at 615 My (Muhongo et al. 2001b; Kröner et al. 2003).

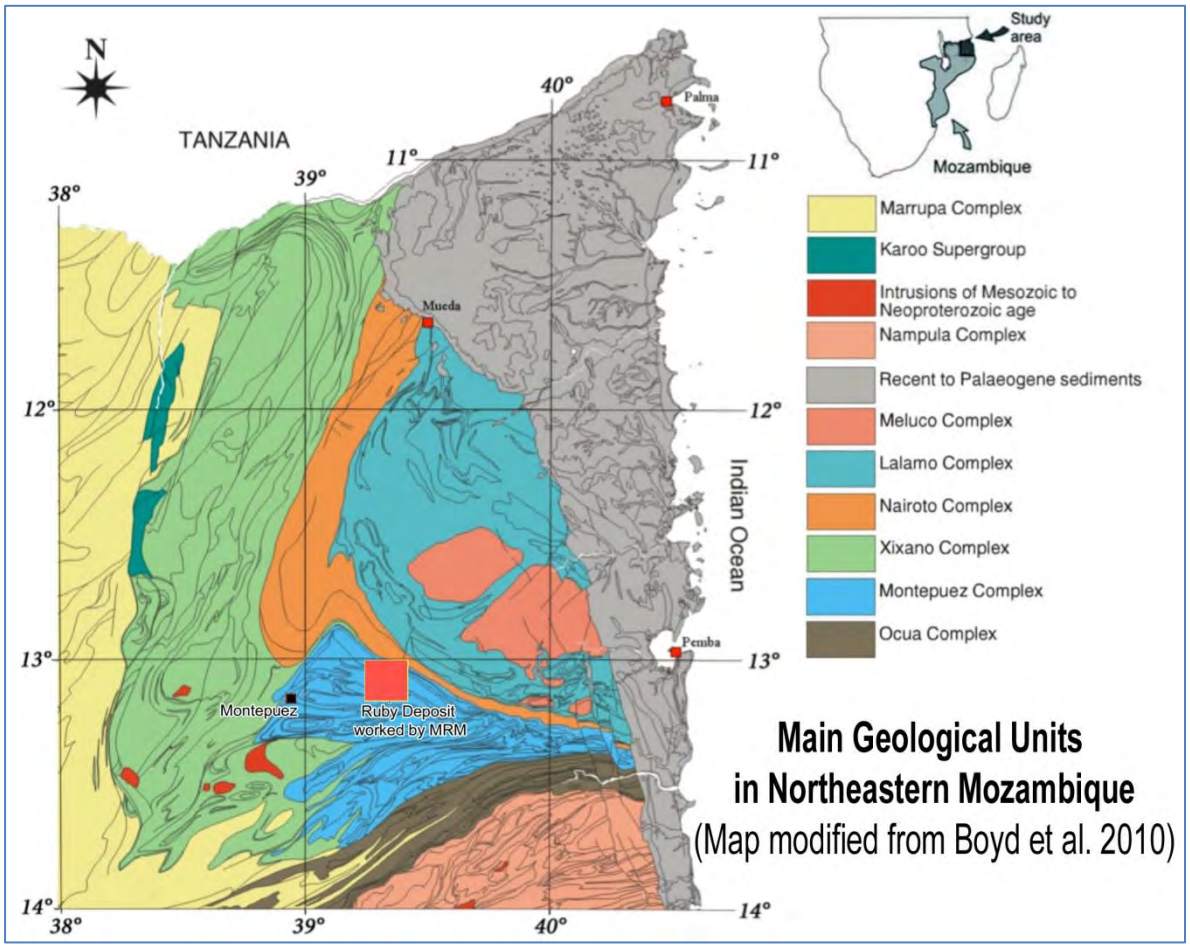

Figure 5: The north of Mozambique is a complex organization of distinct geological units that compose the Mozambique Belt. The ruby deposit of Montepuez is localized in the Montepuez complex. (Map modified from (Boyd 2010)

The ruby deposit of Montepuez is localized in the eponymous tectonic unit (see Figure 5). This unit is mainly composed of strongly deformed gneiss and quartzite, with a few marble lenses (Boyd et al., 2010).

In December 2009 and September 2012, we were able to visit several deposits previously worked by artisanal miners, and in 2012 (at Glass, Nova Mina, Central, Maninge Nice and Namujo/Torro) we were able to study several exploration trenches and pits dug by MRM.

Thanks to these field observations we were able to confirm that in the areas known as “Glass” and “Namujo/Torro”, rubies are found in secondary deposits along streams extending more or less north to south. The rubies found in these secondary deposits are commonly tumbled and rather clean as they possibly survived hundreds of millions of years of weathering in gravels.

In the “Central” area we were able to find and study a primary deposit where rubies existed in amphibolitic lenses (Figure 6, Figure 7). Studies at the GIA Laboratory on some of the material collected, using Raman spectroscopy, confirmed that the host rock is composed of green amphibole with small lenses rich in white feldspar. Using the RRuff database as a reference the closest matches were pargasite for the amphibole and anorthite for the feldspar (Figure 8). Nevertheless X-ray powder diffraction analysis at GIA Carlsbad could not confirm whether pargasite was the amphibole present. This was due to the lack of a clear match for the pattern being obtained and the sodium level being too low for pargasite. According to Shane McClure, Nathan Renfro and Mike Breeding, the samples studied appeared to be more of a solid solution of amphiboles with actinolite being the main component, but in-depth microprobe analysis would be required to obtain better results.

In “Central” we found rubies from two types of deposits; some rubies were found associated with gravels in the eluvial/detritic deposit overlying the primary deposit, while others were found in situ in association with these lenses. Overall the rubies found in the eluvial/detritic deposit were significantly less included than those found in situ in the lenses. This is logical as over the course of millions of years nature has turned most of the highly fractured stones into “powder” and as a result clean stones became concentrated in these eluvial/alluvial/detritic/secondary deposits.

Figure 6: Left to right: Boris Chauviré, Sameer Maniyar (Process Engineer, MRM) and Paul Allan (Project Geologist, MRM) studying the rocks inside a test pit close to the Central - Maninge Nice area. The area studied was dampened in order to reduce the dust and allow the mineral association in the exploration trench to be studied. The dark green areas are mainly composed of amphibole and weathered mica while the white veins are rich in weathered feldspar. The rubies are found mainly inside or near the feldspar rich veins, as indicated by Boris Chauviré. Photo: Vincent Pardieu © GIA.

Figure 7: Detailed view of the rubies found in situ associated with amphibole (dark green), mica (yellowish) and feldspar (white) on the wall of the test pit shown in the previous photo. It is interesting to note that a white feldspar rim surrounds most rubies. Photo: Vincent Pardieu © GIA.

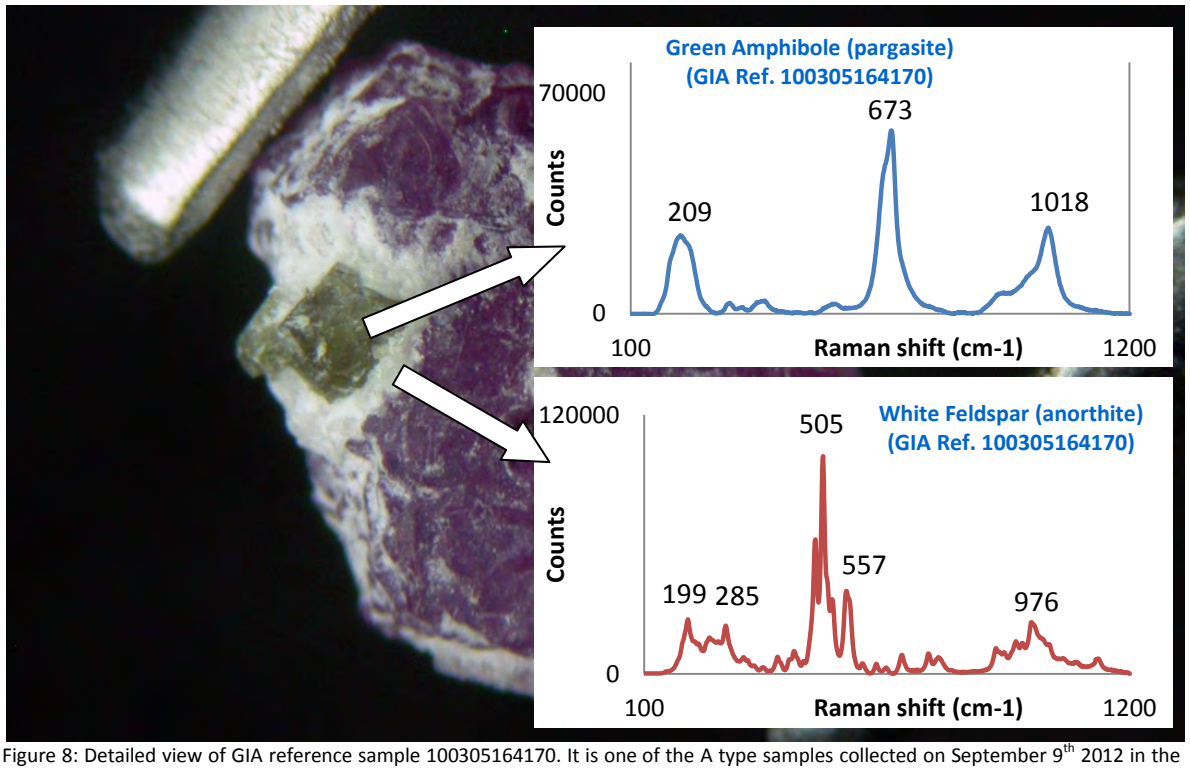

Figure 8: Detailed view of GIA reference sample 100305164170. It is one of the A type samples collected on September 9th 2012 in the prospection trench shown in previous images. As you can see clearly here, the ruby crystal is associated with some white and green minerals that were later studied via Raman spectroscopy at the GIA Laboratory Bangkok and identified as amphibole (closer match being pargasite) and feldspar (anorthite as closer match) respectively, using the RRuff database as a reference. Photo: Vincent Pardieu © GIA.

These results are quite similar to those obtained by Prof. Lawrence Snee who visited the area in April 2010, a few months after author VP's first visit. They can be found in a concise field report published on page 151 in the summer issue of "Gems & Gemology" (Snee and Wu 2010):

"Our exploration activities revealed that the rubies are hosted by eluvial material as well as the underlying weathered bedrock. The bedrock consists of the Montepuez Complex, a Neoproterozoic suite of metamorphosed sedimentary rocks (amphibolite-grade schists and gneisses) that were intruded by granite, granodiorite, and tonalite. In the deeply weathered area we examined, the eluvium appeared to lie directly on Montepuez gneisses, which were crosscut by light-colored veins (now mostly weathered to clay). These veins ranged up to 20 cm thick, and probably originally consisted of syenitic (silica deficient) pegmatites and aplites. Ruby was seen in these veins and also in the overlying boulder-rich eluvium."

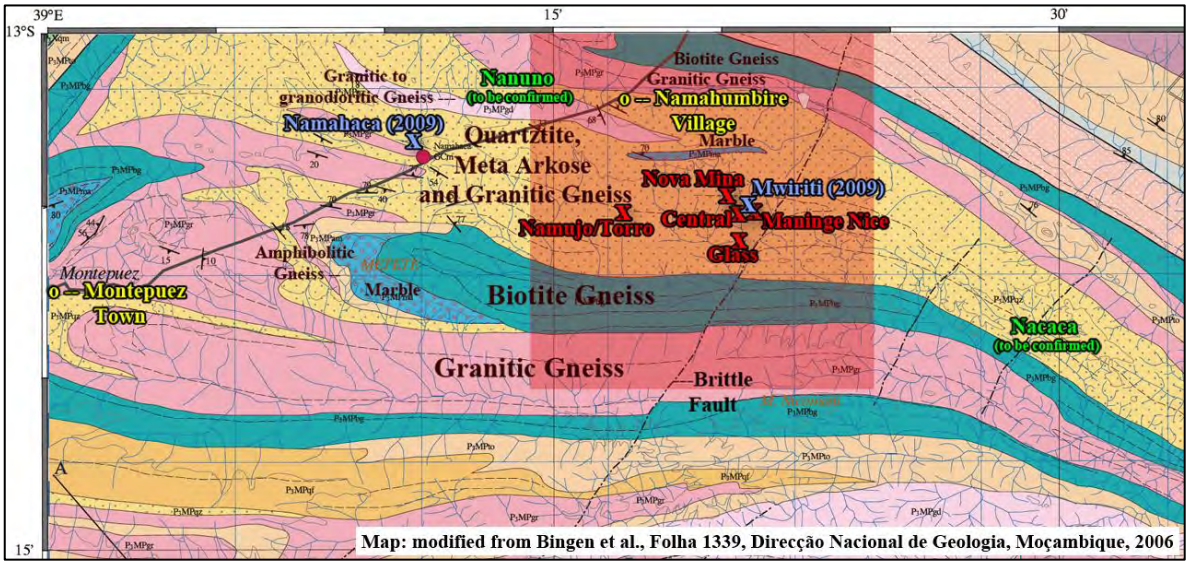

Figure 9: On this geological map, modified from Bingen et al. (2006), we placed the MRM mining concession (red shaded area), Montepuez town and Namahumbire village (in yellow) and the different ruby producing areas author VP and his teams visited in December 2009 (in blue) and in September 2012 (in red). The areas in green are new mining areas that the author heard about at the end of September 2012 a few days after his last visit, but their exact location is still to be confirmed.

However on geological map number 1339 by Bingen et al. published in 2006 (Bingen et al. 2006) by the "Direcção Nacional de Geologia" (Figure 9), the areas in which we found the ruby deposits (in blue in December 2009 and in red in September 2012) are shown as quartzite, meta-arkose and quartzitic gneiss. The lenses of amphibolitic rocks we observed are not illustrated.

Studying this map in relation to the location of the known deposits, it is interesting to see that those from Namahaca to Torro, Central, Maninge Nice and also Nacaca seem to be aligned along the same structural trend. This could possibly indicate the existence of a ruby rich vein extending from Namahaca to Nacaca and possibly further west or east.

More analysis on the host rocks associated with these rubies and of the region will provide some additional information about the genesis of Montepuez rubies and the extent of the ruby producing area, nevertheless it already seems that the ruby producing area extends about 50 kilometers west to east and few kilometers north to south. This is appears to be the case owing to the fact that the ruby producing area is intersected by several streams along which some interesting secondary deposits are located as seen at Namujo/Torro, Glass and Nacaca.

RUBIES FROM MONTEPUEZ, MOZAMBIQUE:

DESCRIPTION OF THE ROUGH RUBIES FROM MONTEPUEZ, MOZAMBIQUE:

Most of the ruby production from Montepuez consists of tabular hexagonal crystals (probably mined from a primary type deposit). Nevertheless since the spring of 2009 part of the production has also been composed of some rough showing abraded features (probably mined from a detritic or secondary type deposit).

The euhedral material obtained from primary deposits is commonly associated with some whitish (feldspar), yellowish (mica) or greenish (amphibole) associated minerals. Such material is usually highly fractured and included with amphibole and mica crystals as the main inclusions, but some of these crystals also have some clean transparent areas that can be clipped to produce clean rough material.

The material that shows some abraded features comes from alluvial / detritic deposits located above the primary deposit or along streams that pass over it. These slightly tumbled crystals or broken pieces of ruby are usually more transparent, on average, and less included than rubies coming from primary deposits. This most likely resulted from natural erosion. Over millions of years some of the ruby rich rocks were eroded, the rubies enclosed within these rocks survived the erosion process and were eventually concentrated in the gravels found over the primary deposit (called eluvial/detritic deposit as there is no water transportation involved) or were transported by the water (alluvial/secondary deposit) to a new location. In these secondary deposits, tumbled rubies are trapped with other heavy minerals in some specific areas sporadically located along current or former stream routes. Weathered over millions of years, the heavily fractured and included material is broken down and altered into particle sized grains as though in a tumbler. At the same time, clean and hence more durable gem material will be tumbled and concentrated in the gem rich gravels. Thus, and this is an interesting observation for miners, the proportion of clean material for such a hard mineral as corundum is much more important in the secondary/alluvial/colluvial/detritic deposits than in the primary deposits.

Figure 10: Rubies, believed to have been mined in the "Central" area, seen in the market in Mozambique in 2009. Photo: Vincent Pardieu © GIA.

It was interesting to see that the color and general appearance of the stones found in the markets in Thailand changed between 2009 and 2013. At first it seemed that most of the mining took place around the area known as “Central” today (see map: Figure 4). This area typically produced pinkish to red stones (Figure 10) from either primary or secondary deposits.

Around 2011 some new very attractive material with high transparency and good luster called “Bo Nam” (Figure 11) and “Bo Daeng” (Figure 12) began to appear in the Thai market. In Thai “Bo Nam” means “*the water mine*” and “Bo Daeng” means “*the red mine*”. The rubies we observed in Thailand, reportedly from “Bo Nam” or “Bo Daeng”, showed no indications of water transportation and looked as though they originated from a primary type deposit. Most of them had clean surface reaching fissures that were not filled with limonite or other foreign substances. In Mozambique garimpeiros told us that “Bo Nam” stones mainly originated from streams and swamps where rubies are found in alluvial gravels like the “Glass” area (see map: Figure 4). These stones are typically weathered and rather clean as it is mainly a secondary deposit. If such stones possess surface reaching fissures they are often filled with yellowish to brownish or orange limonite type material. Nevertheless the parcel said to be “Bo Nam” material obtained in the Thai market (Figure 11) at the end of 2012 showed no indications of water transportation, and possessed clean surface reaching fissures, thus they were obviously mined from a primary type deposit. In fact it seems that rough rubies are sorted more according to their color and clarity in the Thai market than based on the origin of the rough. This unsurprisingly leads to some inconsistencies where Thai buyers working in Mozambique might use “Bo Nam” to mean “tumbled rubies from secondary deposits”, while Thai dealers working between Bangkok and Chanthaburi might consider it more of a quality grade. Such observations show how important/necessary it is to find ways to collect samples on site at the mines when building a solid reference collection.

After studying the stones from these two parcels and comparing them with samples we obtained in the field in Mozambique, it seems highly likely to us that the stones we studied (reportedly from “Bo Daeng” and “Bo Nam”) were both probably mined from “Maninge Nice” (meaning “nice quality”) an area located a few hundred meters to the east of “Central” (see map: Figure 4) where thousands of garimpeiros worked until June 2012.

Figure 11: Parcel of small rubies (about 1 carat per stone) reportedly of the “Bo Nam” type seen in the market in Bangkok, Thailand in January 2012. Note the high transparency and good luster of these stones. Photo: Vincent Pardieu © GIA.

Figure 12: Parcel of small rubies (about 1 carat per stone) reportedly of the "Bo Daeng" type seen in the market in Bangkok, Thailand in January 2012. The stones are typically darker red than the so called "Bo Nam" material but still with a very good transparency and fine luster. Photo: Vincent Pardieu © GIA.

As Montepuez Ruby Mining (MRM) had stepped up security at Central, Maninge Nice and Glass (see map: Figure 4) since their arrival in 2011, the access to these areas became more difficult for the garimpeiros. As MRM's security improved, the garimpeiros had to find new deposits that would allow them to work undisturbed.

In July 2012 most of them moved to a new place near Namujo village called "Torro" (Pardieu and Chauviré 2012; Pardieu and Chauviré 2013) when a rumor spread that it was the source of many large, clean, slightly tumbled stones. "Namujo/Torro", located along a stream produced some material that was called "Bo Som" (meaning the "*Orange mine*" in Thai) when it reached the market in Thailand a few months later. Most stones from "Torro" are darker and more brownish and/or orange than the previous material coming from the Montepuez area.

After studying the material we found that this is mainly due to higher iron content when compared to stones commonly found near "Central" or "Maninge Nice". In fact in many cases, our studies show that the iron content in rubies from the "Torro" area can be very similar to the iron content in Thai/Cambodian rubies (see page 33 and page 39).

Figure 13: Rubies from the Namujo/Torro area collected by author VP for the GIA reference collection at Torro in September 2012 after washing the content of a gravel bag left behind by garimpeiros a few days after the police operation that chased them away from Torro. The stones are between 0.4 to 3 carats and most of them are clean or silky. Note the rounded appearance of the crystals indicating that the rubies probably spent millions of years in the gravel of a secondary deposit. Photo: Vincent Pardieu © GIA.

At the end of September 2012, a Mozambican police operation cleared most of the "Namujo / Torro" area of artisanal mining activity (Pardieu and Chauviré 2012; Pardieu and Chauviré 2013). After a few days many garimpeiros moved to a new area called "Nacaca", located on the east of the MRM ruby mining concession (see map: Figure 4). Note: The exact location of this site is still has to be confirmed, as we were unable to visit it during our last field expedition. According to the garimpeiros we met, the mining area was located near a river and the production was mainly consisted of a few large stones with small stones being rare.

Back in Thailand during winter 2012-2013, the authors witnessed the arrival of small quantities of a new kind of material in the market. The appearance of this new material matched the descriptions given to the authors by the garimpeiros about the new material from the "Nacaca" area. Nevertheless as local buyers buy gems from several miners and then often mix them to create larger or more even parcels; it is likely that most of the parcels destined for Thailand at the time were mixed parcels composed of stones from both the Torro and Nacaca areas. As mining continued in both secondary deposits and produced stones with similar appearances (mostly clean tumbled stones), it is easy to understand that the certainty of a given stone from such a parcel being from Nacaca is very hard to prove without studying each production area on site and noting the differences in material produced from each.

Nevertheless it appears as though the overall color of the stones from parcels reportedly from Nacaca is not as homogeneous as that shown by stones coming from "Central", "Bo Nam", "Bo Daeng" or "Bo Som". It is also interesting to note that Nacaca seems to produce mostly large stones, with very few small stones reportedly being found on site. However most of the Nacaca production is said to be very clean. This is not surprising since being a secondary deposit the mine run probably originated from different areas and subsequently accumulated at Nacaca where they remained for millions of years.

During the winter of 2012/2013 the quantity of stones reaching Thailand reportedly dropped owing to MRM's stricter control of its claim and the exodus of the garimpeiros who moved to Nacaca. Consequently the prices for Mozambique material went up.

Figure 14: Parcel of small rubies reportedly from the "Nacaca" area near Montepuez. This parcel consisted of 76 pieces weighing 50 carats gross and was acquired by the GIA Laboratory from a supplier in Chanthaburi (Thailand). As is clearly visible most of the stones show weathered features, unlike the stones in the parcels in Figure 11 and Figure 12, which proves that they probably settled in a secondary deposit for several million years. Photo: Vincent Pardieu © GIA.

On the whole most of the stones produced from the Montepuez area since the start of production in May 2009 are flat / tabular and fractured; however some of the stones can be very large (the authors saw rough stones of over 100 carats). Thus most of the unheated faceted stones seen in the market are rather small (usually under 3 carats) and often show "windows", nevertheless several noticeable unheated faceted stones over 10 carats were available at the Bangkok and Hong Kong gem shows in September 2013. Blessed with an even coloration and often a very good crystal (meaning a high transparency and a good luster), unheated rubies from Montepuez seem to be very suitable material for the production of small calibrated stones.

Commercial quality rough rubies from Montepuez are commonly heated with borax or other flux-like additives, and since the fractures are healed prior to faceting, larger faceted stones result. Thus flux heated Mozambique rubies of larger sizes (commonly up to 10+ carats) are more readily available in the market than unheated rubies.

Glass filled rubies on the other hand, are only filled with glass (usually with a high lead content) while the stones are still rough instead of having their fractures healed. Since the glass filler acts as binding agent, larger stones, in keeping with the flux treated stones, can once again be faceted, unlike the unheated material which is generally smaller. In this respect lead glass filled rubies of over 10 - 20 carats have often been seen in the market since 2010. Nevertheless it is important to remember that there is an important durability issue to keep in mind with lead glass filled material as the filler can easily be damaged (by heat, acids, etc.) with significant consequences to the stone. In such circumstances fissures may become more noticeable or it is even possible that the stone may break into several pieces.

MATERIALS AND METHODS:

a) <u>Sample selection:</u>

The GIA Laboratory collected several hundred rubies from the Montepuez area in Mozambique during two expeditions: The FE09 field expeditions in September, November and December 2009 and the FE39 field expedition in September 2012.

To collect samples in compliance with GIA Laboratory Bangkok's protocols, GIA field gemologists should collect reference samples as close as possible to the mine (if possible preferably on site at the mines), but also from multiple independent sources.

Besides the samples collected on site at the mines by GIA field gemologists (A or B type samples[1]), some samples were collected either from West African merchants in Pemba and Nampula in 2009 (E type samples1), or from Bangkok and Chanthaburi based merchants in 2012 (F type samples1). These samples, reportedly "mined around Montepuez", were later confirmed to be from Montepuez in the GIA Laboratory Bangkok after study and comparison with A and B type reference samples collected in the field from the same area. Such E or F type samples are typically larger, less fractured, and less included than the A or B type samples collected in the field. Some were particularly interesting for the beauty of their mineral inclusions. They also helped confirm that what we found in the field was similar to that found in the market as reportedly from Montepuez. Such confirmation, or not, also assisted us in knowing if the samples collected in the field are representative of the diversity of the material available in the trade (see the trace element study of the 131 samples collected in the second part of the study).

For the first part of that study we decided to select a few samples collected in the field in Mozambique during the FE39 expedition:

For this study we first selected 131 rubies of interest from the GIA reference collection for a preliminary study of their inclusions and chemistry. Out of these 131 stones, 35 of the cleanest samples were selected and then fabricated as wafers in the GIA laboratory Bangkok in order to collect spectroscopic data using UV-Vis and FTIR spectroscopy.

Lastly 4 key stones, from the 35, were selected as being representative of the diversity of the production from the Montepuez area based on the following criteria:

1) Known A or B type samples. Meaning that we collected the samples on site at the mines, and thus could be as sure as possible that these samples did indeed originate from the specific ruby producing area in question, and that no treatment had been performed on them.
2) One sample was collected from each of the 4 main ruby mining sites visited:
    a. "Central" (believed to have produced stones since the discovery of the deposit in May 2009, and visited in December 2009),
    b. "Glass" (also believed to have produced rubies around the beginning of the deposit's discovery),
    c. "Maninge Nice" (believed to have produced stones since around 2011),
    d. "Torro" (produced stones since July 2012)
3) They were clean enough from which to collect quality spectroscopic data.

[1] According to GIA terminology: See Annex A for the GIA Cataloguing Classification system.

In the second and third parts of this study, we will present:

- A trace element study of the 131 rubies from Mozambique we studied, compared to each other, but also compared to other known ruby deposits.
- An extensive inclusion study with 69 photos showing the diversity of the inclusions we observed while working on the 131 samples studied during the preliminary study.

b) Sample Fabrication:

All the samples in this study were fabricated in the GIA Laboratory Bangkok by Jonathan Muyal. 131 samples were selected for 2 different purposes:

- First 35 samples were fabricated as "spectra quality samples". To fit into this group the samples had to possess a clean area large enough to enable high quality reference spectra to be collected along the c-axis, and eventually also perpendicular to the c-axis.

    - 34 samples were fabricated with one set of surfaces polished perpendicular to the c-axis of the crystal, and subsequently polished with great care to enable good quality spectra to be collected. Optical path lengths of the wafers were measured with a Mitutoyo Series 395 spherical micrometer with an accuracy of 2 microns.
    - As most of the Montepuez material is very flat, only one sample out of the 35 samples was found to be good enough to be fabricated as an optical wafer with two sets of surfaces carefully polished perpendicular and parallel to the c-axis of the crystal.

- The 96 other samples were found to be too included to collect high quality optical data, so they were fabricated in order to document their inclusions. One or several windows were polished perpendicular to the c-axis, in some cases, or in other cases, in directions not specifically related to the c-axis in order to optimize the study of their internal features.

c) Instrumentation:

Sample photography: In order to document the color of our samples in a consistent way, we used a Canon EOS 5D camera with a Canon Macro MP-E 65mm lens adapted to a camera stand. In order to produce consistent results for each GIA reference sample the photographs were taken under exactly the same lighting conditions, with the reference samples being placed in a Logan Electric Tru-View 810 Color Corrected Light Box (5000K lamp). A neutral density filter was used to calibrate the camera - light box combination to produce a neutral gray. High-resolution reference photographs were then collected using transmitted light. As the reference photos were taken of wafers cut perpendicular to the c-axis, the color of the samples on the photographs taken using transmitted light can be considered representative of the color of a nearly pure o-ray.

Note: At this point it is interesting to comment on the color of the wafers in comparison to the color that would be seen if a gem had been faceted from them instead. As the diagram below illustrates, the light just travels through the wafer sample without being reflected. Thus to the observer it might look pink owing to the thin nature of the sample. Now in the case of a faceted stone, the color would be more saturated owing to the longer path length followed within the gem... Furthermore the hue would be slightly different resulting from a combination of some o and e-rays produced by total internal reflection within the stone, while for the wafer, if oriented perpendicular to the c-axis, a purer o-ray hue would be observed.

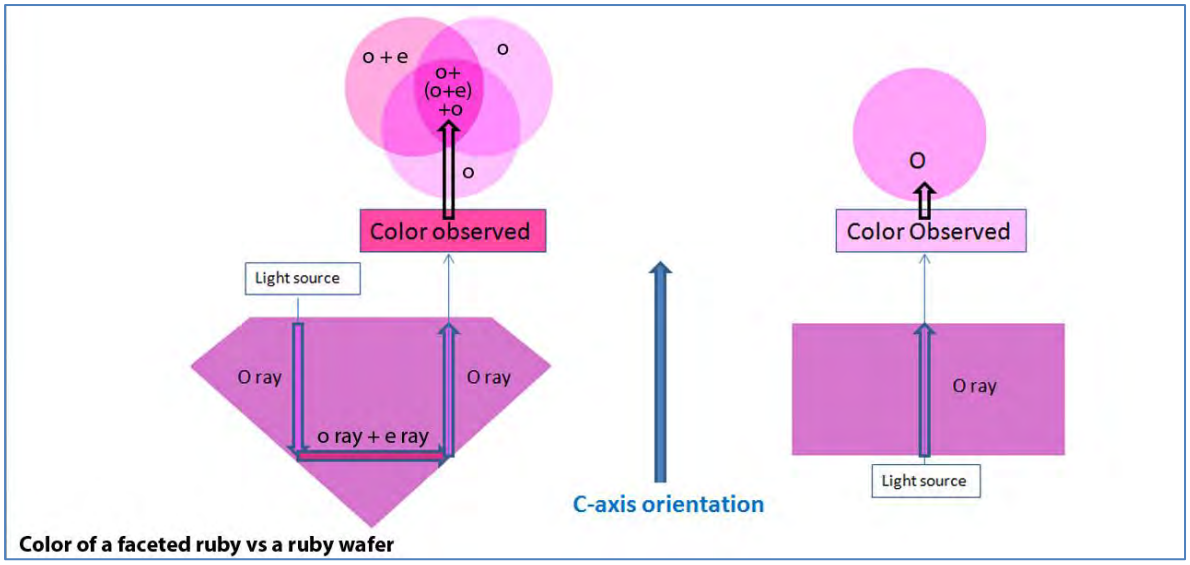

Figure 15: Diagram showing the color of a faceted ruby compared to that of a ruby wafer. In a ruby wafer, light traveling along the c-axis, will results in the color of a perfect o-ray being observed in an ideal case. In the case of an ideal cut faceted ruby observed face-up with the light entering the table, the path followed will initially be down the c-axis (providing the stone has been orientated this way when lapidary work was performed) before being totally internally reflected and travel perpendicular to the c-axis amongst, other directions, before once again being reflected again to continue its journey in the direction of the c-axis. The resulting color seen by the observer will be 1) much more saturated as the path length is greater, and 2) a combination of purplish red (o-ray) and orangy red (e-ray) owing to the various directions taken by the light within the gem.

Gemological microscopy was performed using binocular microscopes with magnification ranging from 10x to 70x using both darkfield and brightfield illumination. Other lighting techniques, including the use of flexible fiber-optic illumination, were also employed to investigate the internal characteristics of the study specimens. Photomicrographs of internal features were captured at up to 180x magnification with a Nikon SMZ 1500 system using dark-field, brightfield, diffused and oblique illumination, together with a fiber optic light source when necessary. Note: The magnification information in the captions associated with the inclusion photos in this study is the magnification power of the microscope at the time the photo was taken. It does not refer to the actual magnification power of the inclusion viewed when this study is printed on A4 size paper or seen on a computer screen. Furthermore most of the original photos were cropped and worked using Photoshop by the lead author V. Pardieu.

Ultraviolet-visible-near infrared (UV-Vis-NIR) spectra were collected using a Hitachi U-2900 spectrophotometer, for unpolarized ordinary ray spectra, at 1.5 nm resolution, and a Perkin Elmer Lambda 950 spectrophotometer, for polarized ordinary and extraordinary rays, at 1.0 nm resolution, operating with integrating sphere accessory, and dual polarizers.

Fourier-transform infrared (FTIR) spectroscopy was performed using a Thermo Nicolet 6700 FTIR spectrometer equipped with XT-KBr beamsplitter and a mercury-cadmium-telluride (MCT) detector operating with a 6x beam condenser accessory and resolution was set at 4 cm^{-1} with 1.928 cm^{-1} data spacing.

Raman spectra were used to identify inclusions using a Renishaw inVia Raman microscope fitted with a 514 nm argon-ion laser. The Raman spectra were collected in the range between 100 and 1500 cm^{-1}. The accumulation was set at 5 to improve the signal to noise ratio of the spectra. Raman Spectra were calibrated using the 520.5 cm^{-1} line of a silicon wafer. In all cases, we used the RRuff database as a reference in our attempts to identify inclusions. Spectra comparisons were performed using Renishaw Wire (version 3.4) and/or Thermo Galactic “Spectral ID” (version 3.02) softwares.

For chemical analysis, we used LA-ICP-MS (Laser Ablation - Inductively Coupled Plasma - Mass Spectrometry) technology with a Thermo Fisher Scientific iCAP Q Induced Coupled Plasma - Mass Spectrometer (ICP-MS) coupled with a Q-switched Nd:YAG Laser Ablation (LA) device operating at a wavelength of 213 nm was employed. Laser conditions used 55 µm diameter laser spots, a fluency of around 10 J/cm^2, and a 15 Hz repetition rate. 8 spots were analyzed on each wafer sample, while only 3 spots were analyzed on faceted samples. For the ICP-MS operations, the forward power was set at ~1350 W and the typical nebulizer gas flow was ~1.00 L/min. The carrier gas used in the laser ablation unit was He, set at ~0.60 L/min. The criteria for the alignment and tuning sequence were to maximize Be counts and keep the ThO/Th ratio below 2%. A special set of synthetic corundum reference standards was used for quantitative analysis. All elemental measurements were normalized on Al (internal element standard), this value approximates to the chemical composition of the corundum.

PRELIMINARY STUDY OF FOUR GIA REFERENCE SAMPLES:

a) Summary of the physical properties of the 4 samples detailed in this study:

The gemological properties of the samples are summarized in table 1. The refractive indices obtained varied between 1.761 to 1.763 for n_e and 1.770 to 1.771 for n_o with a birefringence ranging between 0.008 and 0.009.

Table 1: Properties of rubies showing R.I and S.G. values, reactions through the Chelsea Color Filter, and LWUV /SWUV reactions.

Reference #	RI o-ray	RI e-ray	Birefringence	Chelsea filter	LWUV	SWUV
100305163907	1.770	1.761	0.009	red	Strong Red	Weak
100305163897	1.771	1.763	0.008	red	Medium to Strong Red	Weak
100305164174	1.770	1.761	0.009	red	Strong Red	Weak
100305163945	1.771	1.762	0.009	red	Weak to Medium Red	none

Table 2: Introduction to the 4 selected rubies from Montepuez detailed in this report.

Reference #	Sample Category & Origin	Wafer Weight (carats)	Polished wafer orientation	Wafer path length	Color (transmitted light) along C-axis
100305164174	A1 - "Central"	0.642 carat	Perpendicular to the c-axis	2.648 mm	Purplish red
100305163907	A2 - "Glass"	0.133 carat	Perpendicular to the c-axis	0.702 mm	Pink
100305163897	A2 - "Nova Mina" / "Maninge nice"	0.078 carat	Perpendicular to the c-axis	0.590 mm	Purplish pink
100305163945	B2 - "Torro"	0.066 carats	Perpendicular and parallel to the c-axis	0.510 mm	Brownish pink

b) GIA Reference Specimen Number 100305164174 (from the "Central" area):

GIA reference sample 100305164174 is an A1 type sample (see Annex C for a description of GIA cataloguing classification) collected on September 10th 2012 while visiting the "Central" area where MRM had dug a prospection trench at (13°04'18"S latitude and 39°20'42"E longitude). The

sample was extracted from the secondary/colluvial deposit located just over the amphibolitic lenses we studied in the exploration trench (see Figure 6). It appeared red and weighed 1.530 carats before fabrication (see Figure 16).

Figure 16: GIA reference sample 100305164174 (A1 type; see Annex C for a description of the classification system), weighing 1.530 carats seen before fabrication via transmitted light. The sample is clean on the left side and heavily included on the right side. Thus we decided to cut it in two pieces and use the left side for spectroscopy. This stone was collected on site in an exploration trench at "Central" on September 10th 2012. Photo (color calibrated): Sasithorn Engniwat © GIA.

As one half of the sample was transparent and clean while the other half was heavily included, we opted to cut it into two pieces. The clean part was fabricated into a wafer with one set of parallel windows perpendicular to its c-axis at the GIA Laboratory Bangkok. Particular care was taken to orientate the reference sample correctly, minimize the formation of a wedge shape and obtain a good polish. The final research sample weighed 0.642 carats (see Figure 17).

Figure 17: Two views of GIA reference sample 100305164174 (B2 type; see Annex C for a description of the classification system), weighing 0.642 carats seen after fabrication. The optical path length (the thickness of the sample studied) is 2.648 mm. The color, via transmitted light, is purplish pink with a homogenous color distribution. Photos: Sasithorn Engniwat © GIA.

When viewed under long-wave ultraviolet (LWUV) light the stone exhibited a strong even red reaction and a weak reaction under short-wave ultraviolet (SWUV) light was observed.

The stone is predominantly clean but also hosts a few thin, long and short rutile needles, broad, flat, free-shaped orientated platelets, and a few surface reaching unhealed fissures.

An unpolarized UV-Vis-NIR spectrum (ordinary ray only as the sample is very flat) was collected for the specimen using the Hitachi U-2900 spectrophotometer in the direction of the c-axis.

The resulting spectrum (see Figure 18) showed a chromium spectrum with broad bands at 407 and 558 nm. Besides these bands the smaller chromium related absorption features known as the R and B chromium lines located at 693 nm for the R line (associated with small absorption features at 655, 663 and 697 nm) and at 467 and 474 nm for the dichroic B lines, respectively, are notable. The spectrum is modified by iron with a broad band at 330 nm, a feature associated with Fe^{3+} pairs (Ferguson and Fielding 1971), two barely visible absorption features at 378 nm (Fe^{3+} pairs) and 388 nm (isolated Fe^{3+} ions) forming a shoulder on the broad chromium band centered at 407 nm, with another band at 540 nm which also forms a small shoulder on the chromium broad band centered at 558 nm. The spectrum cut off is at 298 nm. A slight difference in the maximum absorption levels

of the chromium related broad bands at 407 nm and the 558 nm is also clearly evident. In theory this should not be the case for the O ray in a pure ruby spectrum, but it is a common observation in iron rich natural rubies.

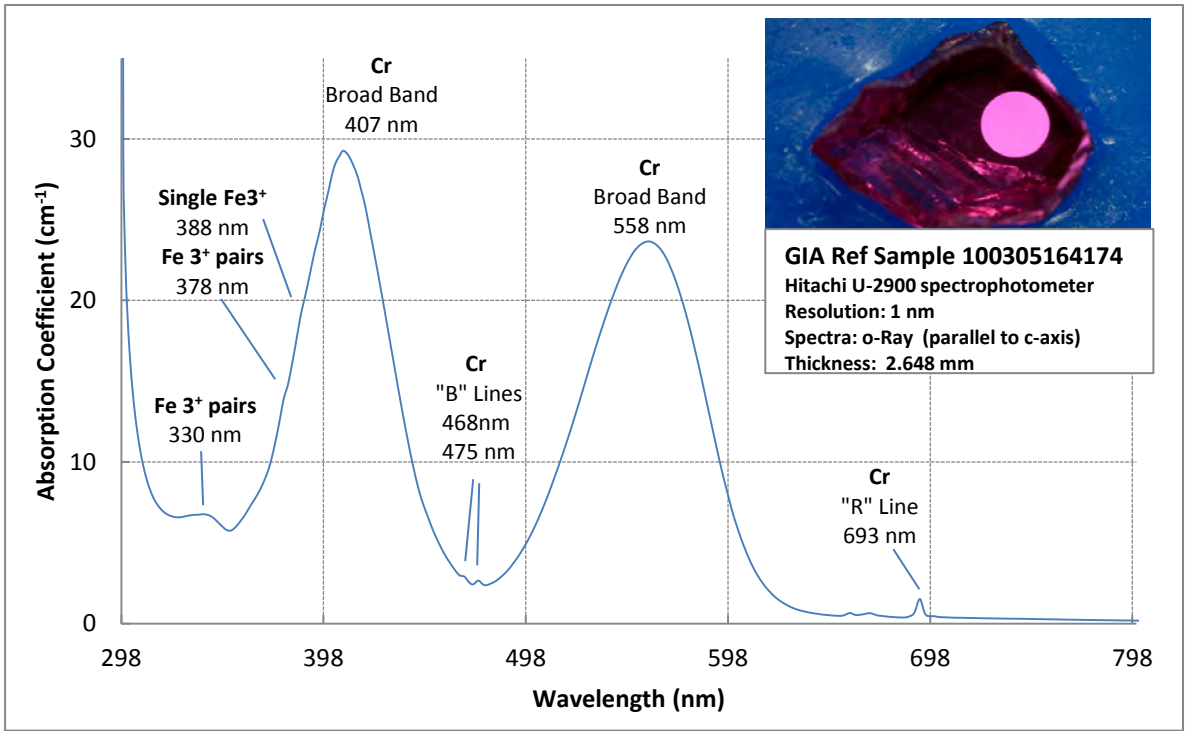

Figure 18: Ordinary ray of the unpolarized UV-Vis-NIR absorption spectra of GIA reference sample 100305164174 taken down the c-axis. In the top right hand corner the ruby can be seen being held in position with blue wax on its aluminum sample holder. The fabricated sample was placed over the (1.5 mm diameter) hole in the center of the sample holder. The lighter purplish pink circle is the area studied with UV-Vis-NIR and FTIR spectrometry. As can be seen it appears clean and the polished window is slightly larger than the area studied, thus enabling a better quality spectrum. The optical path length (the thickness of the sample studied) is 2.648 mm. and the sample weighs 0.642 carat. The wafer was carefully fabricated to be orientated perpendicular to the c-axis, minimizing any formation of a wedge-shape between the 2 polished windows either side of the sample, and particular care was given to the polish. Nevertheless a few needle type inclusions are present in the area studied. As a result of all these factors a background level of 0.18 absorption coefficient at 800 nm, was recorded which is acceptable to us for a sample with minor needle type inclusions. The spectrum as would be expected is mainly a chromium (Cr) spectrum modified by iron (Fe) with a cut off at 298 nm. Note: We purposely decided to start the wavelength scale at 298nm as a convenient way to make the cut off information more clearly visible to the reader.

Infrared spectra were collected for the stone through the same area and orientation used to collect the UV-Vis spectrum (see Figure 19). A weak absorption feature was observed at 3309 cm^{-1}.

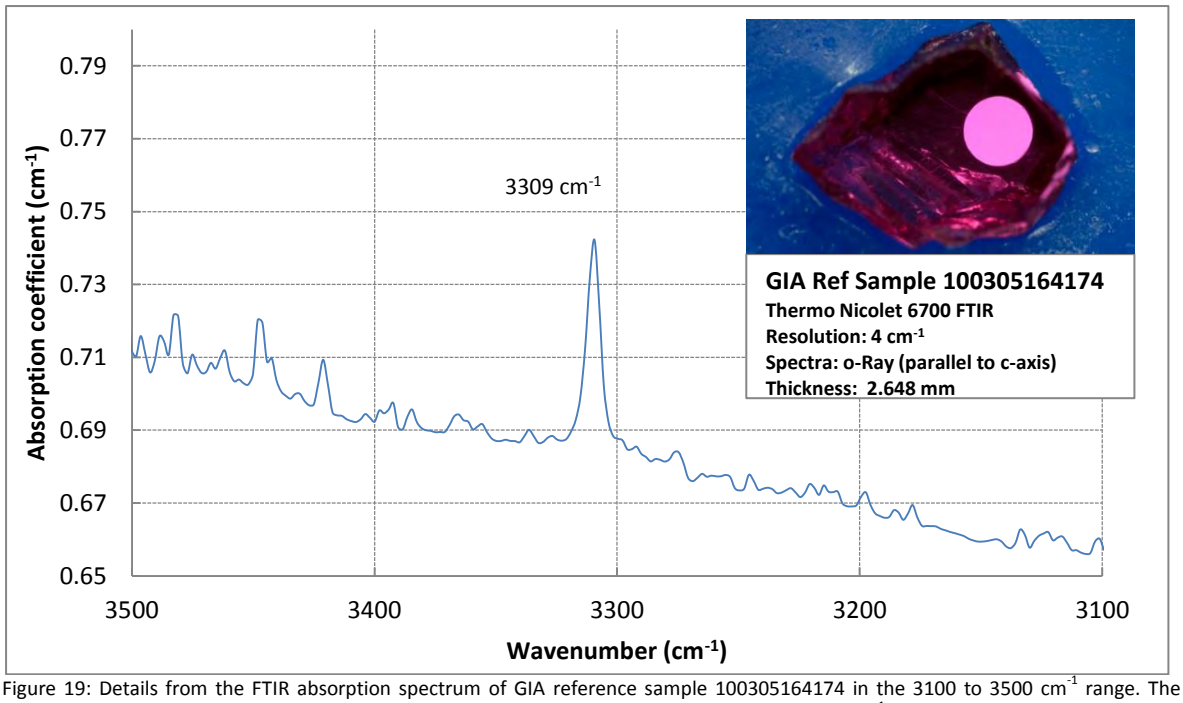

Figure 19: Details from the FTIR absorption spectrum of GIA reference sample 100305164174 in the 3100 to 3500 cm^{-1} range. The spectrum was taken in the direction of the c-axis with an optical path length of 2.648 mm. A 0.06 cm^{-1} (weak) high absorption feature at 3309 cm^{-1} is clearly visible.

LA-ICP-MS chemical data (Table 4) was collected on each side of the specimen. Four spots were analyzed on each side, eight spots in total (see Figure 20) on the same area studied with FTIR and UV-Vis spectroscopy. This method enables the comparison between the chemistry and spectra collected from the sample.

Figure 20: Two views of GIA reference sample 100305164174 (A1 type; see Annex C for a description of the classification system), seen after fabrication, showing the positions of the eight LA-ICP-MS spots. Photos (color calibrated): Sasithorn Engniwat © GIA.

It is interesting to note that the chemistry of sample 100305164174 (See Table 3) showed medium chromium (Cr) content (870 to 1040 ppma) and a significant iron (Fe) content (400 to 490 ppma) as was expected from looking at the UV-Vis spectrum obtained. Interestingly enough it also it had a much higher magnesium (Mg) content (23 to 60 ppma) when compared to the titanium (Ti) content (11 to 26 ppma). This explains the lack of blue color zoning in this ruby from Montepuez (Note: no blue color zoning was observed in any of the rubies from Montepuez studied) since in metamorphic type rubies or sapphires, blue color zoning mainly results from Fe - Ti intervalence charge transfer which is only possible if the host's titanium (Ti) content is higher than its magnesium (Mg) content (Emmett, Scarratt et al. 2003). Finally the vanadium (V) content (1.4 to 2.3 ppma) was rather low while the gallium (Ga) content (6.8 to 7.8 ppma) is at about average levels when compared to those usually encountered in natural rubies.

Table 3: LA-ICP-MS results for GIA reference sample 100305164174. "Bdl" stands for "Below Detection Limit"

Specimen 100305164174 Spot number (color of the spot area)	Concentration (PPMA)						
	Be	**Mg**	**Ti**	**V**	**Cr**	**Fe**	**Ga**
Spot 1 (purplish pink)	bdl	34.2	15.2	1.9	964.7	434.5	7.4
Spot 2 (purplish pink)	bdl	60.1	26.7	2.2	1039.2	489.3	7.8
Spot 3 (purplish pink)	bdl	29.4	13.7	1.9	980.4	456.4	7.4
Spot 4 (purplish pink)	bdl	60.1	27.4	1.9	1027.4	478.3	7.8
Spot 5 (purplish pink)	bdl	24.3	13.6	1.7	952.9	452.7	7.0
Spot 6 (purplish pink)	bdl	24.8	11.3	1.6	968.6	408.9	6.8
Spot 7 (purplish pink)	bdl	23.2	13.3	2.3	874.5	430.8	6.8
Spot 8 (purplish pink)	bdl	24.7	13.0	1.4	945.5	401.6	6.8
Detection Limits	0.4	0.2	3.0	0.4	0.6	1.5	0.2

c) GIA Reference Specimen Number 100305163907 (from the "Glass" area):

GIA reference sample 100305163907 is an A2 type sample (see Annex C for a description of GIA cataloguing classification) collected on September 11th 2012 while visiting the "Glass" area formerly mined by garimpeiros. The sample was found on the ground while exploring the area at (13°05'48"S latitude and 39°20'37"E longitude). Its color is pink with a slightly uneven patchy color distribution. The specimen weighed 0.172 carat before fabrication and has a very transparent central area (see Figure 21).

Figure 21: Two views of GIA reference sample 100305163907 (A2 type; see Annex C for a description of the classification system), weighing 0.172 carat seen before fabrication. The color is pink with a slightly uneven color distribution. The stone was collected on the ground at the "Glass" mining area on September 11th 2012 from a secondary deposit which explains why the sample shows some orange features (commonly called "iron stain" or "limonite") in surface reaching fissures. Photos (color calibrated): Sasithorn Engniwat © GIA.

As the tabular sample was very flat, the stone was fabricated with only one set of parallel windows perpendicular to its c-axis in the GIA Laboratory Bangkok. Particular care was taken to orientate the reference sample correctly, minimize the formation of a wedge shape and obtain a good polish. The final research sample weighed 0.133 carat (see Figure 22).

Figure 22: Two views of GIA reference sample 100305163907 (A2 type; see Annex C for a description of the classification system), weighing 0.133 carat seen after fabrication. The optical path length equals: 0.702 mm. The color, via transmitted light, is purplish pink with an even color distribution. Photo (color calibrated): Sasithorn Engniwat © GIA.

After fabrication the stone had a central area mostly free of any inclusions and some strain, but not as much as is apparently visible in (Figure 23) as viewed through cross-polar filters. The central area was selected for the collection of the spectroscopic data.

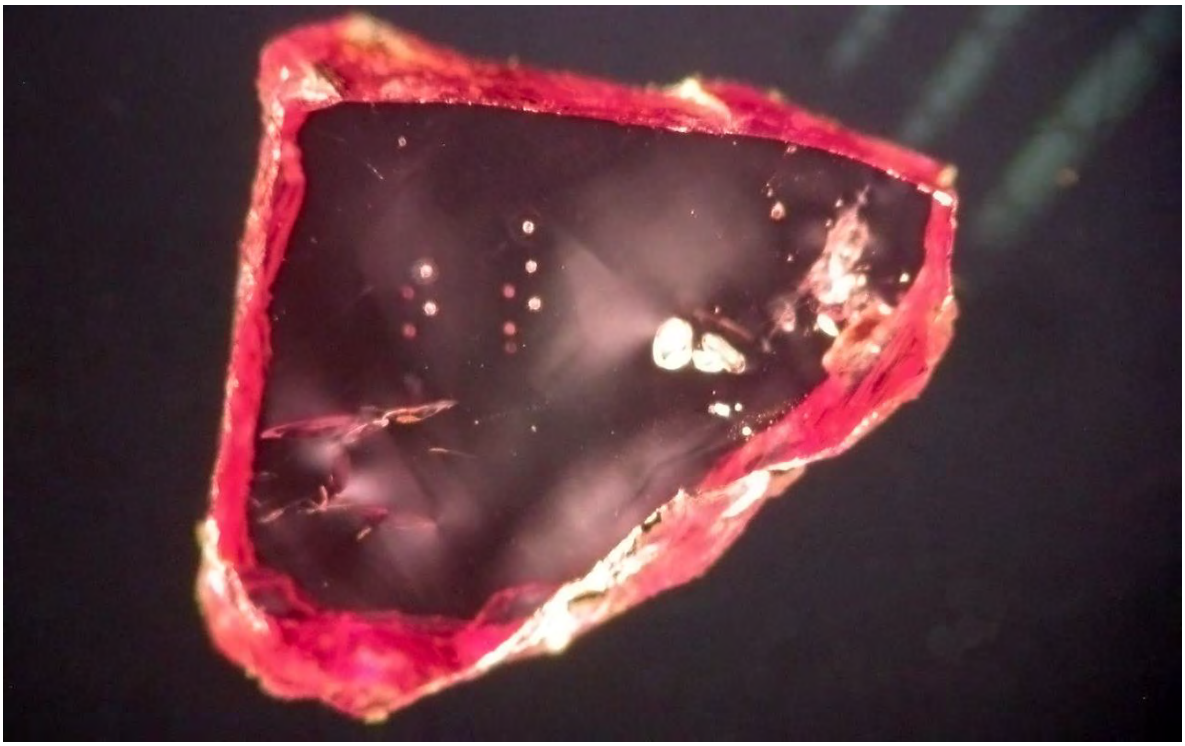

Figure 23: Sample 100305163907 seen through cross-polar filters. The LA-ICP-MS spots (4 on each side) in the central area are clearly visible. On the lower to mid left-hand side of the stone some surface reaching fissures associated with strain (cloud looking features) are apparent while on the right hand side of the sample a group of amphibole and mica crystals (very bright appearance) are evident. Photo: Vincent Pardieu © GIA.

Several interesting internal features are visible on the side of the sample. Firstly a group of rounded, greenish, randomly orientated doubly refractive crystals were identified as amphibole by Raman spectroscopy (Figure 24 and Figure 25) using the RRuff database as reference. Then a few unhealed surface reaching fissures, some small hexagonal tabular crystals identified as mica by Raman (Figure 24), a group of flat negative crystals associated with fringe like features (Figure 26), and a healed fissure composed of flat negative crystals (Figure 27) were all noted.

Besides these inclusions the stone also hosted a cloud composed of thin needles and broad particles associated with intersection like tubes. No twinning was visible under cross-polars but nevertheless the sample showed some strain, particularly in the area where several surface reaching fissures are visible.

Such mineral associations were one of the most common inclusions scenes encountered while studying Montepuez rubies. Another interesting feature observed in this particular sample is the slightly uneven patchy color zoning (Figure 25) which is rarely seen in such rubies.

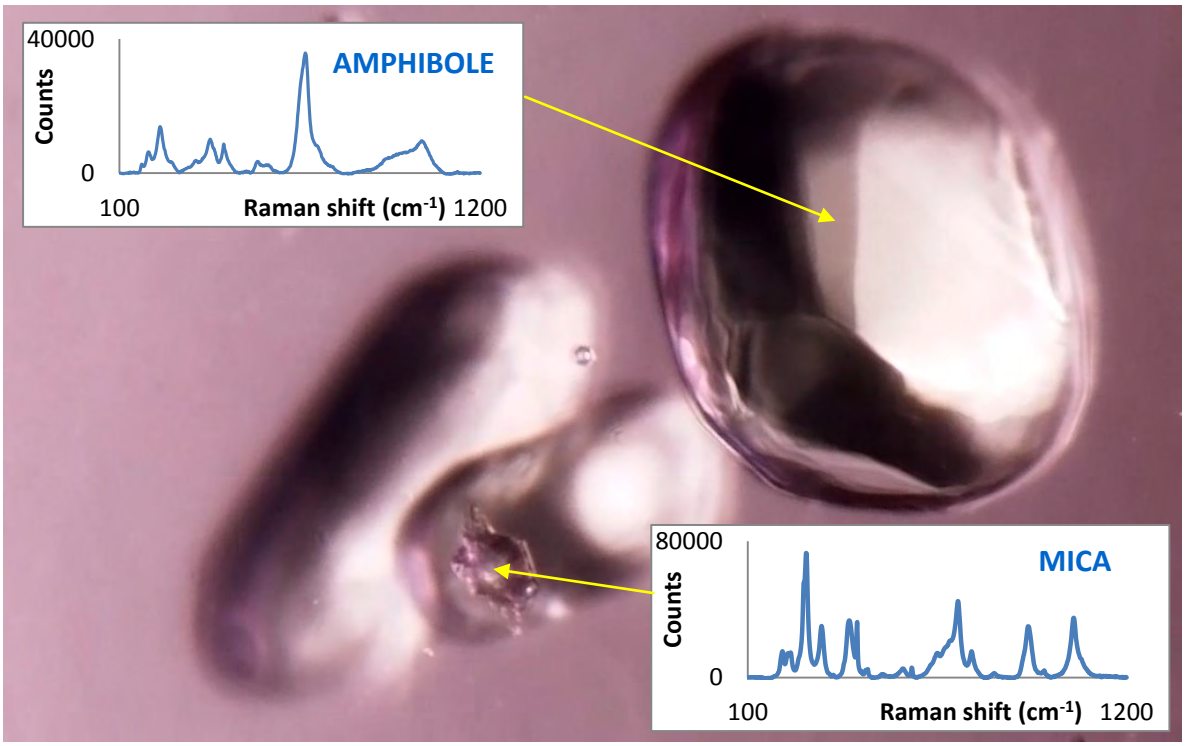

Figure 24: A group of transparent, rather rounded crystal inclusions (identified by Raman as amphibole) associated with two small hexagonal tabular euhedral crystals (identified by Raman as mica). The largest mica crystal is associated with a fringe like feature, a very common characteristic in rubies and sapphires from Montepuez. GIA type A reference sample number 100305163907. Transmitted + fiber optic illumination, magnified 180x. Photo: Jonathan Muyal © GIA.

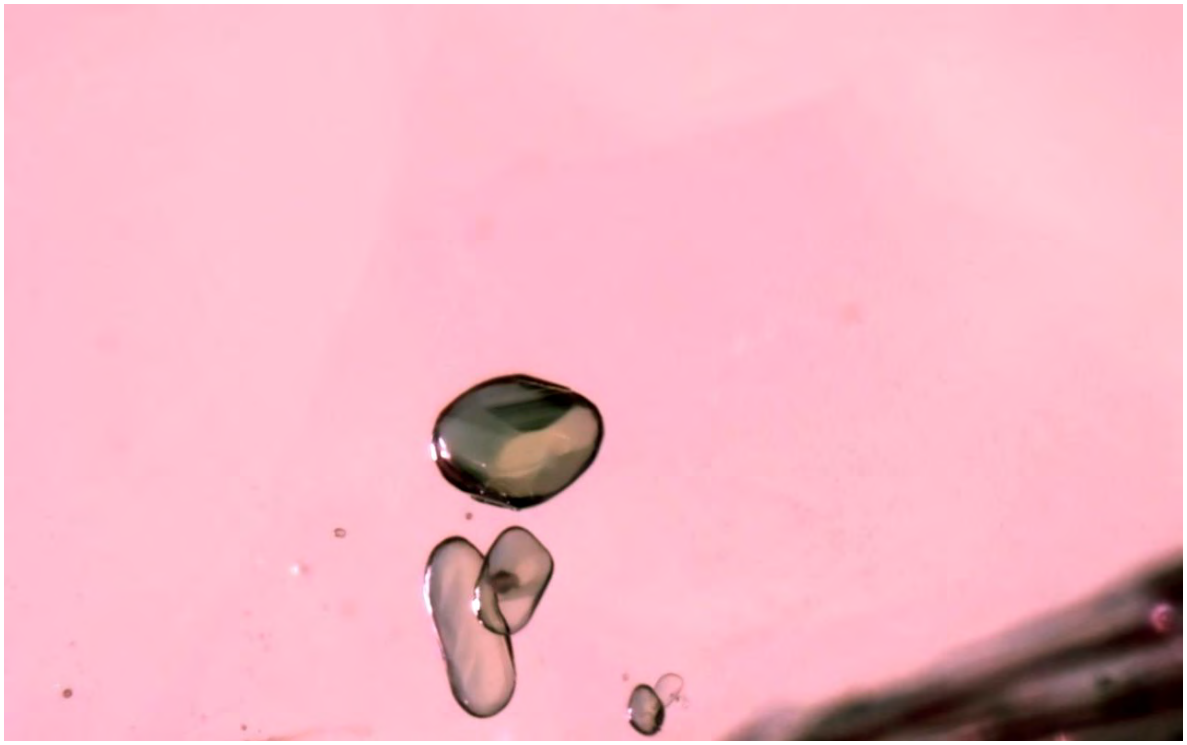

Figure 25: Another view of the crystals shown in Figure 24, this time using diffused lighting. The crystals no longer appear colorless. The largest reveal its brownish green coloration which is typical of amphibole crystals. The other feature worth noting is the uneven patchy color zoning in this sample. GIA type A reference sample number 100305163907. Diffused + fiber optic illumination, magnified 70x. Photo: Jonathan Muyal © GIA.

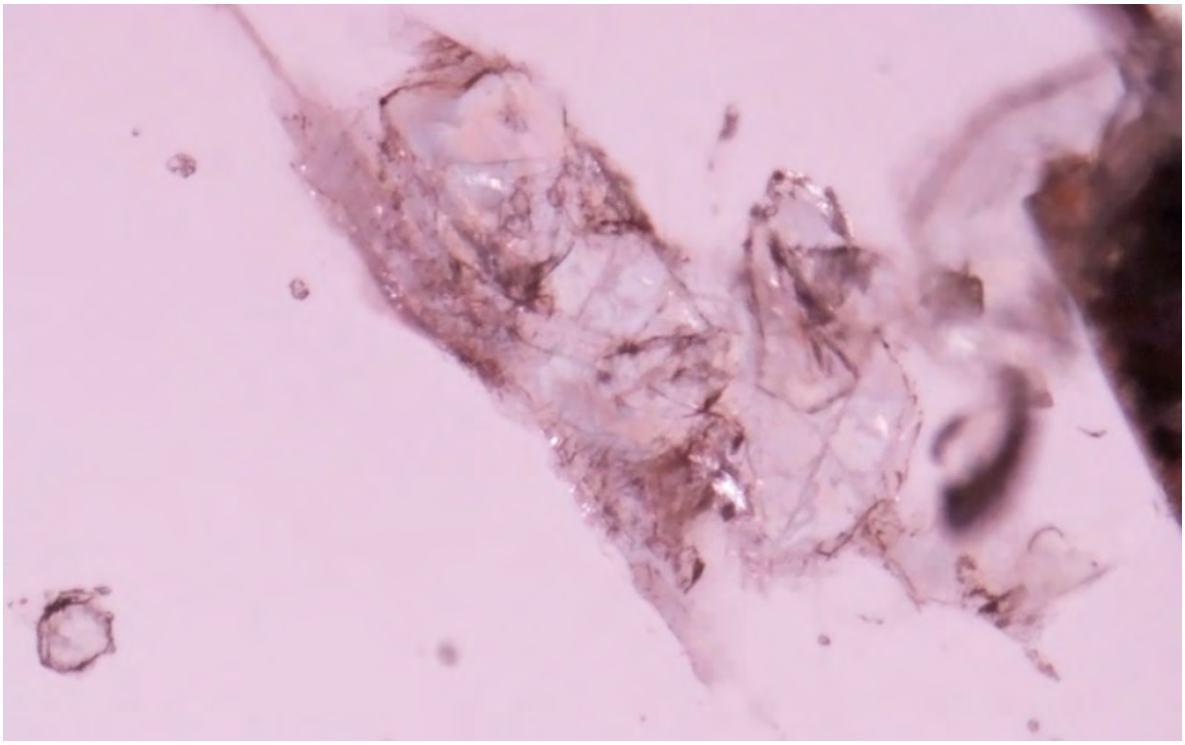

Figure 26: Tabular negative crystals associated with fringe-like fissures. GIA type A reference sample number 100305163907. Diffused + fiber optic illumination, magnified 112.5x. Photo: Jonathan Muyal © GIA.

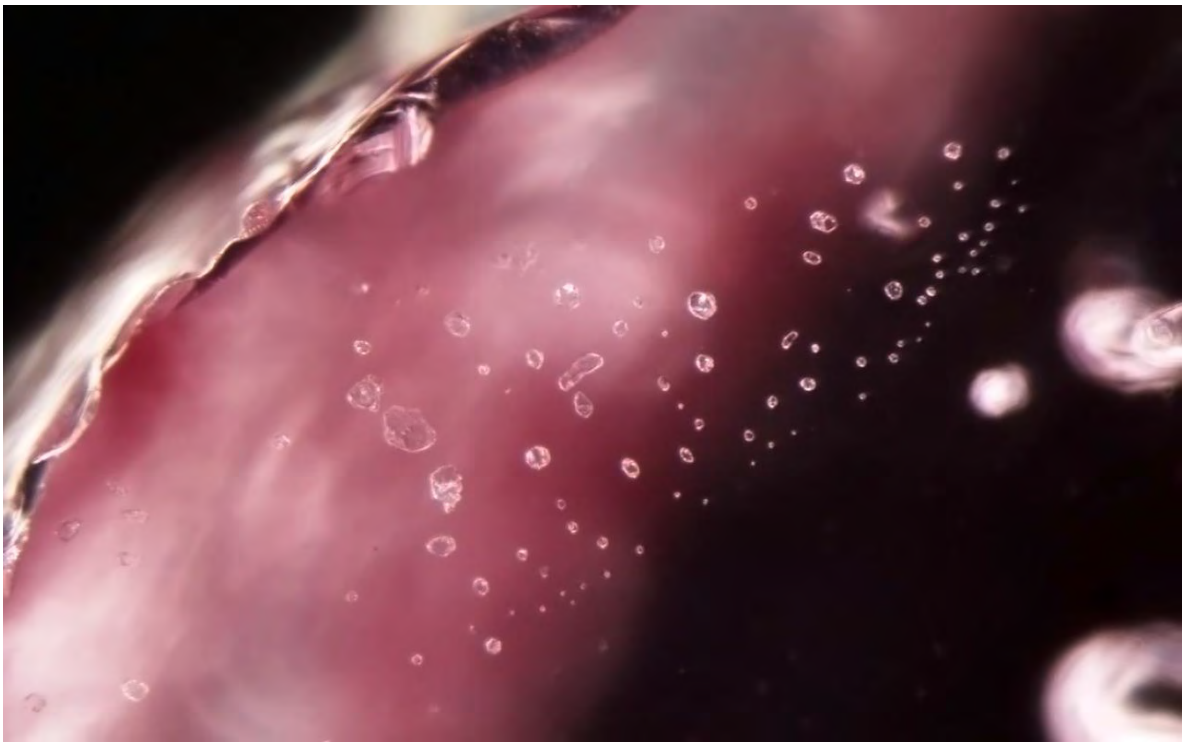

Figure 27: A healed fissure composed of tabular negative crystals. GIA Reference type A sample number 100305163907. Diffused + fiber optic illumination, magnified 100x. Photo: Jonathan Muyal © GIA.

When viewed under long-wave ultraviolet (LWUV) light the stone exhibited a medium to strong homogeneous red and a weak reaction under short-wave ultraviolet (SWUV) light was observed.

An unpolarized UV-Vis-NIR spectrum was collected for the specimen. The sample was carefully fabricated and then placed on a sample holder for spectroscopy to be carried out down the c-axis. The unpolarized spectrum obtained was in fact a very pure o-ray spectrum. The specific area chosen for the study appeared light pink and did not contain any visible inclusions.

The resulting spectrum (see Figure 18) showed a chromium spectrum with broad bands at 407 and 558 nm. Besides these bands the smaller chromium related absorption features known as the R and B chromium lines located at 693 nm for the R line (associated with small absorption features at 655, 663 and 697 nm) and at 467 and 474 nm for the dichroic B lines, respectively, are notable. The spectrum is modified by iron with a broad band at 330 nm, a feature associated with Fe^{3+} pairs (Ferguson and Fielding 1971), two barely visible absorption features at 378 nm (Fe^{3+} pairs) and 388 nm (isolated Fe^{3+} ions) forming a shoulder on the broad chromium band centered at 407 nm, with another band at 540 nm which also forms a small shoulder on the chromium broad band centered at 558 nm. The spectrum cut off is at 298 nm. A slight difference in the maximum absorption levels of the chromium related broad bands at 407 nm and the 558 nm is also clearly evident. In theory this should not be the case for the O ray in a pure ruby spectrum, but it is a common observation in iron rich natural rubies.

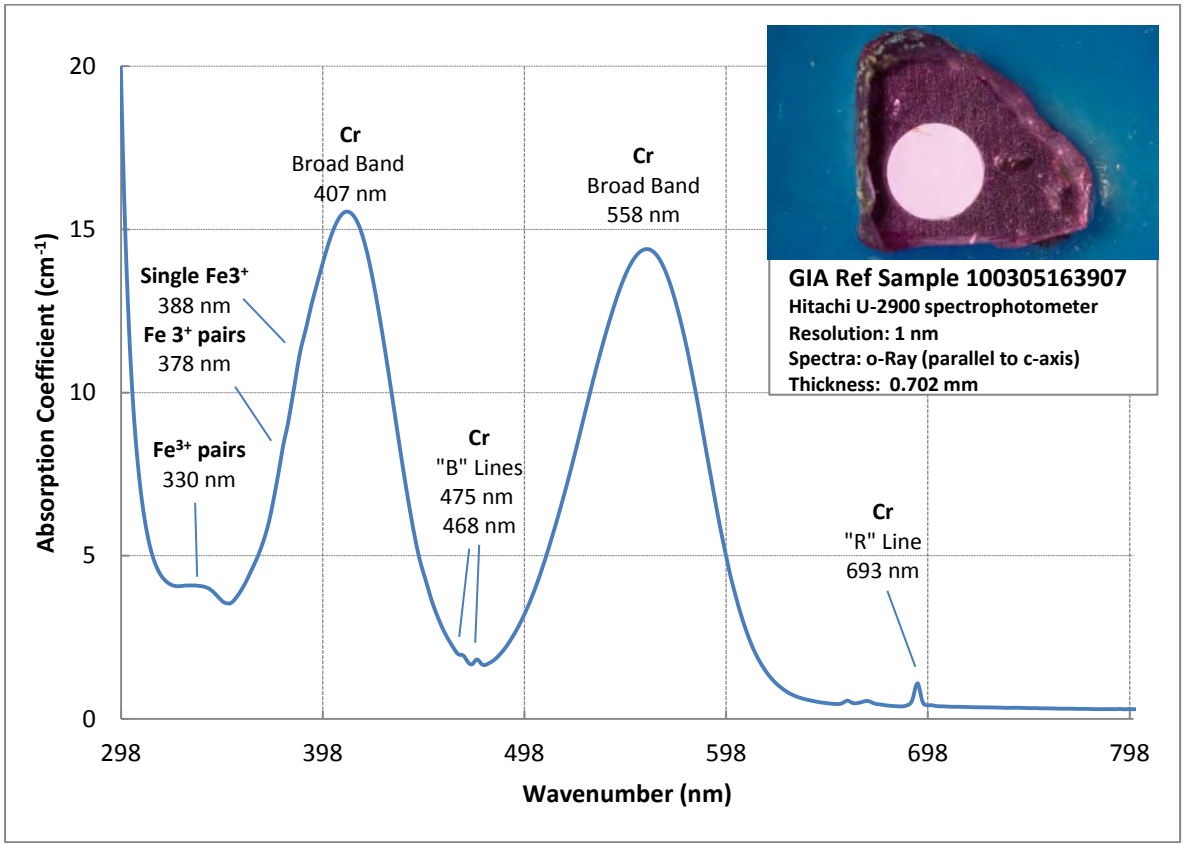

Figure 28: Unpolarized UV-Vis-NIR absorption spectra of GIA reference sample 100305163907 taken down the c-axis. In the top right hand corner the ruby can be seen being held in position with blue wax on its aluminum sample holder. The fabricated sample was placed over the (1.5 mm diameter) hole in the center of the sample holder. The much lighter pink circle is the area studied with UV-Vis-NIR and FTIR spectrometry. As can be seen it appears mostly clean (bar a small healed fissure) and the polished window is slightly larger than the area studied, thus enabling a better quality spectrum. The optical path length (the thickness of the sample studied) is 0.702 mm, and the sample weighs 0.133 carat. The wafer was carefully fabricated to be orientated perpendicular to the c-axis, minimizing any formation of a wedge-shape between the 2 polished windows on either side of the sample and particular care was given to the polish. Nevertheless a small healed fissure is present in the area studied in addition to some strain as seen through cross-polars in Figure 23. As a result of all these factors a background level of 0.29 absorption coefficient at 800 nm, was recorded which is not ideal for a natural sample. The spectrum as would be expected is mainly a chromium (Cr) spectrum modified by iron (Fe) with a cut off at 298 nm. Note: We purposely decided to start the wavelength scale at 298nm as a convenient way to make the cut off information more clearly visible to the reader.

Infrared spectra were collected for the stone through the same area and orientation used to collect the UV-Vis spectrum. No useful features were recorded.

LA-ICP-MS chemical data (Table 4) was collected on each side of the specimen. Four spots were analyzed on each side, eight spots in total (see Figure 29) on the same area studied with FTIR and UV-Vis spectroscopy.

Figure 29: Two views of GIA reference sample 100305163907 (A2 type; see Annex C for a description of the classification system), seen after fabrication, showing the positions of the eight LA-ICP-MS spots. Photos (color calibrated): Sasithorn Engniwat © GIA.

It is interesting to note that the chemistry of sample 100305163907 showed medium chromium (Cr) content (435 to 500 ppma) and a significant iron (Fe) content (320 to 380 ppma). Interestingly enough it also had much higher magnesium (Mg) content (35 to 62 ppma) when compared to the titanium (Ti) content (16 to 22 ppma). This is very common in the rubies from Montepuez we studied and explains why these rubies don't show any blue color zoning. Vanadium (V) and gallium (Ga) are even and low.

Table 4: LA-ICP-MS results for GIA reference sample 100305163907. "Bdl" stands for "Below Detection Limit"

Specimen 100305163907 Spot number (color of the spot area)	**Concentration (PPMA)**						
	Be	**Mg**	**Ti**	**V**	**Cr**	**Fe**	**Ga**
Spot 1 (pink)	bdl	62.1	22.5	1.3	435.3	331.9	6.2
Spot 2 (pink)	bdl	38.3	19.0	1.3	509.8	320.2	6.2
Spot 3 (pink)	bdl	57.5	19.1	1.3	458.8	377.7	5.9
Spot 4 (pink)	bdl	35.5	18.9	1.5	654.9	337.3	6.1
Spot 5 (pink)	bdl	45.8	17.4	1.4	458.8	326.7	6.7
Spot 6 (pink)	bdl	38.7	16.2	1.2	478.4	330.0	6.1
Spot 7 (pink)	bdl	61.8	16.9	1.1	462.7	341.9	5.9
Spot 8 (pink)	bdl	49.4	19.1	1.1	494.1	338.4	6.3
Detection Limits	0.1	0.2	1.9	0.2	0.4	1.2	0.1

Observation: An interesting observation with this sample is that with the magnesium (Mg) content being higher than that of the titanium it would have been consistent to observe a series of absorption features centered around 3160 cm^{-1} with the FTIR, as this feature is usually associated with magnesium in association with a trapped hole center. Such features are usually visible in unheated rubies and sapphires when the magnesium content is greater than titanium. When titanium is equal to or greater than magnesium an inter-valence charge transfer usually results and a blue coloration is visible to the human eye (Emmett, Scarratt et al. 2003). Since this sample was collected on the ground at the mining site, and since its inclusions show no indications of heat treatment, the sample is unlikely to have been heated. Of course we cannot totally exclude, as the sample was found on the ground in the mining area, the possibility that it may have been exposed to the effects of a bush fire or even the remote chance that it may have been thrown into a fire intentionally or unintentionally by a miner! So at present there appears to be no clear explanation for the absence of the 3160 cm-1 peak.

d) GIA Reference Specimen Number 100305163897 (from the "Maninge Nice" area):

GIA reference sample 100305163897 is an A2 type sample (see Annex C for a description of GIA cataloguing classification) collected on September 10th 2012 while visiting an area called "Nova Mina". The sample was found with many small amphibole crystals on the ground (Figure 30) near an abandoned garimpeiros hut at (13°04'53"S latitude and 39°20'14"E longitude). During a study of the site with the local staff from MRM, including a former garimpeiro, we were informed that such stones probably originated from "Maninge nice" area. That area, located less than a kilometer to the south east, was famous for deep red rough stones of this appearance.

Figure 30: GIA reference sample 100305163897 (top right) and other small samples associated with small broken pieces of green amphibole as GIA field gemologist VP found them on the ground near an abandoned hut at "Nova Mina" near Montepuez. Photo Vincent Pardieu © GIA.

It is possible that the garimpeiros brought some bags of gem rich ground from "Maninge Nice" to their camp at Nova mina and sorted it in front of their hut. This made more sense as the other stones and mineral associations found at "Nova Mina" were markedly different from these samples. Except for this find, the stones found at "Nova Mina" were mainly weathered light pink stones associated with quartz and garnets, obviously originating from a secondary deposit. The green amphibole crystals and small rubies found on that specific spot were in contrast very sharp and presented no indications of weathering.

Note: This "tale" is interesting because it helps explain why GIA has a different field cataloguing code for samples found on a mining site that depends on how they were collected. If a sample is found on the ground at a mining site it does not prove that it was definitely mined in that specific spot as such samples may have been extracted from a neighboring mining site or possibly an even more distant place and subsequently taken to the spot where it was discovered later by a GIA gemologist. Furthermore, as with the previous stone, in such cases it is also not possible to completely exclude the possibility that the samples were submitted to bush fires or even some kind of camp-fire related "heat treatment". For such reasons GIA differentiates between samples mined by a GIA field gemologist directly from the hard rock in a primary deposit (called A1 type samples in the GIA cataloguing classification system, see Annex C for more details), samples found on the ground while visiting a mining site (called A2 type samples in the GIA cataloguing

classification system) and also samples mined by the gemologist from a secondary deposit (called A3 type samples in the GIA cataloguing classification system, see Annex C for more details). As a result, and it is particularly the case with A2 type samples, careful examination of the area where the samples are found is necessary in order to see if it makes sense that any given sample was indeed mined nearby or not.

Later while studying samples of the "Bo Daeng" type found in the Thai market and believed to have been mined at "Maninge Nice", we discovered that sample 100305163897 and these samples not only shared the same appearance but also the same chemistry. The latter was found to be slightly different, as will be seen further on, from that of the other deposits near Montepuez.

Prior to fabrication the stone was a flat tabular crystal weighing 0.121 carat (see Figure 31).

Figure 31: Two views of GIA reference sample 100305163897 (A2 type; see Annex C for a description of the classification system), weighing 0.121 carat seen before fabrication. The color, via transmitted light is deep purplish pink with a homogeneous color distribution. Photos (color calibrated): Sasithorn Engniwat © GIA.

It was fabricated with one set of parallel windows perpendicular to the c-axis at the GIA Laboratory Bangkok. Particular care was taken to orientate the reference sample correctly, minimize the formation of a wedge shape, and obtain a good polish. The final research sample weighed 0.078 carat (see Figure 32).

Figure 32: Two views of GIA reference sample 100305163897 (A2 type; see Annex C for a description of the classification system), weighing 0.078 carat seen after fabrication. The color is purplish pink with a homogenous color distribution. Photos (color calibrated): Sasithorn Engniwat © GIA.

When viewed under long-wave ultraviolet (LWUV) light the stone exhibited a medium to strong even red reaction and a weak reaction under short-wave ultraviolet (UV) light was observed.

The stone is predominantly clean but also hosted a few interesting inclusions. The main internal features were a transparent apparently colorless rounded crystal (Figure 33) identified by Raman as amphibole. Given that this sample was found at Nova Mina in association with broken amphibole crystals that obviously originated from the rock matrix hosting the rubies this comes as no surprise. The second crystal inclusion observed was a small, dark, opaque, highly lustrous

euhedral crystal (Figure 34) believed to be chalcopyrite after several similar looking inclusions that reached the surfaces of other reference stones were identified as such by Raman.

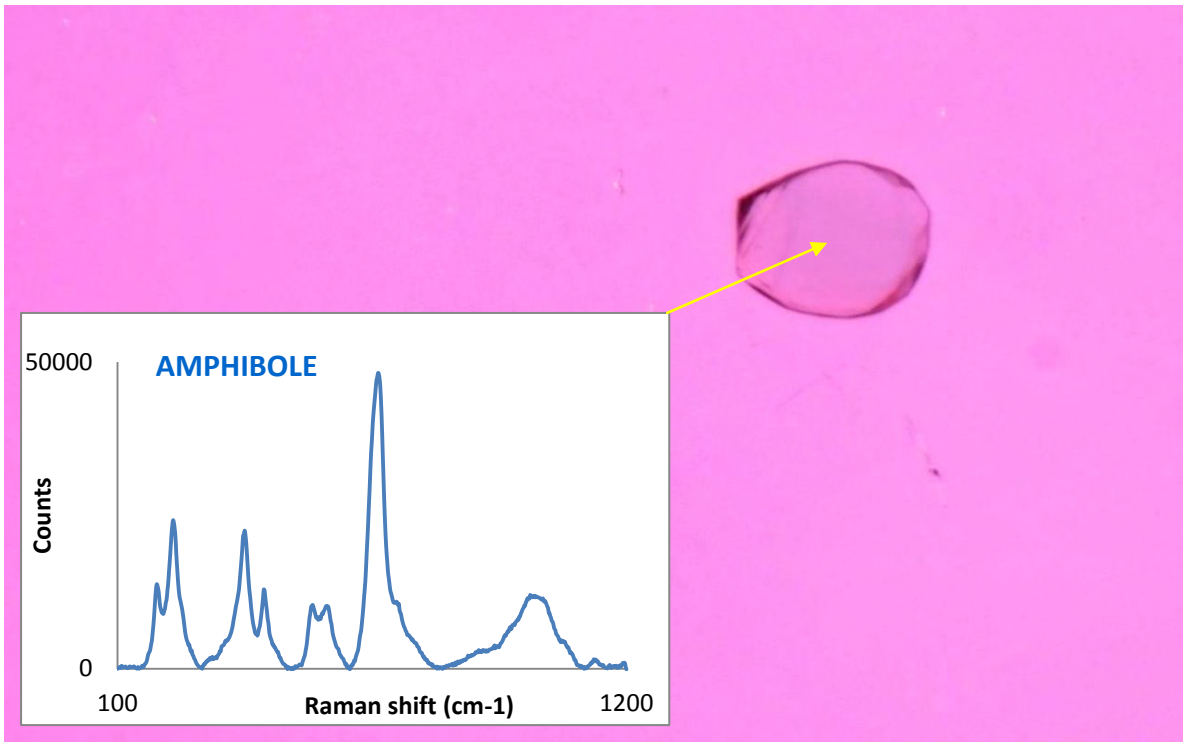

Figure 33: A transparent colorless rounded crystal inclusion (identified by Raman as amphibole) in GIA reference sample number 100305163897. Diffused + fiber optics illumination, magnified 115x. Photo: Jonathan Muyal © GIA.

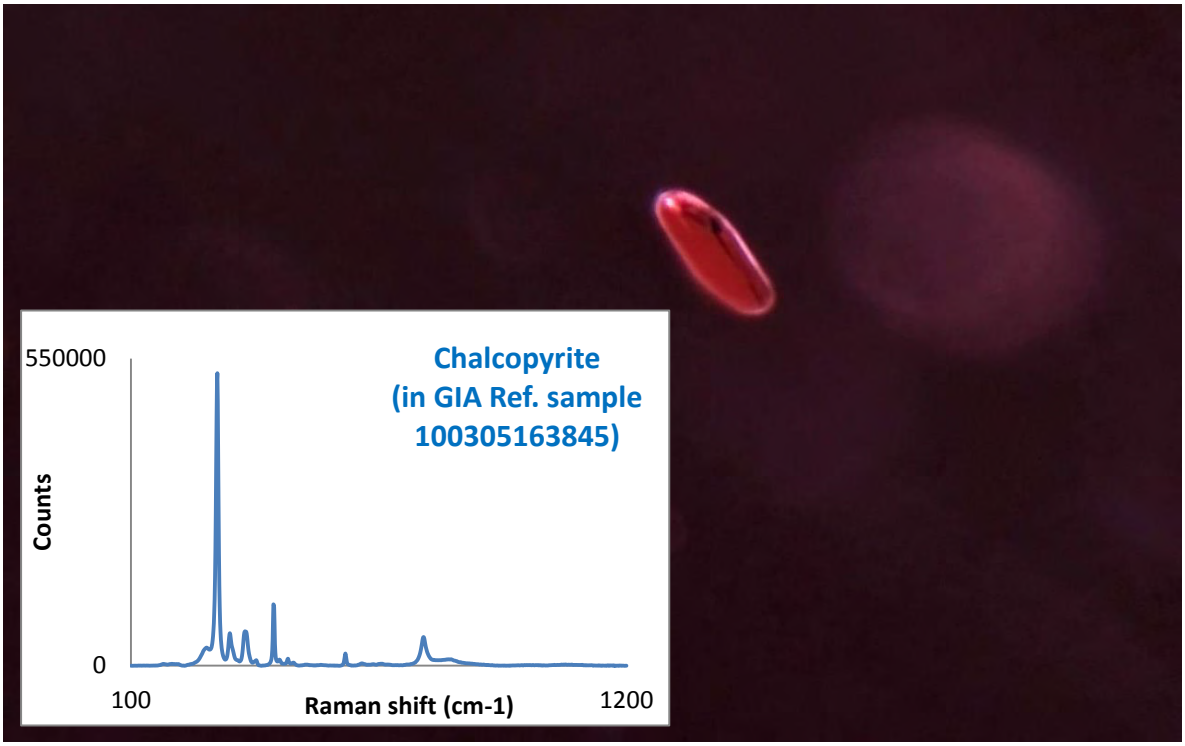

Figure 34: An opaque dark looking crystal inclusion in GIA reference sample number 100305163897. A similar inclusion that reached the surface of another ruby from Montepuez (GIA reference sample 100305163845) was identified as chalcopyrite by Raman. Dark field + fiber optics illumination, magnified 115x. Photo: Jonathan Muyal © GIA.

Overall, the presence of amphibole crystals associated with chalcopyrite seems to be a very common inclusions association in rubies from the Maninge Nice area as it was later confirmed by MRM staff who sorted kilos of the material recovered from their exploration trenches.

An unpolarized UV-Vis-NIR spectrum was collected for the specimen. The sample was carefully fabricated and then placed on a sample holder for spectroscopy to be carried out down the c-axis. The resulting unpolarized spectrum obtained was in fact a very pure o-ray spectrum. The specific area chosen for the study appeared pink and did not contain any visible inclusions.

The resulting spectrum (Figure 35) showed a chromium spectrum with two broad bands at 410 and 559 nm. Besides these bands the smaller chromium related absorption features known as the R and B chromium lines located at 693 nm for the R line (associated with small absorption features at 655, 663 and 697 nm) and at 467 and 474 nm for the dichroic B lines, respectively, are notable. The spectrum also shows a limited iron content (but less than in the case of GIA reference sample 100305163907) with a broad band at 342 nm, a feature associated with Fe^{3+} pairs (Ferguson and Fielding 1971), two barely visible absorption features at 378 nm (Fe^{3+} pairs) and 388 nm (isolated Fe^{3+} ions) forming a shoulder on the broad chromium band centered at 410 nm, with another band (barely visible) at 540 nm which also forms a small shoulder on the chromium broad band centered at 559 nm. The spectrum cut off is at 289 nm which is quite low and is usually seen in rubies with no particles and low iron content. A slight difference in the maximum absorption levels of the chromium related broad bands at 410 nm and the 559 nm is also clearly evident. In theory this should not be the case for the O ray in a pure ruby spectrum, but it is a common observation in iron rich natural rubies.

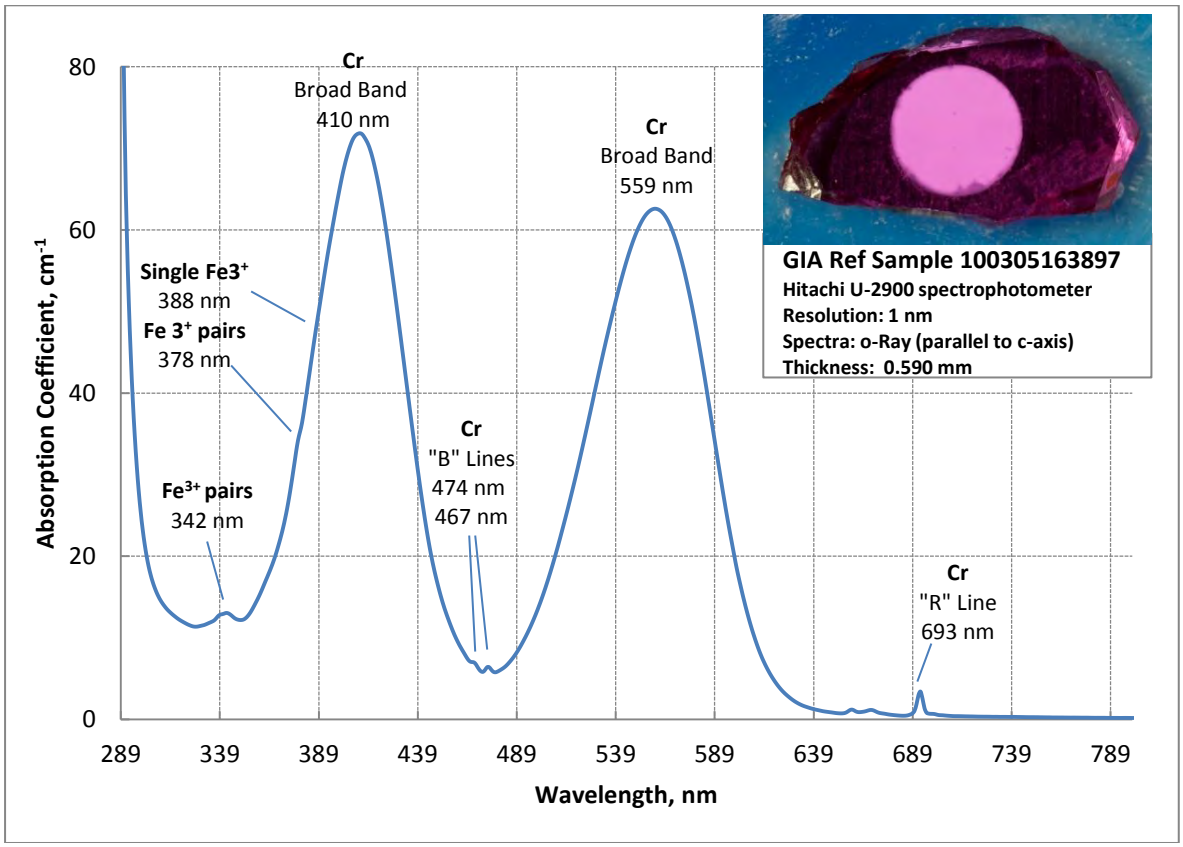

Figure 35: Ordinary ray of the unpolarized UV-Vis-NIR absorption spectra of GIA reference sample 100305163897 taken down the c-axis. In the top right hand corner the ruby can be seen being held in position with blue wax on its aluminum sample holder. The fabricated sample was placed over the (1.5 mm diameter) hole in the center of the sample holder. The pink circle is the area studied with UV-Vis-NIR and FTIR spectrometry. As can be seen it appears mostly clean (a small healed fissure is present) and the polished window is slightly larger than the area studied, thus enabling a better quality spectrum. The optical path length (the thickness of the sample studied) is 0.590 mm, and the sample weighs 0.078 carat. The wafer was carefully fabricated to be orientated perpendicular to the c-axis, minimizing any formation of a wedge-shape between the 2 polished windows either side of the sample, and particular care was given to the polish. The area studied contained very minor inclusions. As a result of all these factors a background level of 0.17

absorption coefficient units at 800 nm was recorded which is acceptable to us for a natural sample. The spectrum as would be expected is mainly a chromium (Cr) spectrum modified by iron (Fe) with a cut off at 289 nm. Note: We purposely decided to start the wavelength scale at 289nm as a convenient way to make the cut off information more clearly visible to the reader.

Infrared spectra were collected for the stone through the same area and orientation used to collect the UV-Vis spectrum. No visible features were recorded.

LA-ICP-MS chemical data (Table 5) was collected on each side of the specimen. Four spots were analyzed on each side, eight spots in total (see Figure 36) on the same area studied with FTIR and UV-Vis spectroscopy in order to compare the results of the trace element chemistry with spectroscopy. The area appeared deep purplish pink and did not contain any visible inclusions.

Figure 36: Two views of GIA reference sample 100305163897 (A2 type; see Annex C for a description of the classification system), seen after fabrication, showing the positions of the eight LA-ICP-MS spots. Photos (color calibrated): Sasithorn Engniwat © GIA.

Table 5: LA-ICP-MS results for GIA reference sample 100305163897. "Bdl" stands for "Below Detection Limit".

Specimen **100305163897** Spot number (color of the spot area)	**Concentration (PPMA)**						
	Be	**Mg**	**Ti**	**V**	**Cr**	**Fe**	**Ga**
Spot 1 (purplish pink)	bdl	40.8	27.9	3.7	2333.3	333.6	6.8
Spot 2 (purplish pink)	bdl	49.0	32.4	3.4	2113.7	335.9	6.5
Spot 3 (purplish pink)	bdl	44.0	27.2	4.0	2337.2	339.5	6.8
Spot 4 (purplish pink)	bdl	36.4	22.8	3.7	2317.6	334.4	6.2
Spot 5 (purplish pink)	bdl	34.6	26.0	4.1	2113.7	307.4	6.4
Spot 6 (purplish pink)	bdl	42.0	29.0	4.0	2352.9	305.9	6.4
Spot 7 (purplish pink)	bdl	44.2	30.3	4.5	2399.9	331.8	6.8
Spot 8 (purplish pink)	bdl	47.9	31.1	4.5	2556.8	246.5	6.4
Detection Limits	0.1	1.8	0.2	0.4	1.1	0.1	0.1

At between 2100 and 2600 ppma, the chromium content in this sample is remarkably high consistent with our findings in most of the other samples from the type referred to as "Bo Daeng" in the Thai trade. At 245 to 340 ppma, the iron content on the other hand is significantly lower than what has been detected in all the other samples from the Montepuez area we have studied. This result makes sense as it is consistent with the UV-Vis spectra obtained where the iron contribution was minor. Such high chromium levels combined with rather low iron content explains the strong red fluorescence seen when viewed under long-wave ultraviolet light. Finally since each spot revealed Mg in greater quantities than Ti, it proved that Ti was unavailable to pair with Fe in a charge-transfer reaction thus resulting in the lack of any blue coloration in the sample.

e) <u>GIA Reference Specimen Number 100305163945 (from the "Torro" area):</u>

GIA reference sample 100305163945 is a B2 type sample (see Annex C for a description of GIA cataloguing classification) collected on September 20th 2012 while visiting an area called “Torro” near Namujo village located at (13°05'23"S latitude and 39°17'09"E longitude). The sample was found on September 24th 2012, a few days after the police chased away thousands of garimpeiros working at “Torro”. During a visit to the former mining site that day we were able to obtain one bag of gem rich gravel left behind by the garimpeiros during their escape. We washed the contents and collected 9 samples. Most of them were very clean as is expected from the majority of samples found in secondary deposits. Among these rubies was GIA reference sample 100305163945, a very clean slightly brownish red stone that weighed 1.611 carats before fabrication (see Figure 37).

Figure 37: Two views of GIA reference sample 100305163945 (B2 type; see Annex C for a description of the classification system), weighing 1.611 carats seen before fabrication via transmitted light. The color is brownish red. Photos (color calibrated): Sasithorn Engniwat © GIA

A very small wafer was fabricated from this sample in order to collect o and e ray spectra. To achieve this, two sets of parallel windows were polished perpendicular and parallel to the c-axis of the stone at the GIA Laboratory Bangkok. Particular care was taken to orientate the reference sample correctly, minimize the formation of a wedge shape and obtain a good polish. The final research sample weighed 0.066 carats (Figure 38).

Figure 38: Two views of GIA reference sample 100305163945 (B2 type; see Annex C for a description of the classification system), weighing 0.066 carats seen after fabrications with windows cut in the direction perpendicular to the c-axis. In this orientation color is homogenous brownish pink. Photos (color calibrated): Sasithorn Engniwat © GIA.

When viewed under long-wave ultraviolet (LWUV) light the stone exhibited a weak to moderate even red reaction and no reaction under short-wave ultraviolet (UV) light was observed.

Two polarized UV-Vis-NIR spectra (o-ray and e-ray) were collected from the specimen. As can be seen (Figure 39) the o and e ray spectra exhibit a mainly chromium (Cr) spectrum modified by iron (Fe) with a cut off at 300 nm for the e-ray and 309 nm for the o-ray. Chromium related absorption bands centered at about 410 and 559 nm (for the o-ray) and 398 and 547 nm (for the e-ray) are also visible. Besides these bands the smaller chromium related absorption features known as the R and B chromium lines located at 693 nm for the R line (associated with small absorption features

at 655, 663 and 697 nm) and at 467 and 474 nm for the dichroic B lines, respectively, are notable. In these two spectra iron related absorption features are significant and clearly evident: We note particularly a noisy broad band that looks like a shoulder at 330 nm (obvious in both o and e rays) (Ferguson and Fielding 1971), and absorption peaks at 376 and 450 nm related to Fe3+ pairs, as well as at 388 nm related to single Fe3+. Note that these features are easier to see in the o-ray.

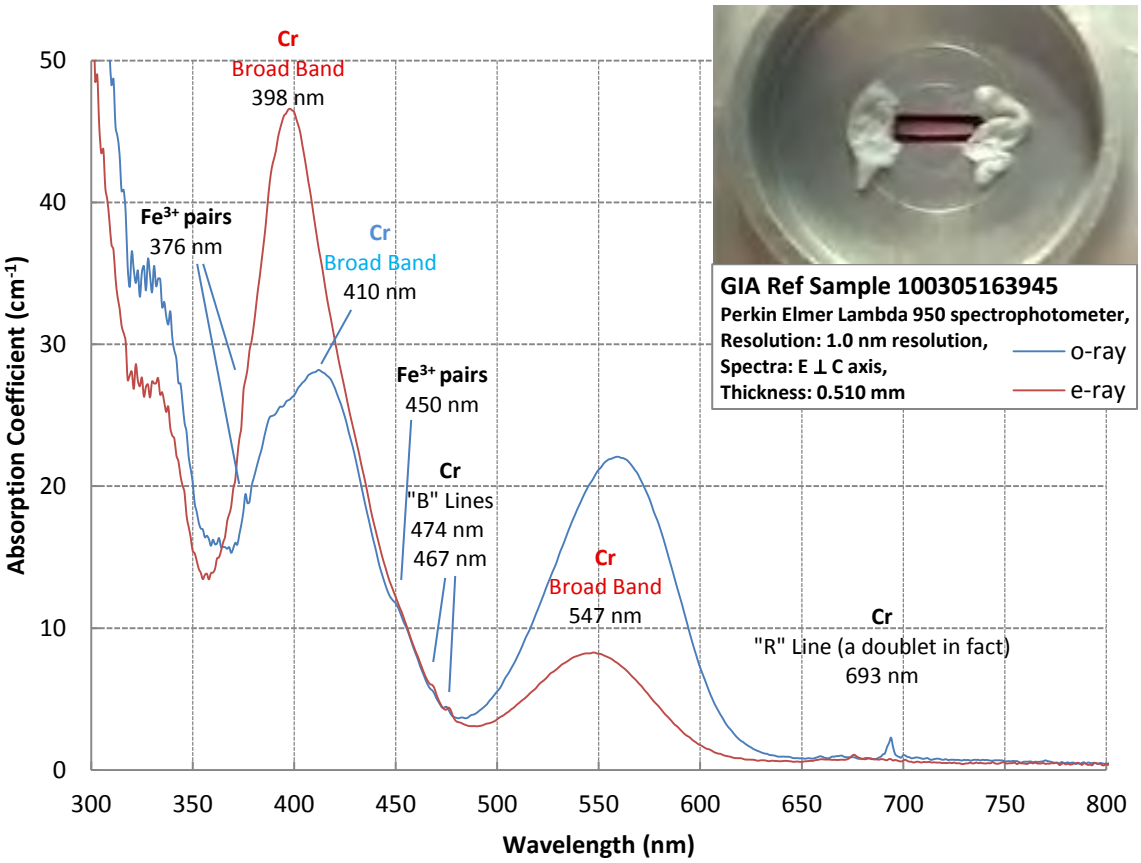

Figure 39: Polarized UV-Vis-NIR absorption spectra of GIA reference sample 100305163945 showing the o and e rays. In the top right hand corner the ruby can be seen being held in position on its aluminum sample holder. The opening of the sample holder is 1.5 x 6mm diameter, which is slightly larger than the sample. In order to obtain an acceptable spectrum we used a plastic mask to reduce the size of the opening. The optical path length (the thickness of the sample studied) was 0.510 mm and the spectrophotometer's slit was 1.0 nm. The sample weighed 0.066 carats, and the color was orange in transmitted light. The fabricated wafer was carefully orientated so that 2 sets of windows were fabricated perpendicular and then parallel to the c-axis, the wedge between the two polished windows was kept to a minimum and particular care was given to the polish, whilst the area studied had no visible inclusions. As a result of all these factors a background level of 0.41 absorption Coefficient units at 800 nm was recorded, which is not ideal but for such a small sample it is quite acceptable to us. As can be seen the spectrum is mainly a chromium (Cr) spectrum modified by iron (Fe).

Infrared spectra were collected for the stone through the same area and orientation used to collect the UV-Vis spectrum (Figure 39). The main features recorded a broad peak centered at 3164 cm^{-1}. This is interesting as such a feature is usually found in unheated natural metamorphic type blue sapphires when the beam passes through colorless or yellow areas where magnesium is typically present in greater quantities than titanium. This feature was also commonly observed in rubies from Winza, Tanzania (Schwarz et al. 2008) and Toamasina or Didy, Madagascar (Pardieu et al. 2012) which are deposits where rubies are also associated with amphibole.

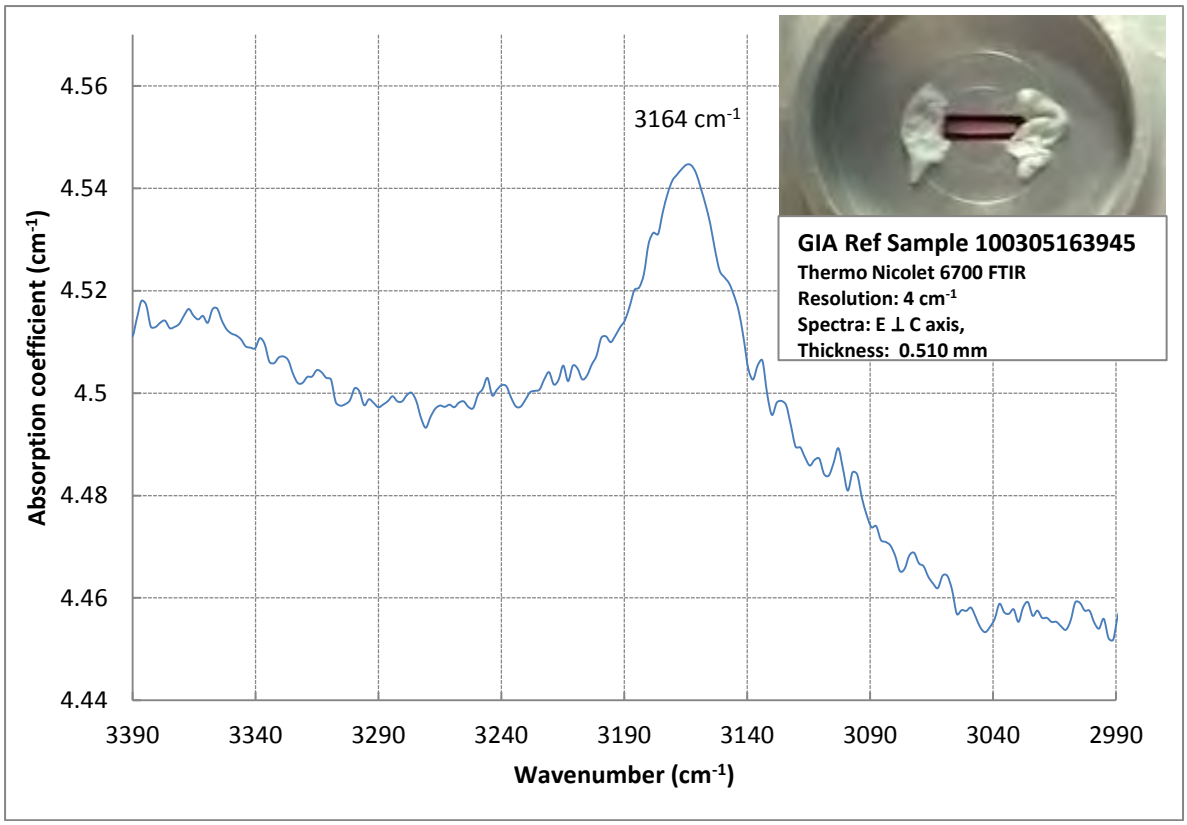

Figure 40: Details from the FTIR absorption spectrum of GIA reference sample 100305163945 taken perpendicular to the direction of C-axis. Approximate optical path length: 0.510 mm. Weight: 0.066 carats, Color: Brownish Pink.

LA-ICP-MS chemical data (Table 6) was collected on each side of the specimen. Four spots were analyzed on each side; eight spots in total (see Figure 41).

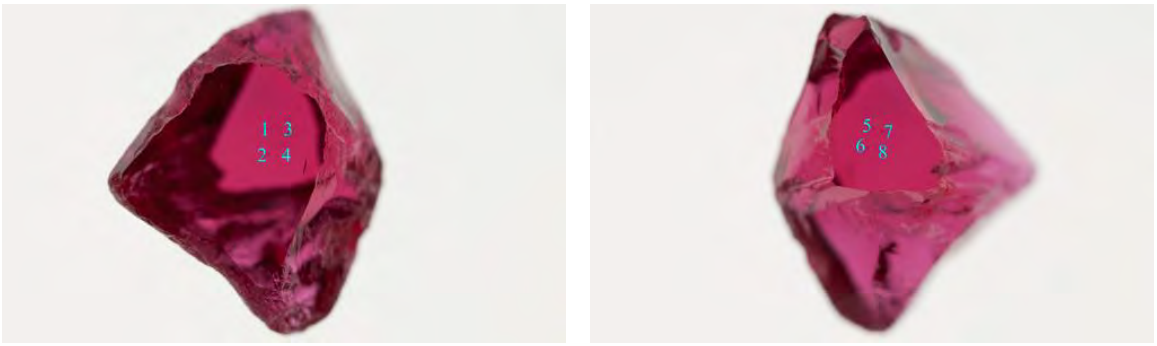

Figure 41: Two views of GIA reference sample 100305163945 (B2 type; see Annex C for a description of the classification system), seen after fabrication showing the positions of the eight LA-ICP-MS spots. Photos (color calibrated): Sasithorn Engniwat © GIA

The area analyzed appeared brownish red and free of any visible inclusions. Looking at the results summarized in Table 6, the first feature of note is the high iron (Fe) content present in this sample (consistent with all the other samples collected and examined by us from "Torro") when compared to other samples from the "Central", "Glass" or "Maninge Nice" areas. Magnesium, titanium, vanadium, gallium contents were consistent with samples analyzed from the other ruby producing areas near Montepuez. Such high quantities of iron explain the weak red fluorescence observed under long-wave ultraviolet light.

Table 6: LA-ICP-MS results for GIA reference sample 100305163945. "Bdl" stands for "Below Detection Limit".

Specimen **100305163945** Spot number (color of the spot area)	**Concentration (PPMA)**						
	Be	**Mg**	**Ti**	**V**	**Cr**	**Fe**	**Ga**
Spot 1 (Red)	bdl	118.2	18.8	3.9	760.7	1391.1	9.1
Spot 2 (Red)	bdl	148.4	26.7	4.3	784.3	1423.9	8.8
Spot 3 (Red)	bdl	119.1	21.2	3.8	843.1	1391.1	8.8
Spot 4 (Red)	bdl	116.6	23.1	4.0	874.5	1358.2	9.2
Spot 5 (Red)	bdl	152.6	21.2	3.8	858.8	1402.0	9.7
Spot 6 (Red)	bdl	153.5	21.0	3.9	1031.3	1402.0	9.5
Spot 7 (Red)	bdl	170.2	20.6	4.4	1043.1	1413.0	9.4
Spot 8 (Red)	bdl	184.5	27.7	4.2	1062.7	1453.1	9.2
Detection Limits	0.1	0.1	2.2	0.2	0.4	1.2	0.1

It is interesting to discuss the chemistry in relation to the FTIR spectrum data collected. As we wrote previously, absorption centered around 3160 cm^{-1} in is commonly seen in some unheated corundum (metamorphic type blue sapphires, rubies from Winza or north east Madagascar) when the beam passes through an area where, as in this case, Mg is present in higher quantities than Ti. Out of 39 samples from the Montepuez area studied with FTIR: 5 of the A type, 4 of the B type and 30 of the E and F types (see Annex C for a description of GIA cataloguing classification) seven samples (including 3 of the B type samples from Torro) exhibited a magnesium content significantly greater than the titanium content detected, but sample 100305163945 was the only one where the 3160 cm^{-1} feature was observed. This indicates that such an FTIR absorption feature in rubies is not simply associated with a higher Mg content when compared to the Ti levels present. That interesting observation and the chemistry of that interesting sample are being further investigated.

DISCUSSIONS:

In order to check whether the data collected makes sense it is always useful to compare a color calibrated photo of the samples studied (obtained using Logan Electric Tru-View 810 Color Corrected Light Box with 5000K lamp used as transmitted light) with color circles obtained via calculation using also 5000k as light temperature for our calculation.

We used two different methods to analyze the chemical data collected and the UV-Vis spectra recorded. In the first method we produced a color circle based on the results of the chromium content obtained and the depth of the sample and then based on the spectra collected used the method developed by E. Dubinsky and J.L. Emmett (Dubinsky and Emmett 2013) to compare the results.

In all three cases the color obtained from the calculations were found to be very similar to those seen in the calibrated images which means that the data collected is reliable.

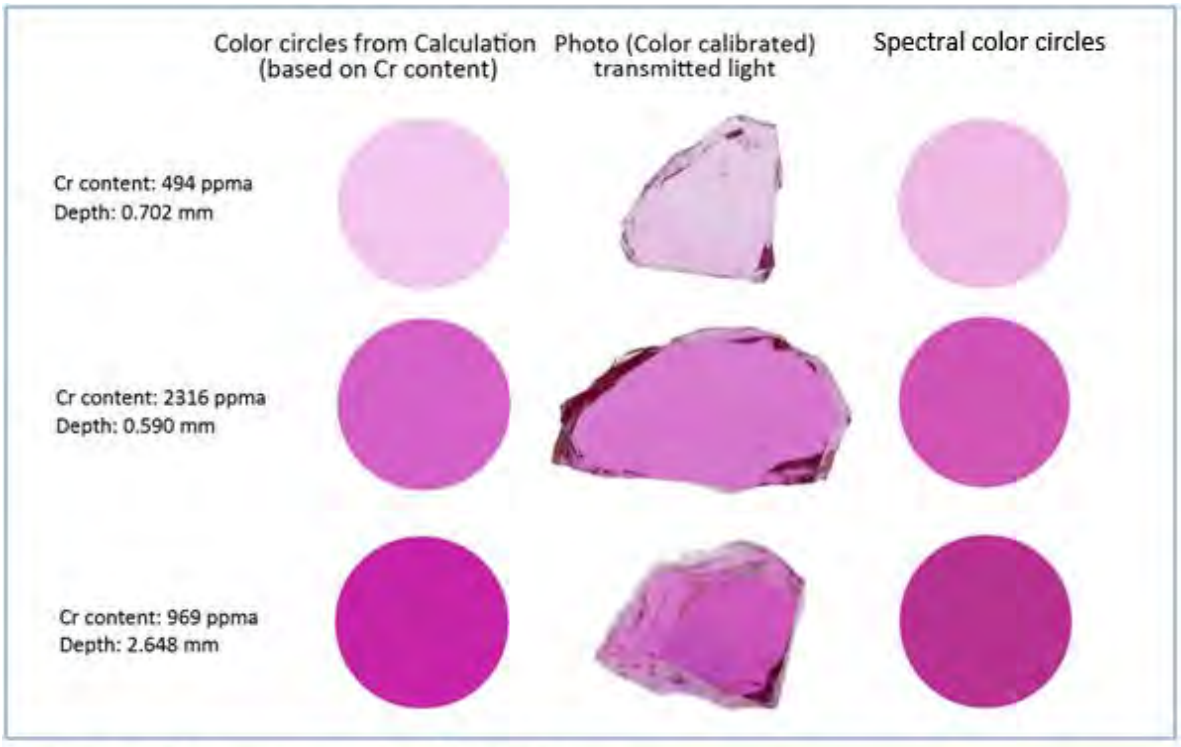

Note: The light temperature used was 5,000K in all cases.

TRACE ELEMENT VARIATIONS AMONGST THE DIFFERENT MINING SITES IN THE MONTEPUEZ AREA AND A COMPARISON WITH OTHER RUBY DEPOSITS (MARBLE, BASALT AND AMPHIBOLE RELATED):

Besides the 4 reference stones already discussed the chemistry of 127 other stones from the Montepuez area were also studied. Some of them were collected on site at the mines (A1, A2 and B2 types, see Annex C for a description of GIA cataloguing classification) whilst others were collected from gem merchants in Mozambique (E type) or in Thailand (F type).

The results were compared to those obtained from other GIA reference samples:

- Rubies from similar amphibole related deposits like M'sawize (Niassa Province, Mozambique), Winza (Tanzania), Didy (Madagascar)
- Well known marble type ruby deposits. We used rubies from the Mogok area in Myanmar (Burma) for this comparison.
- Well known basalt related ruby deposits. We used rubies from the Pailin ruby and sapphire mining area in Cambodia for this comparison.

In order to separate the rubies from the different Montepuez areas with each other and with rubies from other deposits, it is often interesting to study the relative content of trace elements present in rubies from the different deposits studied.

When studying rubies with LA-ICP-MS a very limited number of trace elements are usually found. These trace elements are usually: Magnesium (Mg), Titanium (Ti), Vanadium (V), Chromium (Cr), Iron (Fe) and Gallium (Ga). Most of the other elements are often present in such small quantities that they are under the detection limit of the instrument, or their detection is hindered by interference effects caused by other elements. After looking at all the population fields diagrams comparing trace elements, it was found that the diagram comparing vanadium (V) and iron (Fe) was the most interesting to separate these rubies.
In the following diagrams the differently colors triangles represent the results relating to samples collected in the field at the mines (A or B type). The tiny dots represent data from stones collected from traders in Mozambique or Thailand, and finally the squares represent data collected from other amphibole related rubies, while the circles represent data from marble or basalt related deposits:

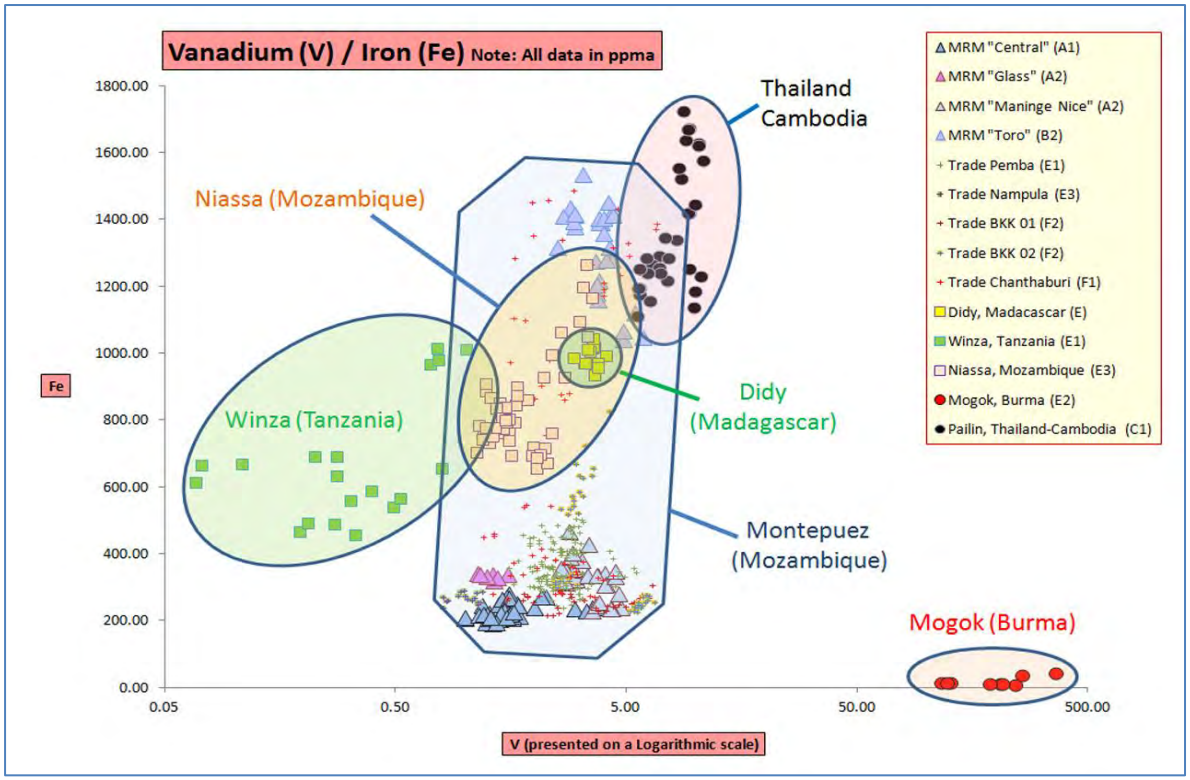

Figure 42: Population field comparing the iron (Fe) and vanadium (V) content (in ppma) in rubies from Montepuez and other known amphibole type ruby producing areas. We added also some Thai Cambodian (basalt type) and Burmese rubies (Marble type) to add some comparison elements: Marble type rubies from Mogok (Burma) are easy to separate using this diagram with amphibole related rubies from East Africa (Winza, Montepuez, Niassa and Didy). However, separating rubies from Thailand/ Cambodia from those of Torro or Nacaca origin using these criteria are not so straightforward using this method.

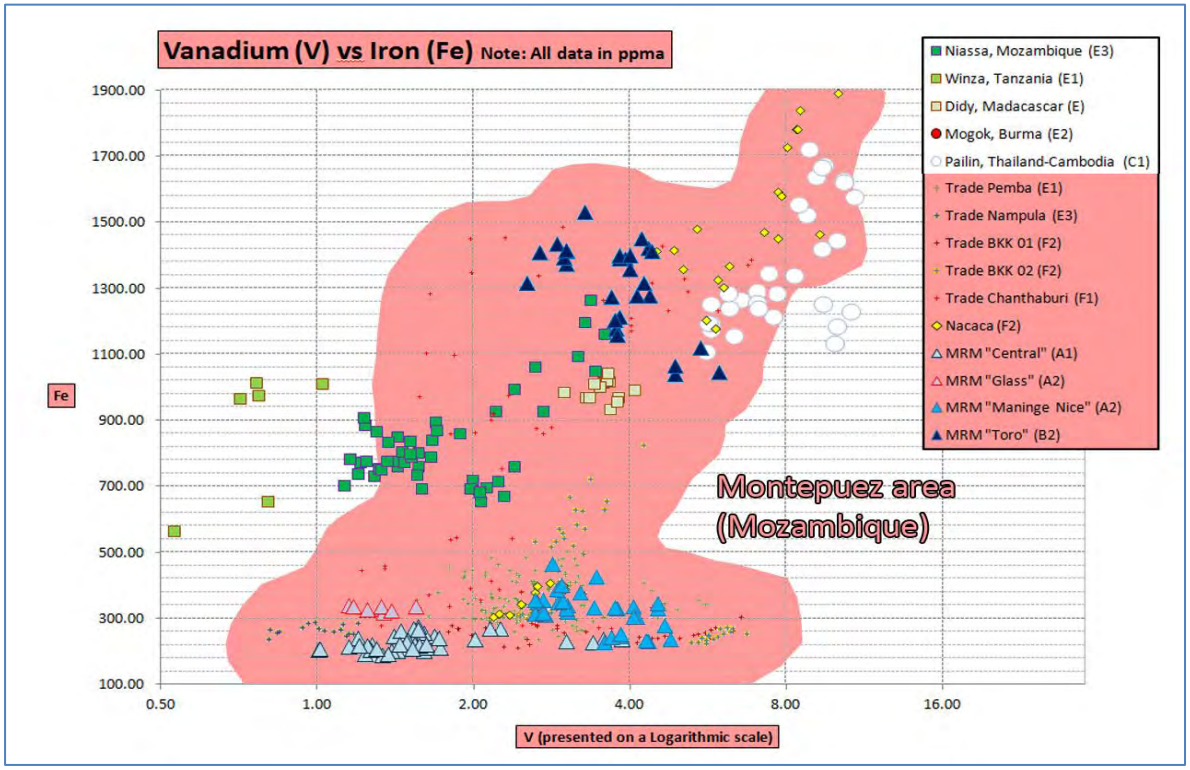

Figure 43: Details of the trace element population field regarding iron and vanadium (in ppma) for Montepuez rubies (orange area) compared to figure 42 we also added the rubies reportedly from the new deposit at Nacaca (small yellow dots). It is interesting to see that there are mainly two types of material in Montepuez: A large population with relatively low iron content (between 180 to 500 ppma of iron) mainly consisting of stones from the "Central", "Maninge Nice", "Glass", and some from the "Nacaca" area, and another population with an iron content typically higher (between 1000 to 2000 ppma of Fe) mainly populated by stones from Torro and Nacaca with an iron content quite similar to that found in Thai/Cambodian rubies.

The first positive fact to note about the results is that the stones collected from traders in Mozambique and Thailand that were claimed to be of Montepuez origin (visible as small dots in the diagrams) are a very close match to those we collected in the field from Montepuez (visible as triangles in the diagram).

It is also apparent that rubies from the Montepuez (and more generally the "non-classic" metamorphic rubies from amphibole related deposits in East Africa and Madagascar) can be characterized by the following features:

1) A moderate to high iron content when compared to the well-known rubies mostly coming from either marble type deposits (such as those from Myanmar (Burma) or basalt related deposits (such as those from the deposits located along the Thai Cambodian border near Chanthaburi and Pailin) that dominated the ruby trade for centuries (see Figure 42).

   The iron content of the Montepuez rubies was found to be similar to that of rubies mined from other amphibole related deposits like Niassa (Mozambique), Winza (Tanzania) and Didy (Madagascar), see Figure 42.

   A point of interest observed while studying the details of the production from Montepuez was that most of the iron rich stones originated from the "Torro" area, while the other mining sites ("Central", "Glass" and "Maninge Nice") appeared to produce stones with significantly lower an iron content than that commonly detected in other amphibole related deposits (see Figure 42). This is not a bad characteristic as the best stones from amphibole related deposits typically combine high chromium and minimal iron content. Since too much iron darkens rubies and lower iron content results in stronger fluorescence it is more desirable to have a low iron content.

2) The vanadium content of these rubies is typically lower than that found in marble type rubies from Burmese deposits (Mogok, Mong Hsu). However, Montepuez rubies usually contained higher vanadium content compared to the amphibole type rubies from Winza (Tanzania). Finally the results of the analysis showed that the vanadium content of rubies from Didy in Madagascar or M'sawize in Mozambique is similar to that found in Montepuez stones (see Figure 42).

THE INTERNAL WORLD OF RUBIES FROM MONTEPUEZ:

A microscopic study of the internal features seen in 131 GIA reference specimens of different types was performed in the GIA Laboratory Bangkok. The types consisted of stones collected on site in the field, others from traders in Mozambique and finally others from traders in Thailand.

The most frequently encountered mineral inclusions observed were amphibole, mica and chalcopyrite crystals associated with needles, platelets, tubes and bands/planes of minute particles. This is interesting because rubies from the neighboring M'sawize deposit, another amphibole related ruby deposit located in the Niassa province of Mozambique, rarely exhibit mineral inclusions while healed fissures associated with needles, platelets and tubes are more commonly encountered.

The amphibole crystals observed in Montepuez rubies are usually found as transparent, slightly rounded crystals (Figure 48), lacking the sharp and euhedral form of those found in rubies from Winza (Pardieu 2009). When seen under dark field illumination these rounded amphibole crystals commonly appear colorless (Figure 44) and could be mistaken for calcite inclusions in marble type rubies like those from Mogok in Myanmar (Burma), but a careful examination under brightfield conditions will reveal that these crystals are in fact greenish or gray blue (Figure 45, Figure 50 and Figure 51). In some rare cases, the amphibole crystals will appear as well formed rods (Figure 58, Figure 59 and Figure 60) quite similar in appearance to the amphibole inclusions found in some emeralds. In Montepuez rubies amphibole crystals sometimes host mineral inclusions themselves (Figure 52, Figure 53, Figure 54 and Figure 55) or cleavage planes (Figure 59).

The mica crystals inclusions found in Montepuez rubies are often very interesting. They very commonly appear as hexagonal whitish, semi-transparent or translucent, tabular crystals often associated with frosty looking fissures (Figure 63, Figure 64, Figure 65, Figure 66, Figure 67, Figure 71, Figure 72 and Figure 74) or in some cases with healed fissures (Figure 70, Figure 71) that may resemble features sometimes observed in some heated stones. These confusing features were found in many A or B type samples collected in the field that were clearly unheated. Some samples also exhibited more classic mica inclusions of a more transparent light brown foliated appearance. These were identified as margarite by Raman (Figure 75, Figure 76 and Figure 77).

Chalcopyrite crystals were also frequently encountered in Mozambique rubies. The, opaque, euhedral crystals usually appear highly lustrous (Figure 104, Figure 105, Figure 106, Figure 107, Figure 108 and Figure 109). These crystals are of particular interest to the traders and burners because they turn into really obvious and unattractive black spots with a black opaque glassy melted core surrounded by a large mostly black discoid after heat treatment.

Negative crystals are present as planes or former healed fissures (Figure 81, Figure 82, Figure 83 and Figure 84). In some cases they also form delicate "rosette" like circular structures (Figure 78). Unlike negative crystals from other corundum locations they never appear to host any gas bubbles or black graphite crystals.

Besides crystal inclusions most rubies also host many exsolved needles, platelets and/or particles. Several types of needles are usually found together in Montepuez rubies. First thin short or long needles intersecting at 60 degrees to one another believed to be rutile needles (Figure 87, Figure 91, Figure 94, Figure 99 and Figure 100) were often encountered. Then other needles, often looking more like platelets, sometimes with a regular outline but more often with a very irregular outline (Figure 87, Figure 88, Figure 99) that we believe to be iron rich exsolutions (possibly hematite, ilmenite or magnetite) were observed. The particles inclusions varied from minute to larger ones often appearing within whitish appearing lines, planes or bands (Figure 88, Figure 89,

Figure 90, Figure 93, Figure 95 and Figure 98). Besides the needles and particles tubes (Figure 101, Figure 102) were also encountered. These were sometimes associated with intersecting twinning planes and were also another common inclusion within these rubies.

The following photo album of 69 high-resolution photos will provide a general overview of the types of inclusions encountered in Montepuez rubies:

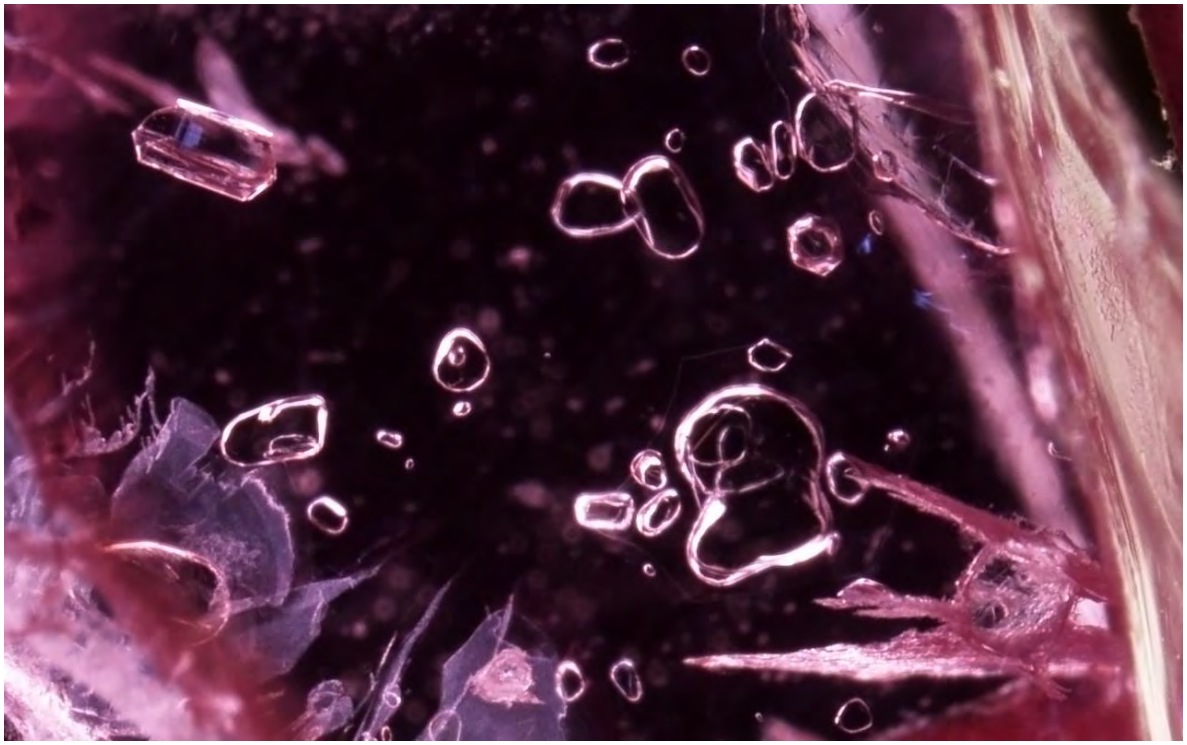

Figure 44: A group of mixed crystals in GIA reference sample number 100305163938 from the “Central” area, collected on site (A type) in September 2012, showing the variety of the crystals found in Montepuez rubies. Translucent, hexagonal crystals (probably mica) associated with frosty looking fringes (lower right hand corner), and many transparent, mostly rounded, colorless crystals (probably amphibole) are visible.. Darkfield + fiber optic illumination, magnified 40x. Photo: Jonathan Muyal © GIA.

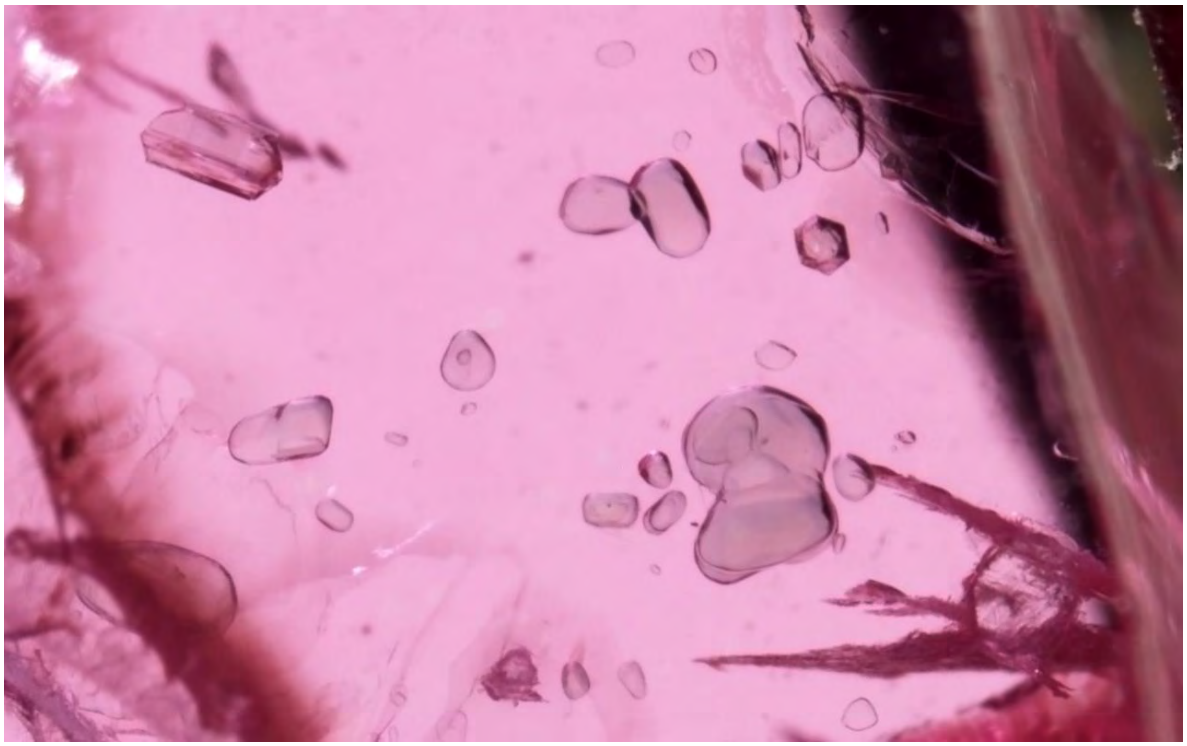

Figure 45: The same group of mixed crystal inclusions seen in the previous photo in diffused lighting conditions. It is now obvious that the larger crystals are not colorless but in fact greenish. This does not confirm that these crystals are amphibole, but it is a good indicator of their probable amphibole nature. Confirmation came using Raman and the RRuff database as a reference. The hexagonal crystal associated with frosted looking features on the lower right was identified as mica by Raman using the RRuff database as a reference. GIA reference sample number 100305163938 from the “Central” area. Diffused + fiber optic illumination, magnified 40x. Photo: Jonathan Muyal © GIA.

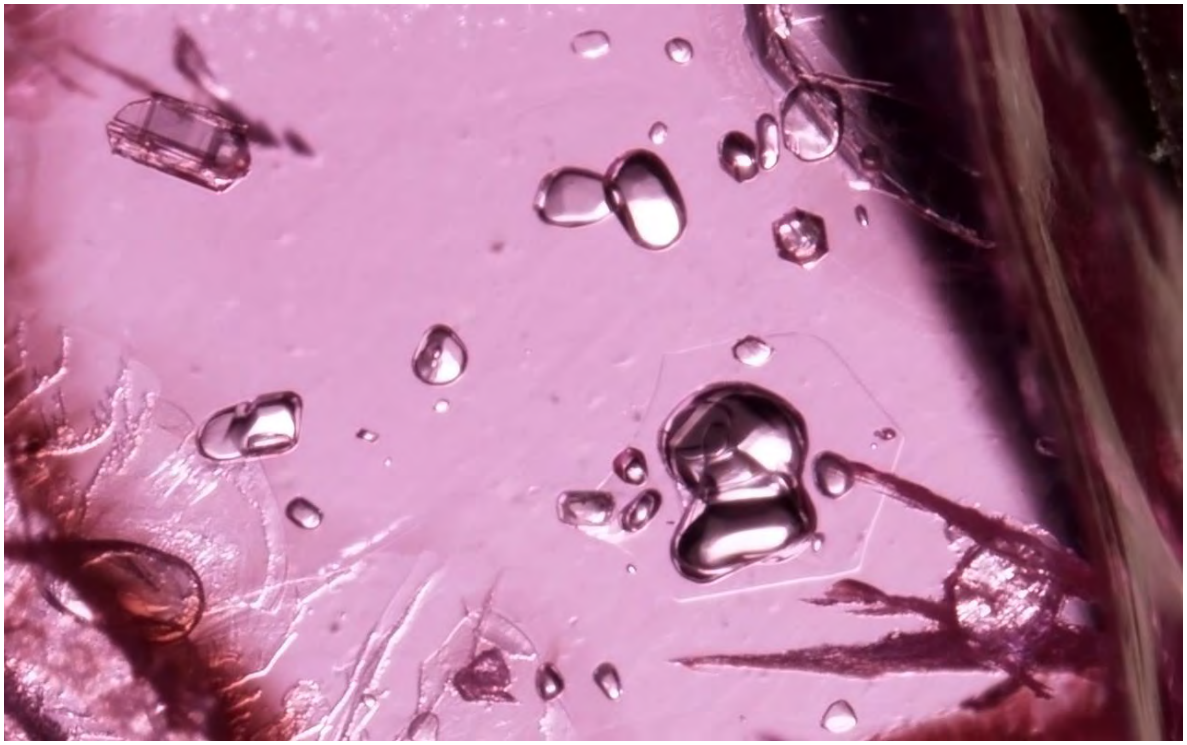

Figure 46: In this third photo of the same group of crystals, the importance of using different types of lighting environments while working with a microscope is clearly illustrated. Using transmitted light, the crystals still look transparent however several interesting growth features associated with the crystal inclusions now become more apparent. GIA reference sample number 100305163938 from the "Central" area. Brightfield + fiber optic illumination, magnified 40x. Photo: Jonathan Muyal © GIA.

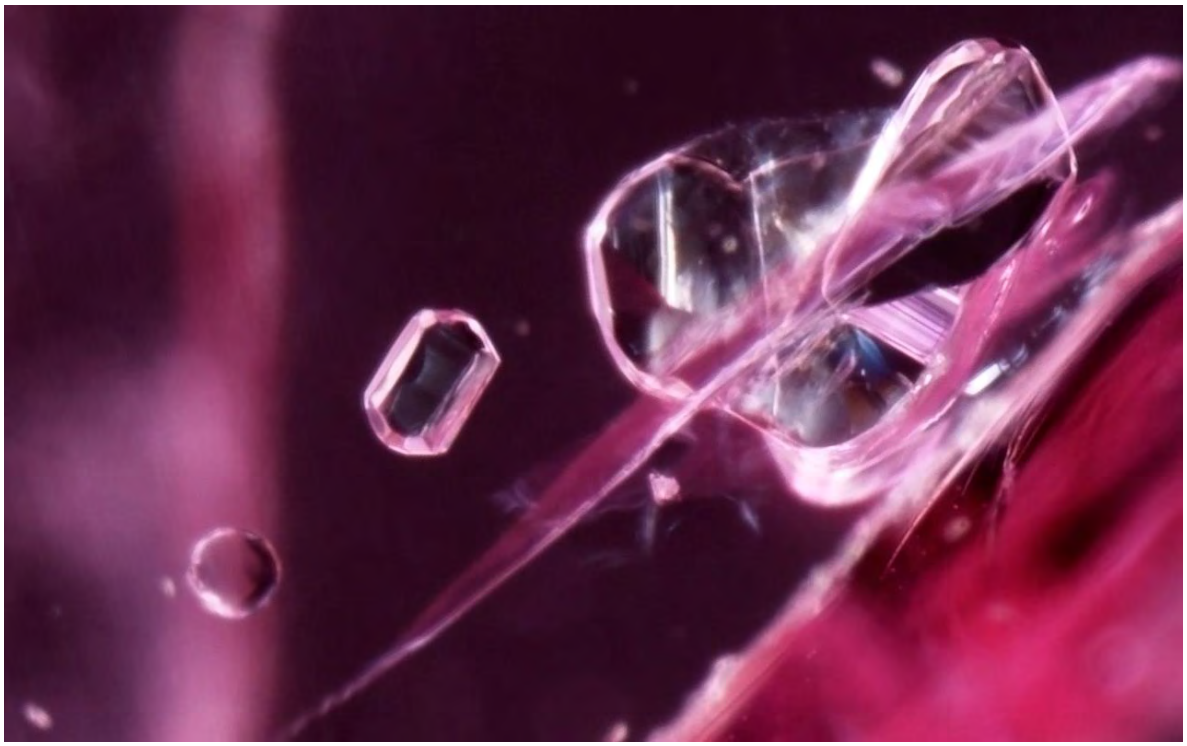

Figure 47: A group of transparent colorless euhedral and rounded crystals (identified by Raman as amphibole using the RRuff database as a reference) in GIA reference sample number 100305163941 from the "Central" area collected on site (A type) in September 2012. Whilst fine euhedral amphibole crystals are rare in Montepuez rubies, they can be found from time to time as this sample proves. Darkfield + fiber optic illumination, magnified 90x. Photo: Jonathan Muyal © GIA.

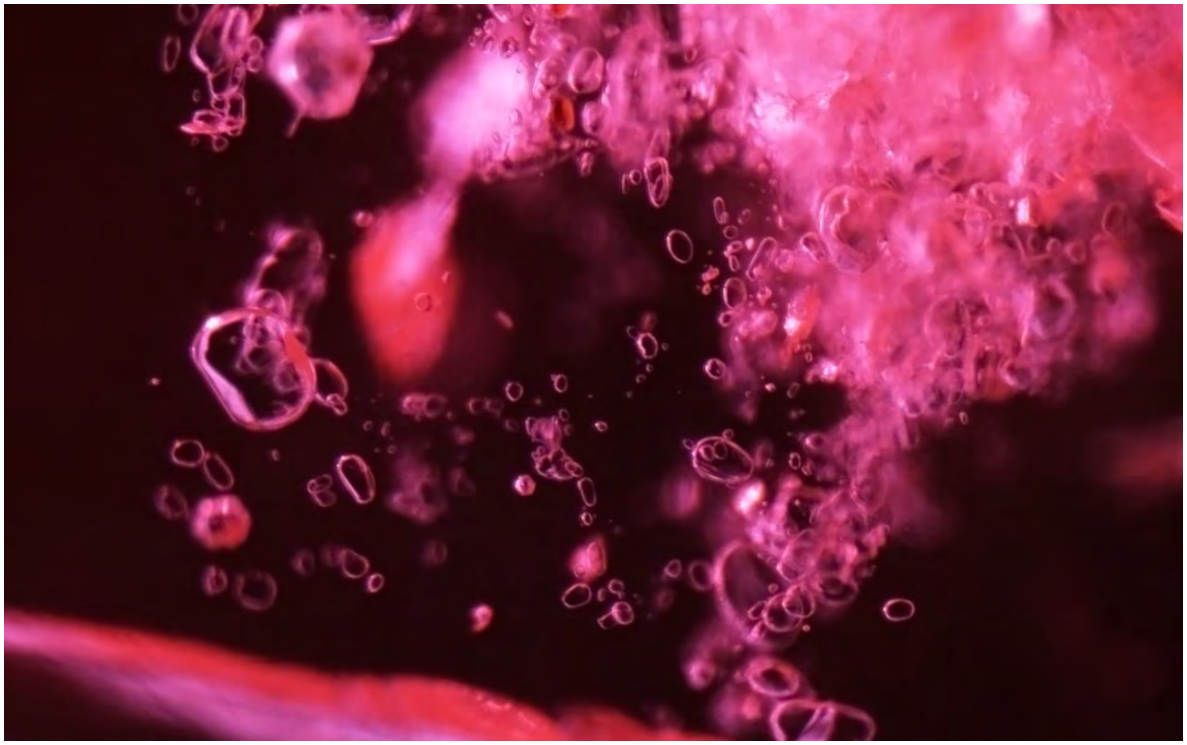

Figure 48: A “galaxy” of small, more or less rounded , transparent crystals reminiscent of calcite crystals seen in marble type rubies. Nevertheless these crystals were identified by Raman (using the RRuff database as a reference) as amphibole. GIA reference sample number 100305163835 from a “Bo Nam” parcel (F type sample) acquired in January 2013 in Thailand. Darkfield + fiber optic illumination, magnified 90x. Photo: Jonathan Muyal © GIA.

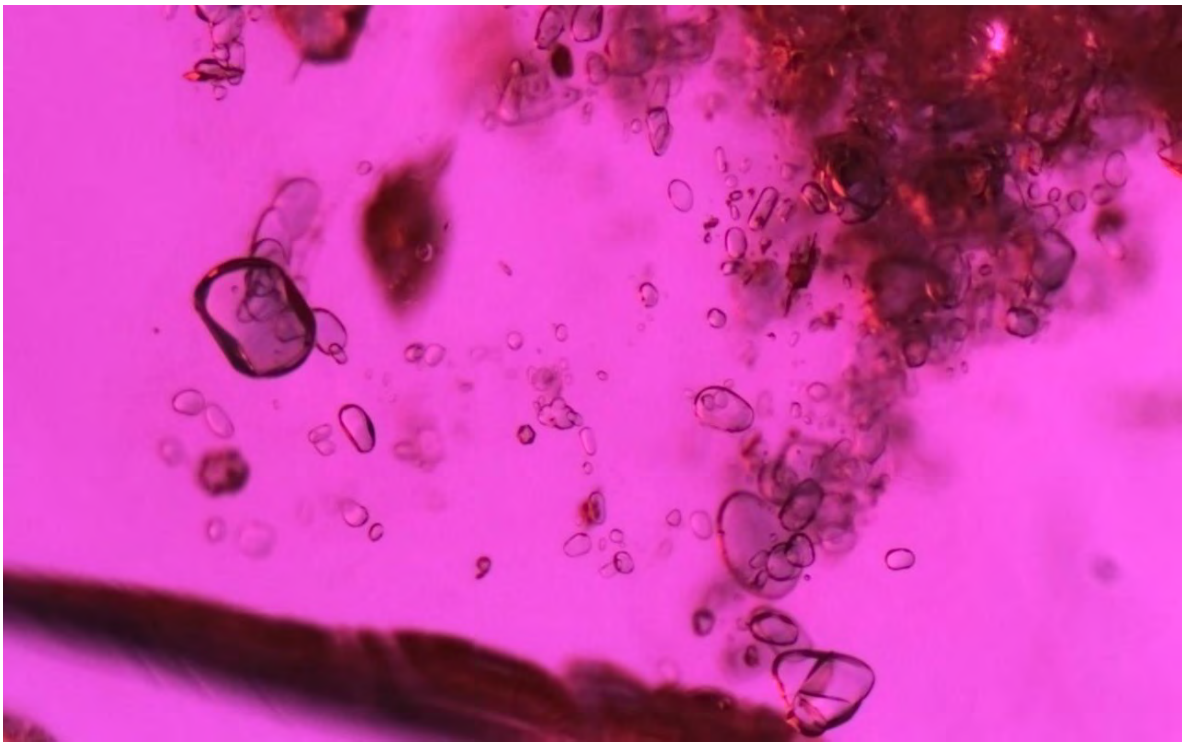

Figure 49: The same group of transparent crystals seen in the previous photo, but this time seen via diffused lighting. Such a technique enables the observer to see that the large crystals are not colorless as would be expected for calcite, but rather more greenish, indicating that they are more likely amphibole crystals. GIA reference sample number 100305163835 from a “Bo Nam” parcel (F type sample) acquired in January 2013 in Thailand. Diffused + fiber optic illumination, magnified 90x. Photo: Jonathan Muyal © GIA.

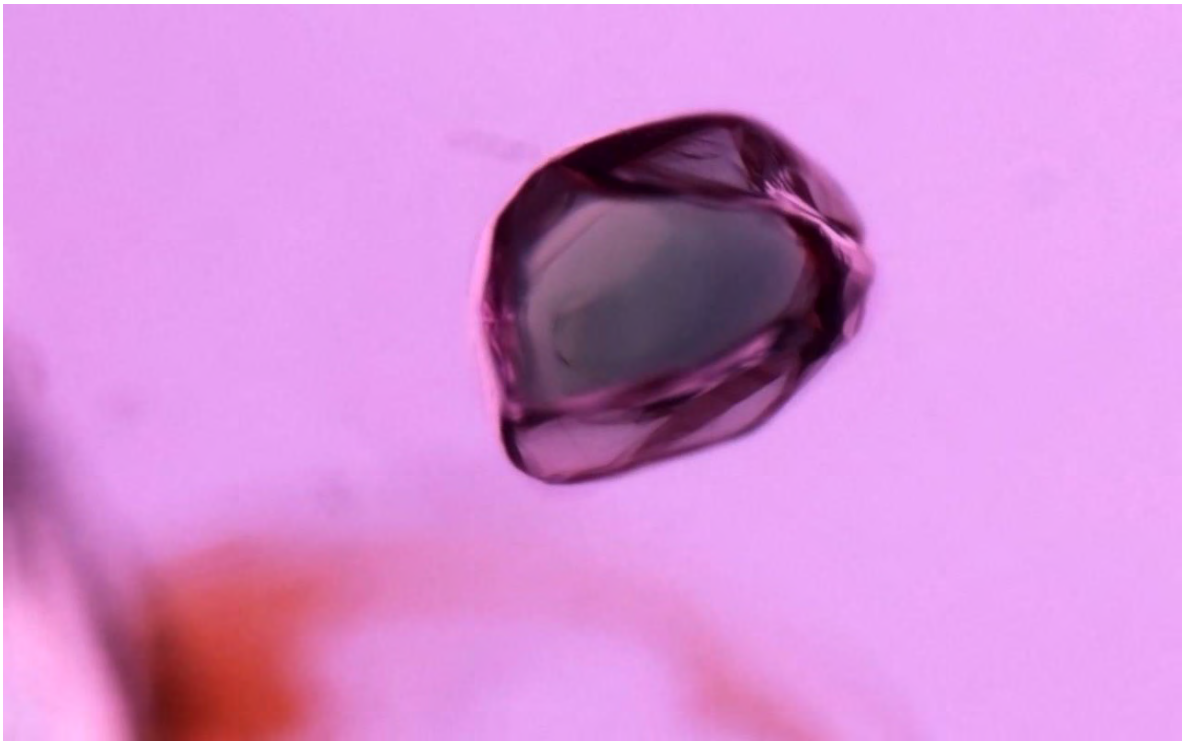

Figure 50: A euhedral greenish amphibole crystal (identified by Raman using the RRuff database as a reference) seen in GIA reference sample number 100305162444 from a parcel bought in Nampula (E type sample), Mozambique in 2009. Diffused illumination, magnified 80x. Photo: Jonathan Muyal © GIA.

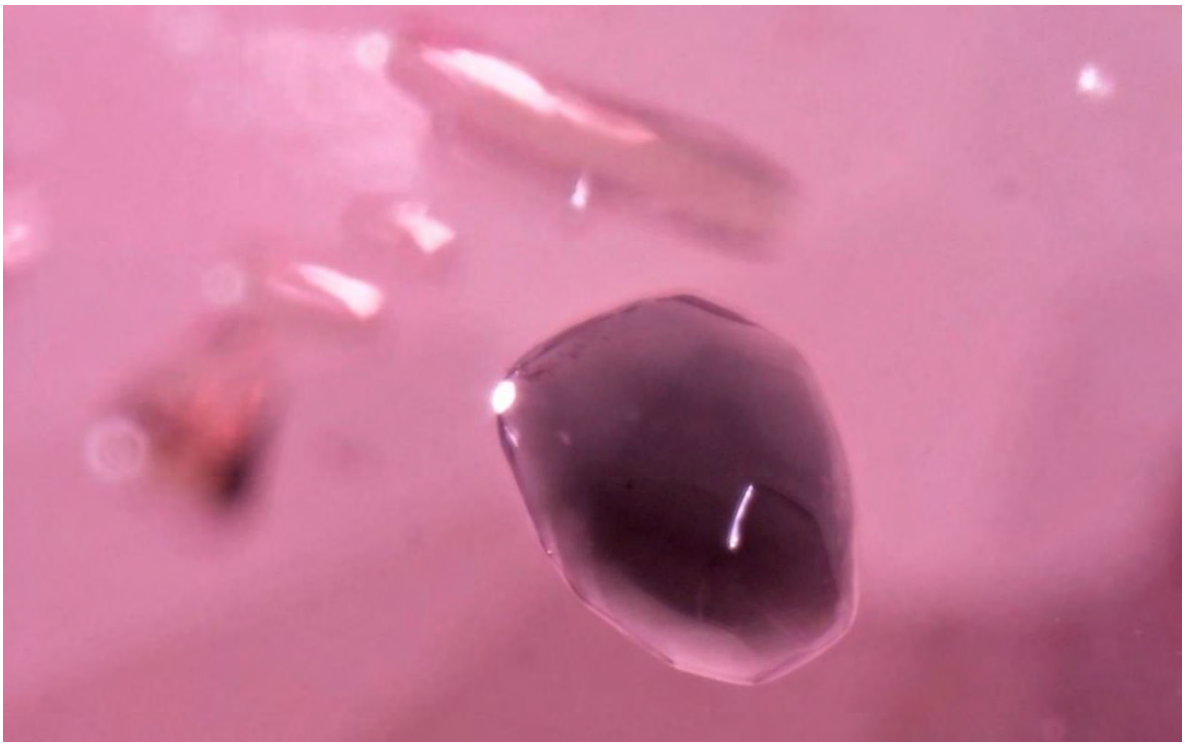

Figure 51: A greenish transparent crystal (identified by Raman as amphibole using the RRuff database as a reference) in GIA reference sample 100305164548, an F type sample bought in Chanthaburi, Thailand in January 2013. Diffused + fiber optic illumination, magnified 80x. Photo: Jonathan Muyal © GIA.

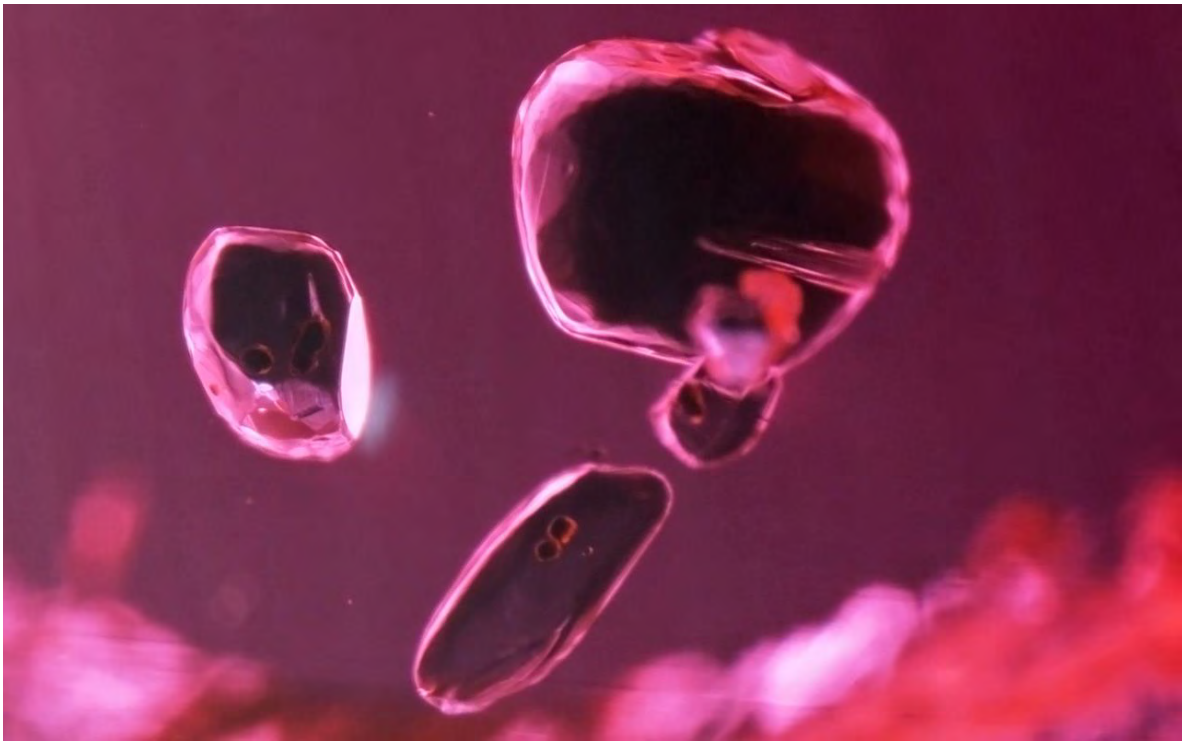

Figure 52: A group of dark green transparent crystals (probably amphibole) within which several mineral inclusions are visible. GIA reference sample number 100305163834, an F type sample obtained in Thailand in January 2013 in a parcel of "Bo Daeng" rough . Darkfield + fiber optic illumination, magnified 60x. Photo: Jonathan Muyal © GIA.

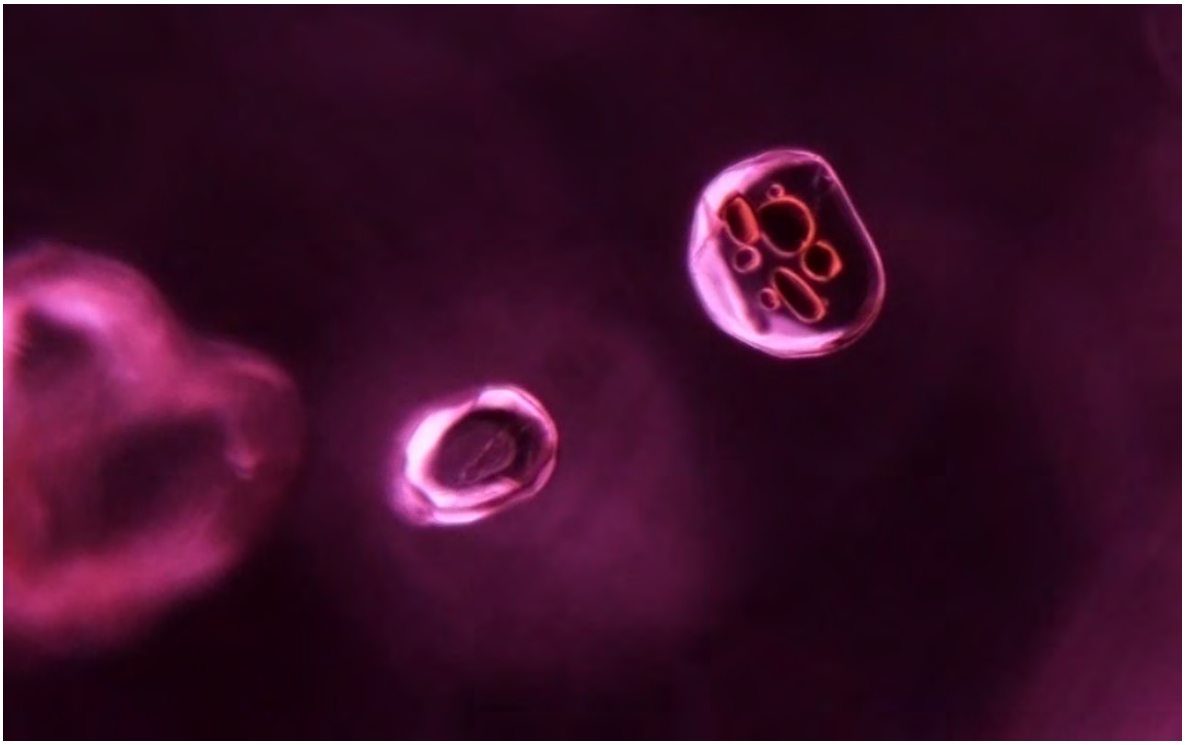

Figure 53: A group of transparent crystals (probably amphibole) within which several dark rounded mineral inclusions are cleary evident.GIA reference sample number 100305163855, an F type sample obtained in Thailand in January 2013 in a parcel of "Bo Nam" rough. Darkfield illumination, magnified 140x. Photo: Jonathan Muyal © GIA.

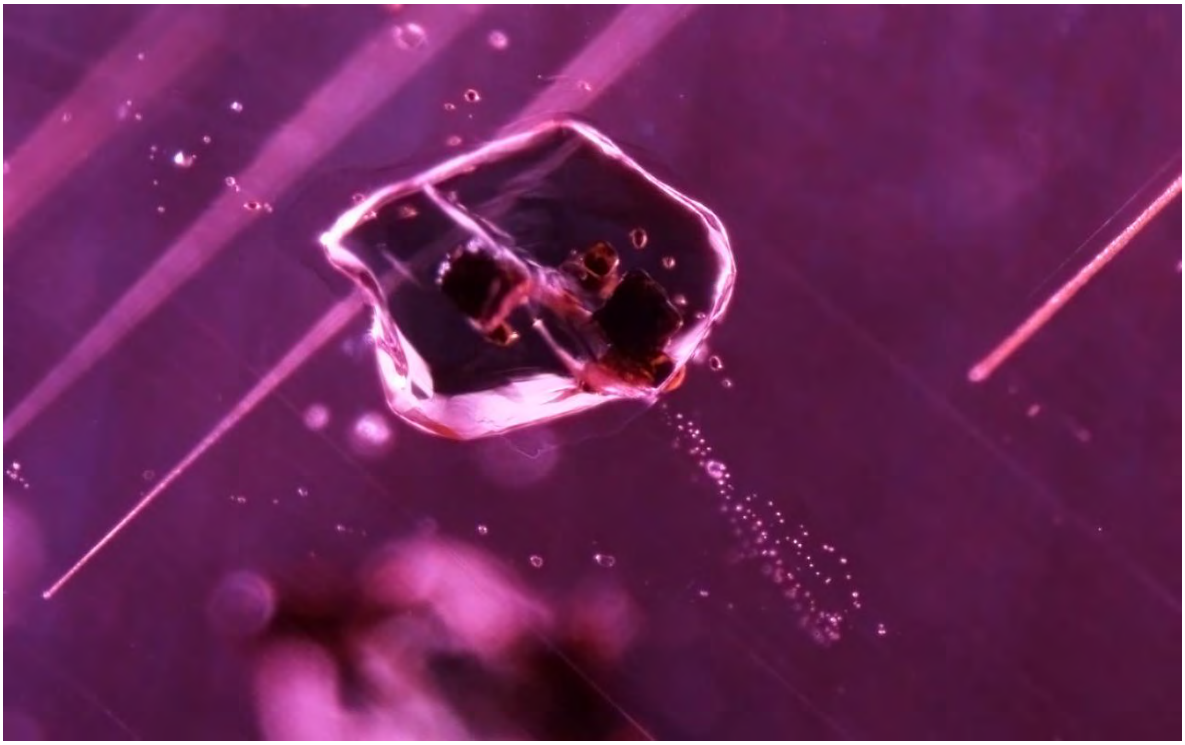

Figure 54: A dark transparent crystal (probably amphibole) hosting several orangy mineral inclusions in GIA reference sample number 100305163854, an F type sample obtained in Thailand in January 2013 in a parcel of “Bo Nam” rough. Darkfield + fiber optic illumination, magnified 60x. Photo: Jonathan Muyal © GIA.

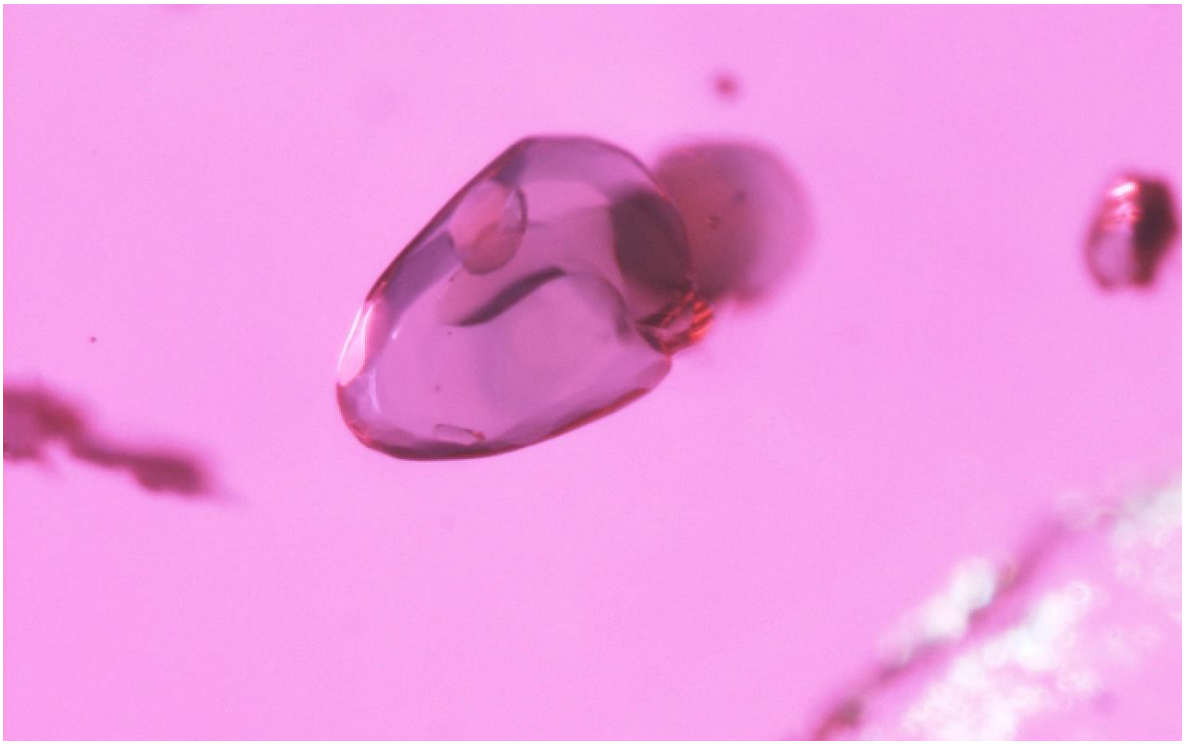

Figure 55: A rounded transparent doubly refractive crystal inclusion (probably amphibole) within which orange transparent mineral inclusions are visible.GIA reference sample number 100305163839, an F type sample obtained in Thailand in January 2013 in a parcel of “Bo Daeng” rough. Diffused + fiber optic illumination, magnified 90x. Photo: Jonathan Muyal © GIA.

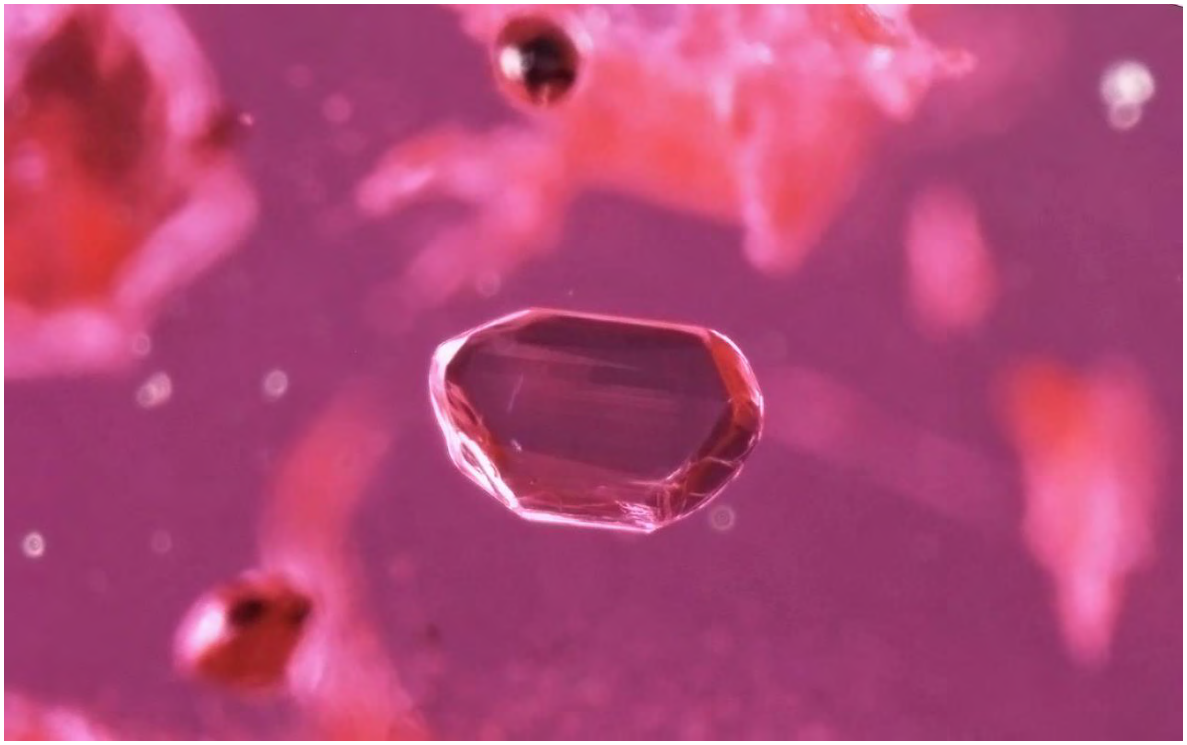

Figure 56: Euhedral transparent crystal (probably amphibole) seen in GIA reference sample number 100305163864, an F type sample obtained in Thailand in January 2013 in a parcel of “Bo Nam” rough. Darkfield + fiber optic illumination, magnified 60x. Photo: Jonathan Muyal © GIA.

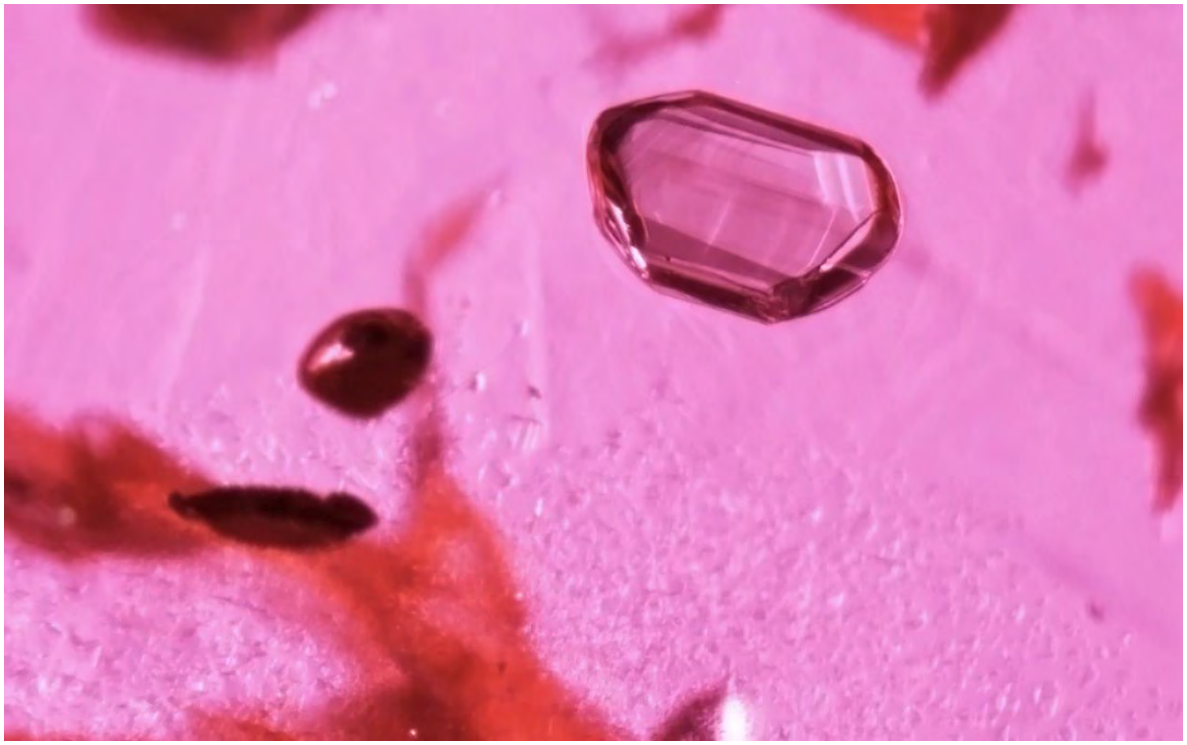

Figure 57: Euhedral transparent crystal (probably amphibole) with a likely opaque chalcopyrite crystal to the left seen in GIA reference sample number 100305163864, an F type sample obtained in Thailand in January 2013 in a parcel of “Bo Nam” rough. Transmitted + fiber optic illumination, magnified 60x. Photo: Jonathan Muyal © GIA.

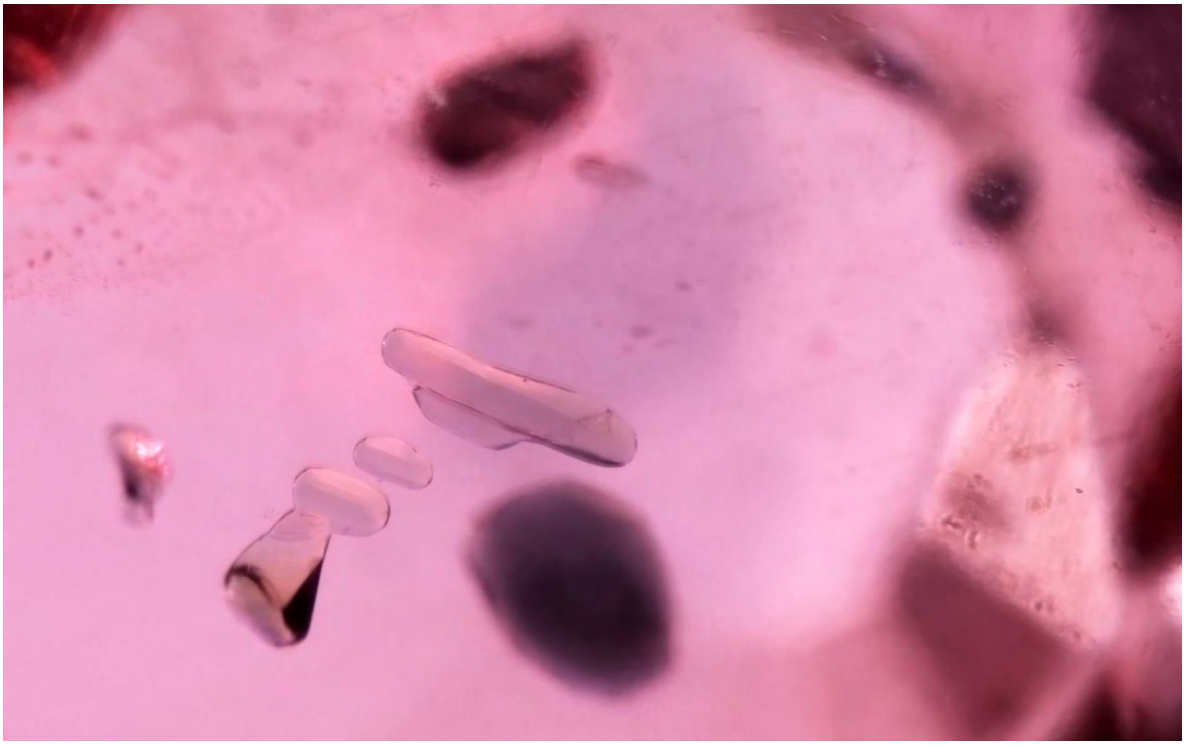

Figure 58: A group of “elongated” transparent crystals (probably amphibole) associated with broad orientated particles in GIA reference sample number 100305164548, an F type sample obtained in Thailand in January 2013 in a parcel of “Bo Nam” rough. Diffused + fiber optic illumination, magnified 50x. Photo: Jonathan Muyal © GIA.

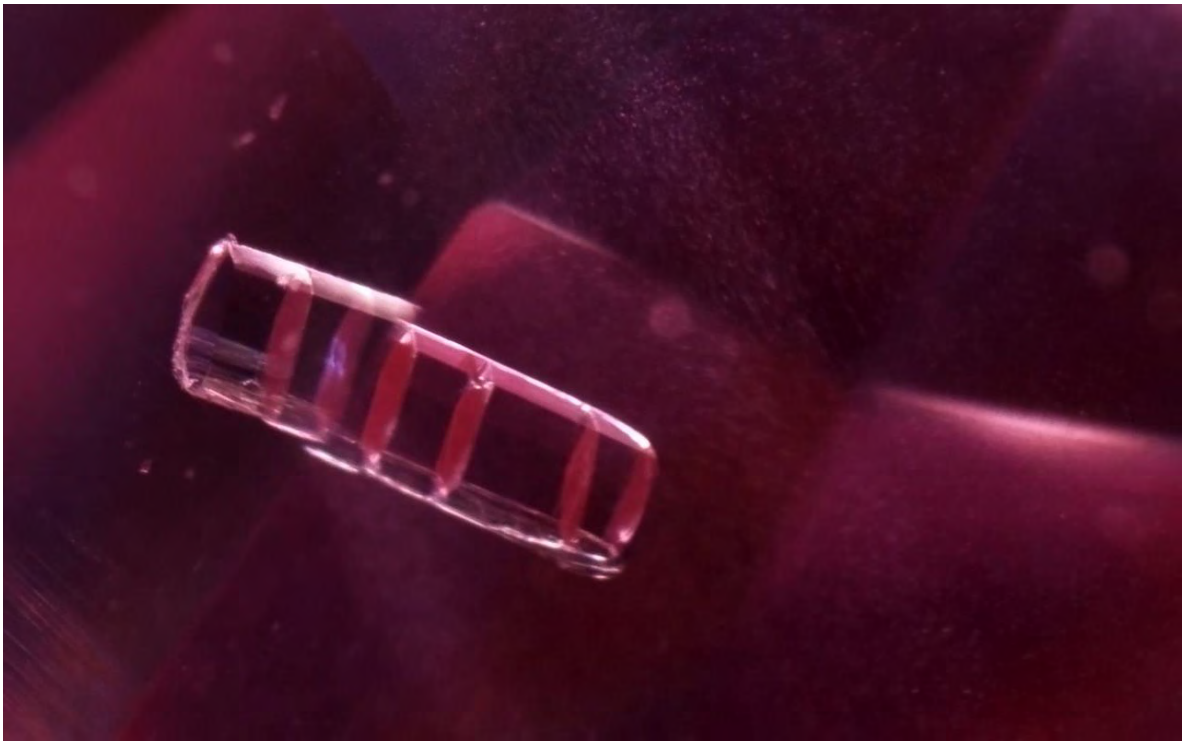

Figure 59: A single, transparent, crystal (identified by Raman as amphibole using the RRuff database as reference) exhibiting several cleavage planes in GIA reference sample number 100305164534, an F type sample obtained in Chanthaburi, Thailand in January 2013. Darkfield + fiber optic illumination, magnified 50x. Photo: Jonathan Muyal © GIA.

Figure 60: A group of long transparent acicular looking crystals (identified by Raman as amphibole using the RRuff database as a reference) associated with bands of minute particles seen in GIA reference sample number 100305164551, an F type sample obtained in Chanthaburi, Thailand in January 2013. Darkfield + fiber optic illumination, magnified 50x. Photo: Jonathan Muyal © GIA.

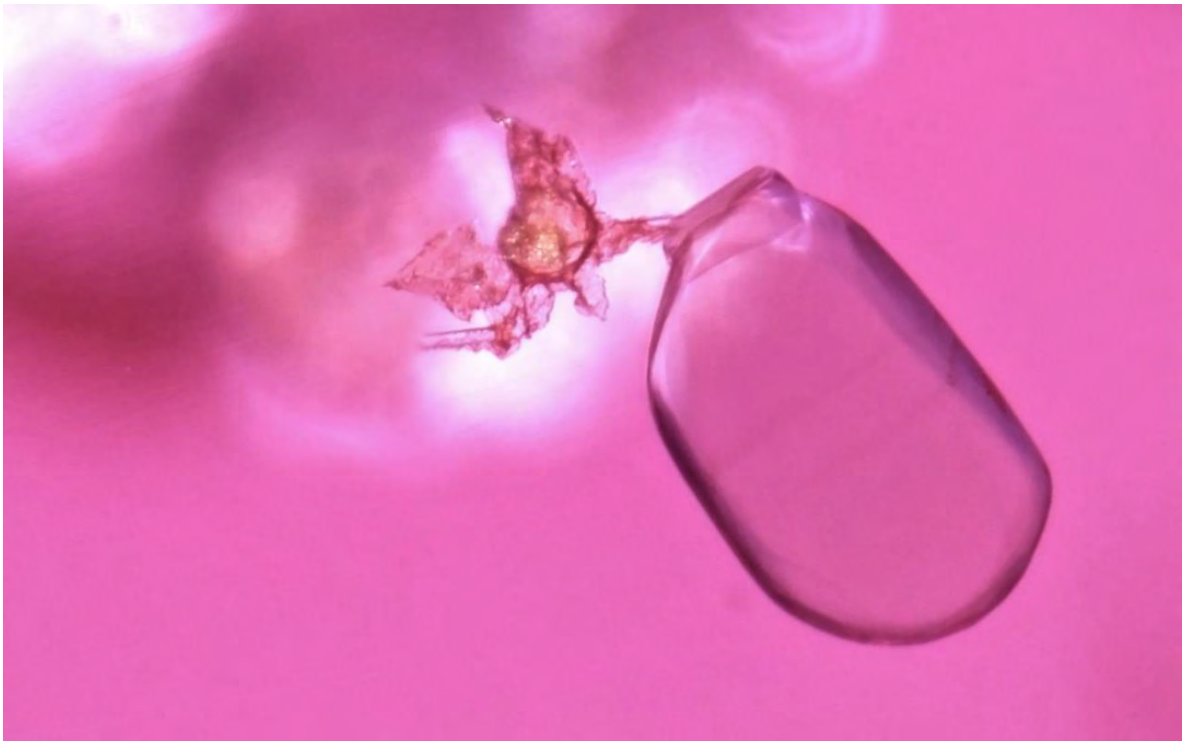

Figure 61: A transparent rounded transparent crystal (identified by Raman as amphibole using the RRuff database as a reference) associated with a smaller hexagonal crystal (identified by Raman as mica using the RRuff database as a reference) which itself is associated with frosty fringes in GIA reference sample number 100305163842, an F type sample obtained in Thailand in January 2013 in a parcel of "Bo Nam" rough. Darkfield + fiber optic illumination, magnified 112.5x. Photo: Jonathan Muyal © GIA.

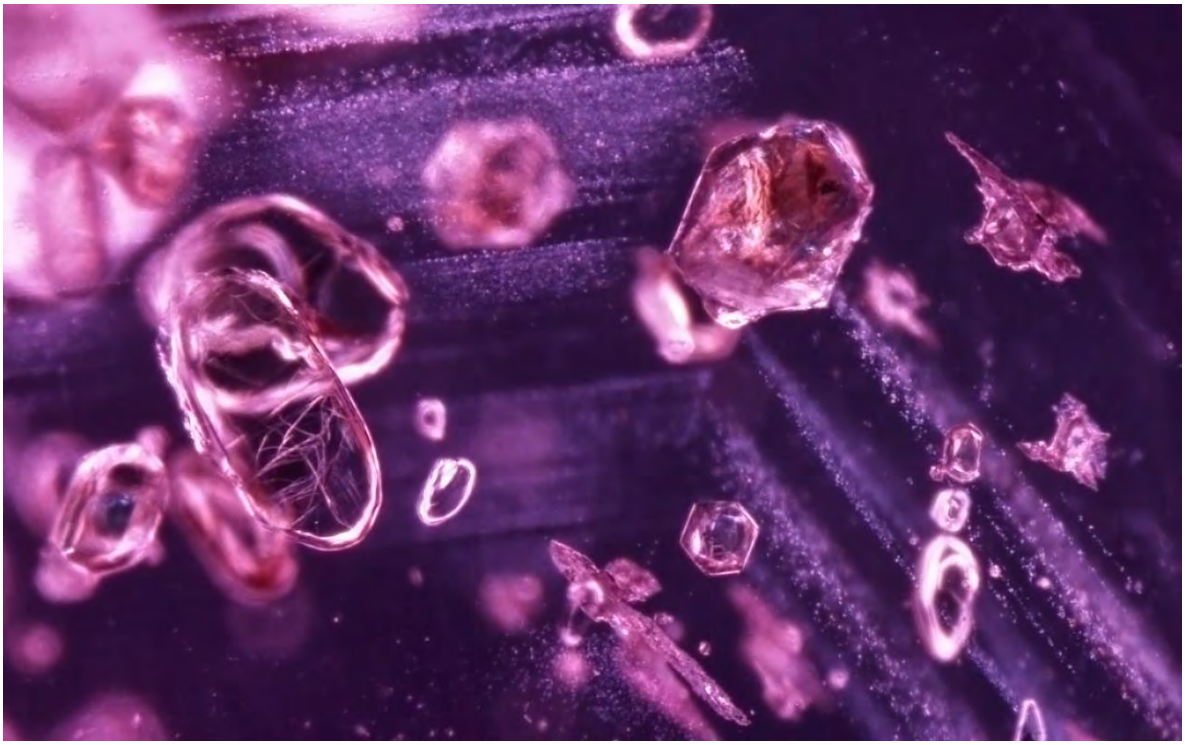

Figure 62: Bands of minute particles and rounded transparent crystals (probably amphibole) associated with hexagonal mostly translucent whitish crystals (identified by Raman as mica using the RRuff data base as a reference). Interestingly some of the hexagonal tabular crystals in the lower center and upper right areas of the photo are associated with a large frosted fringe, while the others are not. GIA reference sample number 100305163861, an F type sample obtained in Thailand in January 2013 in a parcel of "Bo Nam" rough. Darkfield illumination, magnified 60x. Photo: Jonathan Muyal © GIA.

Figure 63: Mica crystals seen in a highly fractured stone. They are easy to spot with their tabular, hexagonal, translucent whitish appearance and associated frosty looking fringe. GIA reference sample number 0668538802, an E type sample most likely from the "Central" area obtained in Mozambique in September 2009. Darkfield + fiber optic illumination, magnified 40x. Photo: Jonathan Muyal © GIA.

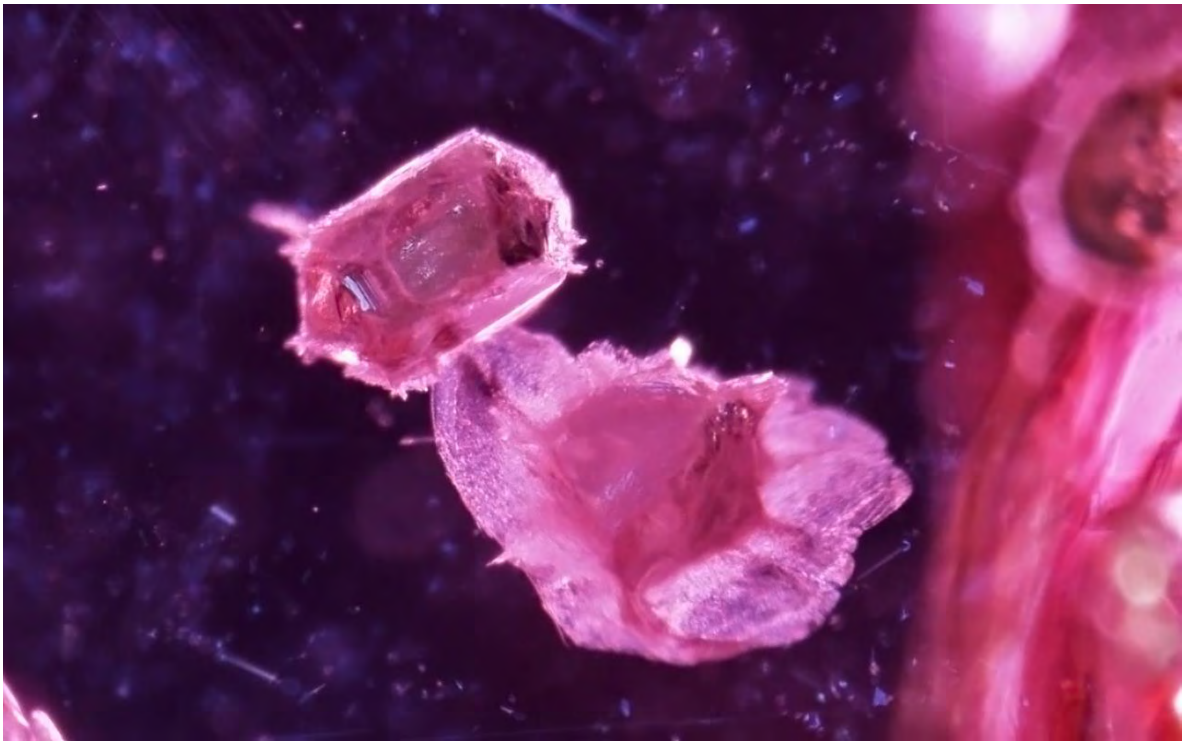

Figure 64: Mica crystals tend to be easy to spot with their tabular, hexagonal, more translucent than transparent appearance and common association with frosty looking fringes. GIA reference sample number 100305163848, an F type sample obtained in Thailand in January 2013 in a parcel of “Bo Nam” rough. Darkfield + fiber optic illumination, magnified 60x. Photo: Jonathan Muyal © GIA.

Figure 65: A group of hexagonal, translucent mica crystals associated with their characteristic frosty looking fringes. GIA reference sample number 100305163853, an F type sample obtained in Thailand in January 2013 in a parcel of “Bo Nam” rough. Darkfield + fiber optic illumination, magnified 70x. Photo: Jonathan Muyal © GIA.

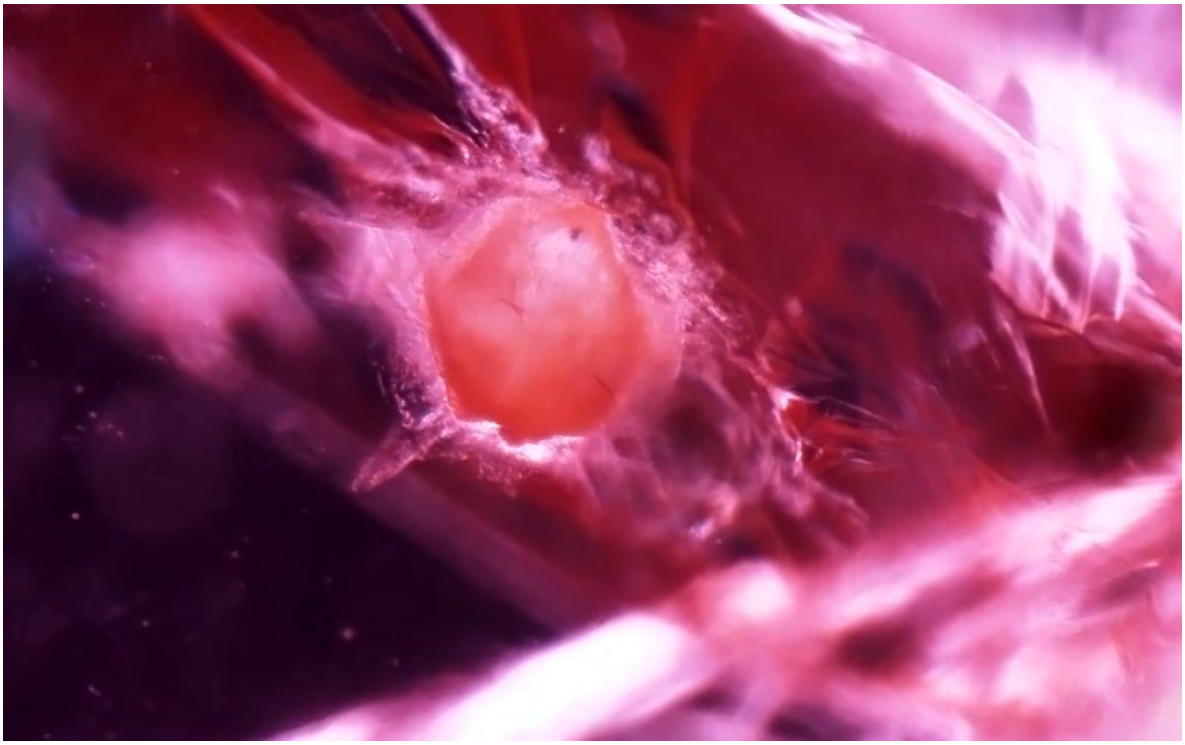

Figure 66: A translucent tabular, hexagonal, mica crystal associated with a frosty looking fringe. GIA reference sample number 0668538702, an E type sample probably from the "Central" area obtained in Mozambique in September 2009. Darkfield + fiber optic illumination, magnified 100x. Photo: Jonathan Muyal © GIA.

Figure 67: Mica crystals of varying sizes that are easy to recognize owing to their tabular, hexagonal, more translucent appearance and their characteristic associated frosty looking fringes. GIA reference sample number 0668531802, an E type sample (probably from the "Central" area) obtained in Mozambique in September 2009. Darkfield + fiber optic illumination, magnified 80x. Photo: Jonathan Muyal © GIA.

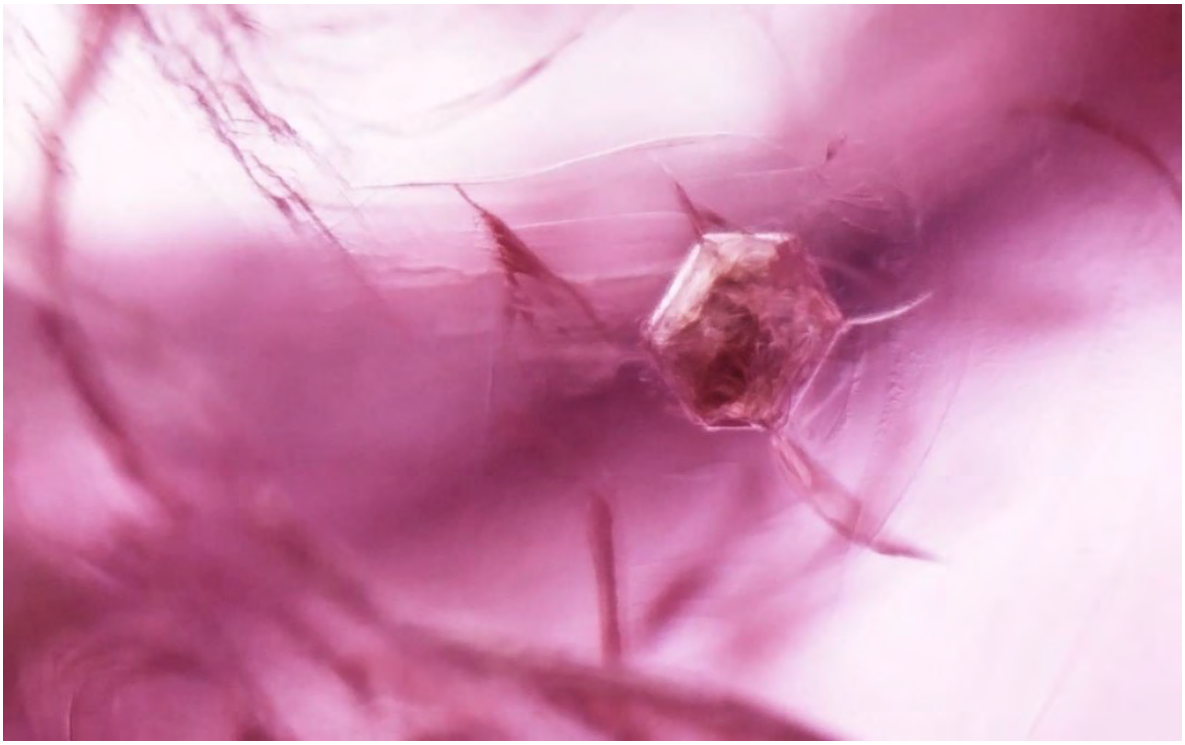

Figure 68: A single translucent hexagonal, tabular mica crystal (identified by Raman using the RRuff database as a reference) associated with unhealed fissures and growth features in GIA reference sample 100305163924, an A type sample collected in September 2012 at "Central". Darkfield + fiber optic illumination, magnified 112.5x. Photo: Jonathan Muyal © GIA.

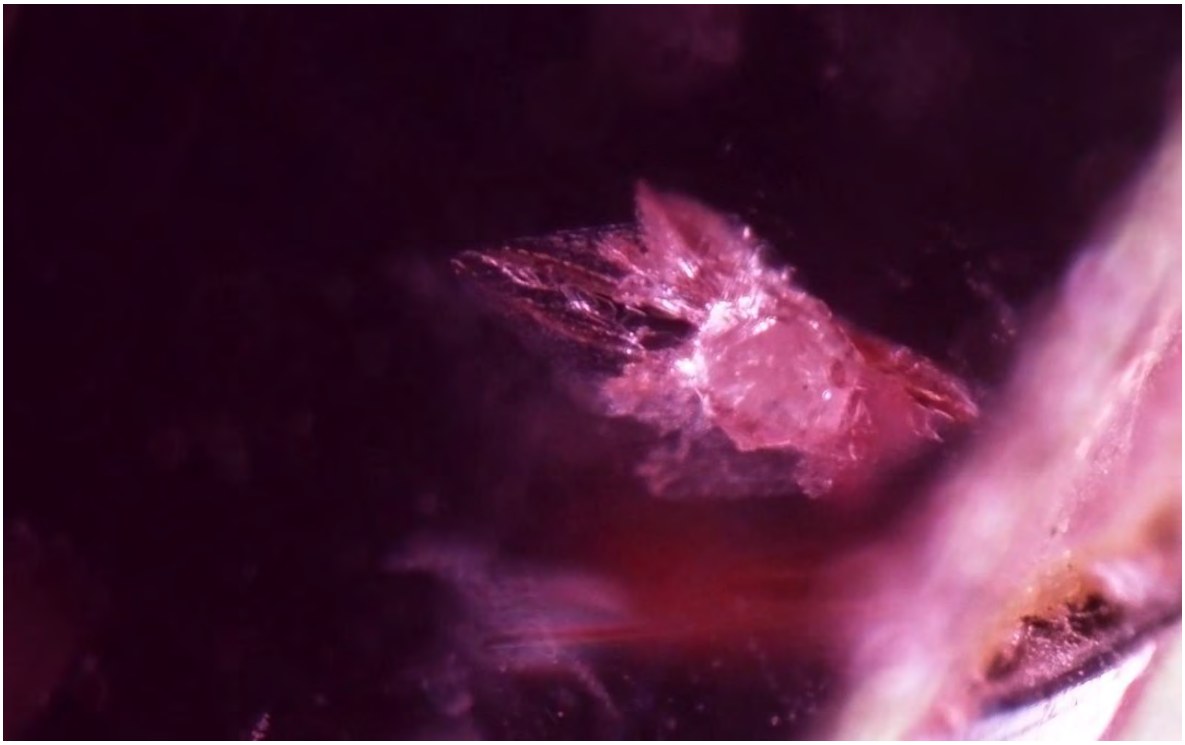

Figure 69: An interesting single translucent hexagonal, tabular mica crystal (identified by Raman using the RRuff database as a reference) associated some healed and frosty looking fissures in GIA reference sample 100305163940, an A type sample collected in the "Central" area in September 2012. Darkfield + fiber optic illumination, magnified 112.5x. Photo: Jonathan Muyal © GIA.

Figure 70: Not all mica crystals are associated with frosty fringes in Montepuez rubies. In some cases they are found in association with healed fissures reminiscent of those found in heated stones; however the absence of the “atoll like” rim commonly associated with altered inclusions in heated stones is not present in this unheated ruby. GIA reference sample number 100305163841, an F type sample obtained in Thailand in January 2013 in a parcel of “Bo Daeng” rough. Darkfield + fiber optic illumination, magnified 50x. Photo: Jonathan Muyal © GIA.

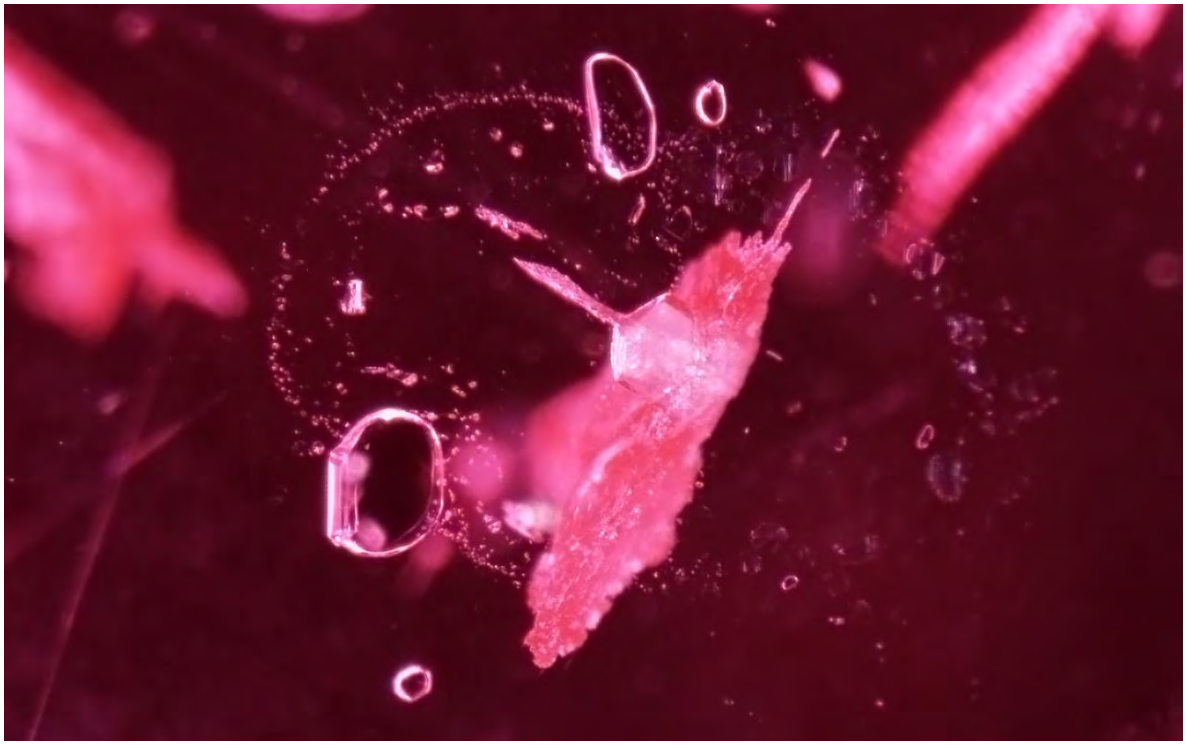

Figure 71: A hexagonal translucent mica crystal with associated frosty fringes and an extended healed fissure composed of flat negative crystals in a Ruby from Montepuez. The mica crystal is associated with several rounded amphibole looking crystals. GIA reference sample number 100305163868, an F type sample obtained in Thailand in January 2013 in a parcel of “Bo Nam” rough. Darkfield + fiber optic illumination, magnified 70x. Photo: Jonathan Muyal © GIA.

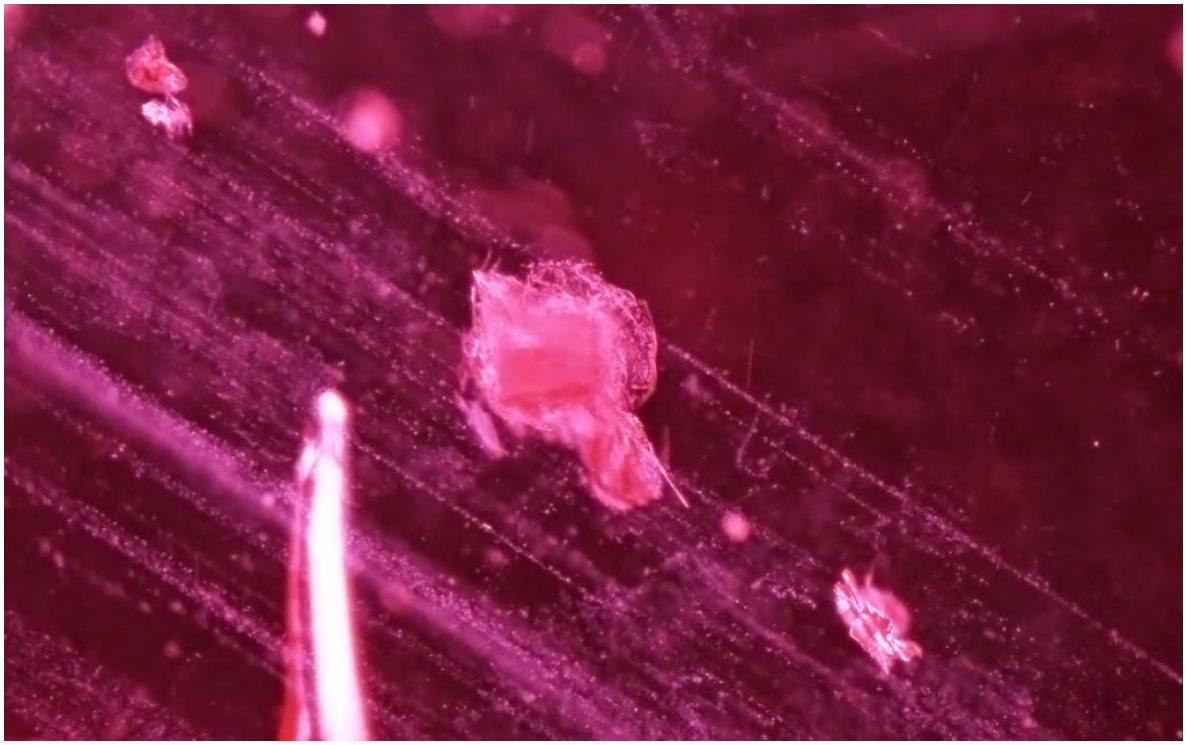

Figure 72: Hexagonal translucent mica crystals with associated frosty fringes accompanied by bands of minute particles and a few short needles in a Ruby from Montepuez. GIA reference sample number 100305163866, an F type sample obtained in Thailand in January 2013 in a parcel of "Bo Nam" rough. Darkfield + fiber optic illumination, magnified 50x. Photo: Jonathan Muyal © GIA.

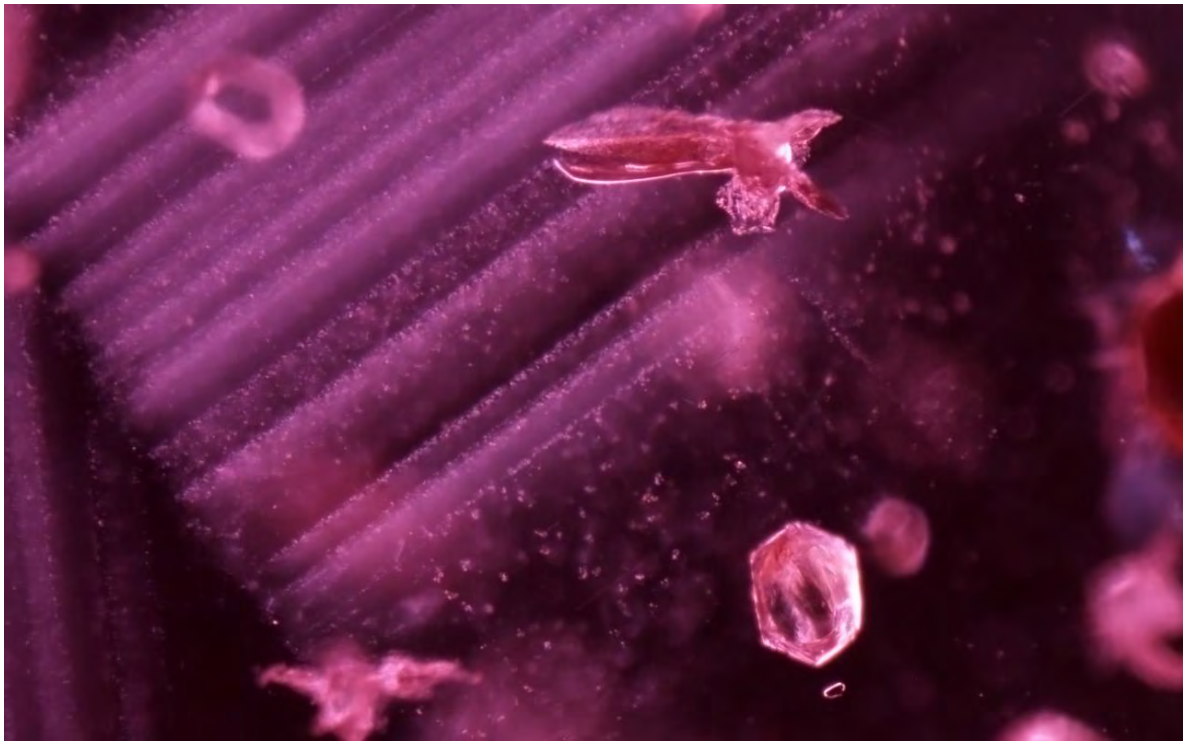

Figure 73: Bands of minute particles form a nice backdrop to hexagonal translucent mica crystals that show not all mica crystals are associated with frosty fringes in a Ruby from Montepuez. GIA reference sample number 100305163842, an F type sample obtained in Thailand in January 2013 in a parcel of "Bo Nam" rough. Darkfield illumination, magnified 70x. Photo: Jonathan Muyal © GIA.

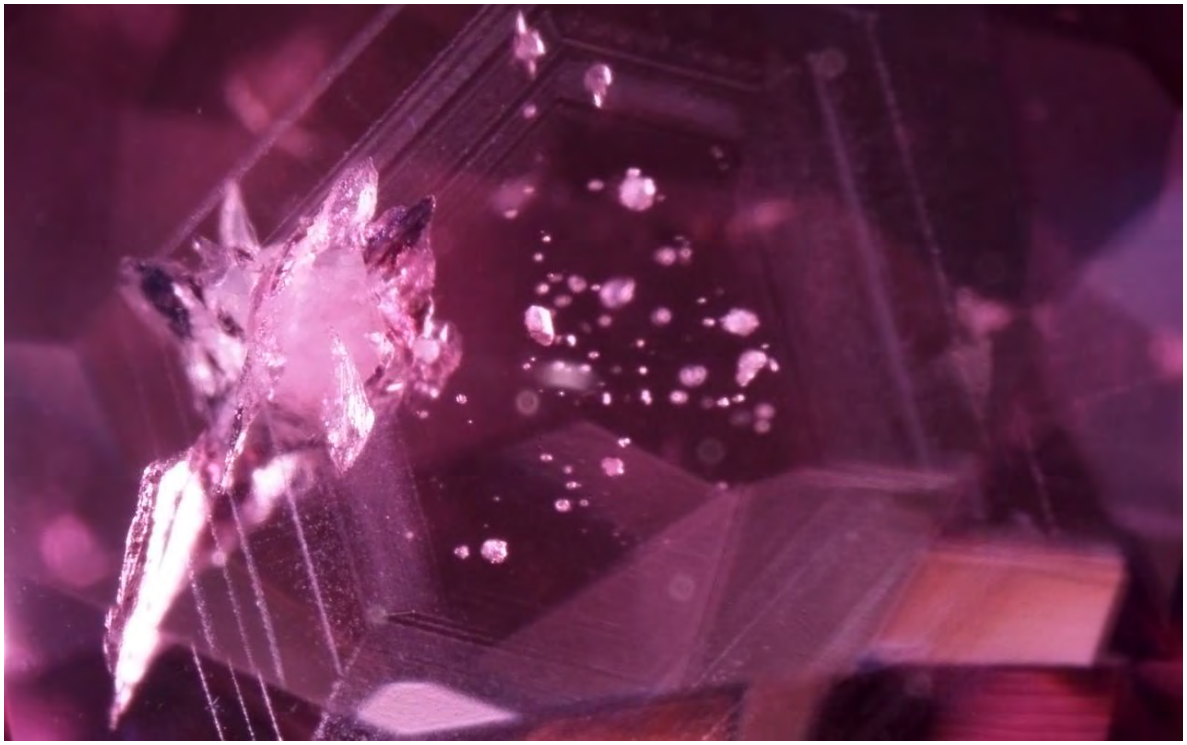

Figure 74: A hexagonal translucent mica crystal associated with numerous frosty fringes, several smaller crystals and many low density bands of minute particles forming a hexagonal pattern in a Ruby from Montepuez. GIA reference sample number 100305164550, an F type sample obtained in Chanthaburi Thailand in January 2013. Diffused + fiber optic illumination, magnified 30x. Photo: Jonathan Muyal © GIA.

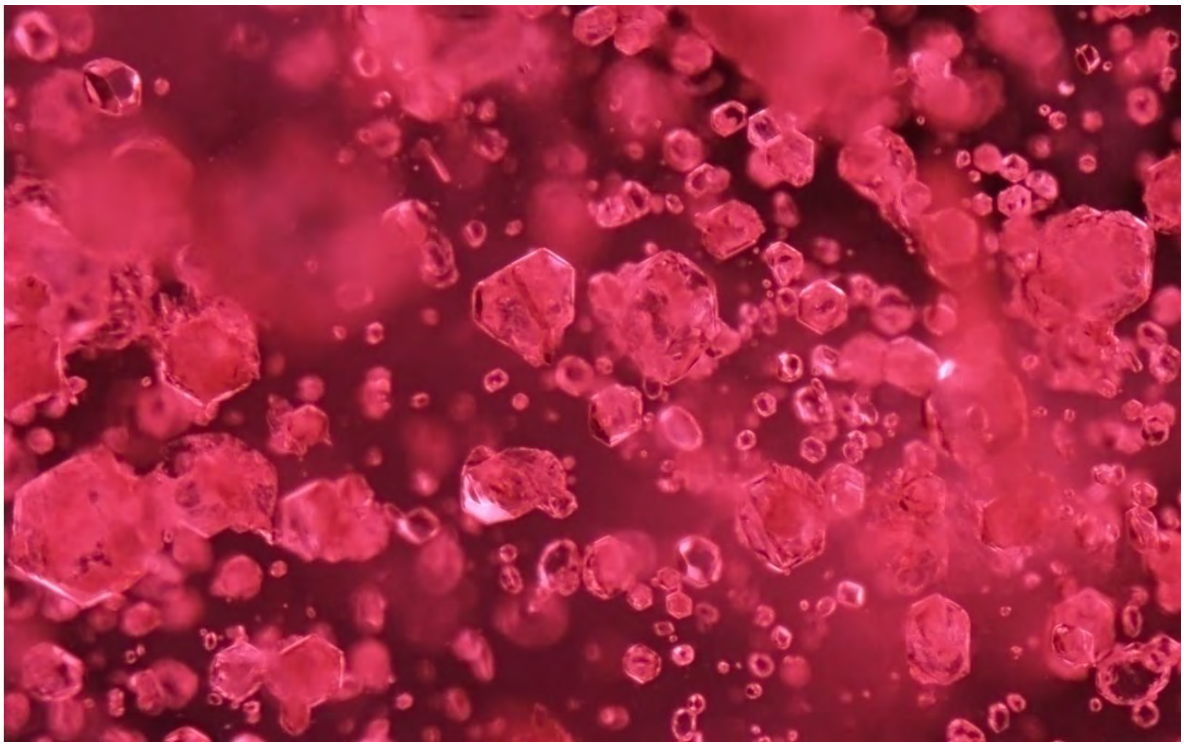

Figure 75: Galaxy of hexagonal translucent margarite crystals (identified by Raman using the RRuff database as a reference) in a Ruby from Montepuez. GIA reference sample number 100305164535, an F type sample obtained in Chanthaburi Thailand in January 2013. Diffused illumination, magnified 80x. Photo: Jonathan Muyal © GIA.

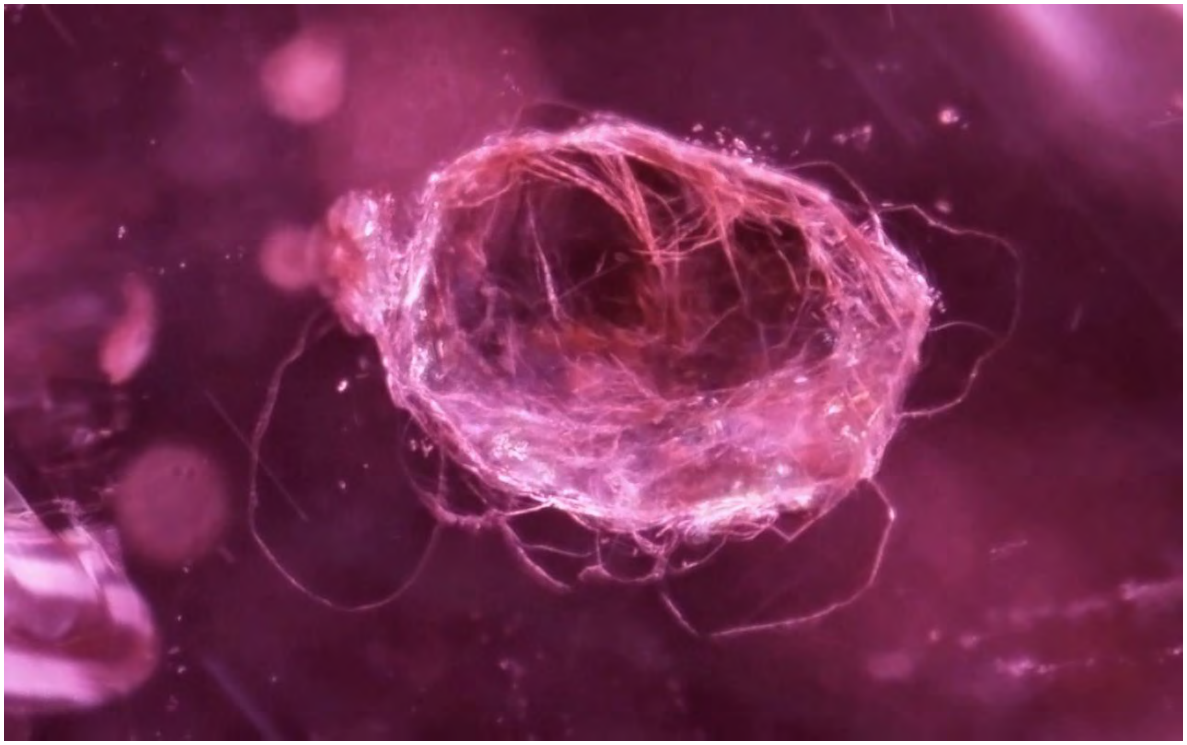

Figure 76: Margarite crystal (identified by Raman using the RRuff database as a reference) exhibiting a characteristic mica habit consisting of numerous “sheets” in a Ruby from Montepuez. GIA reference sample number 100305163865, an F type sample obtained in Thailand in January 2013 in a parcel of “Bo Nam” rough. Darkfield + fiber optic illumination, magnified 80x. Photo: Jonathan Muyal © GIA.

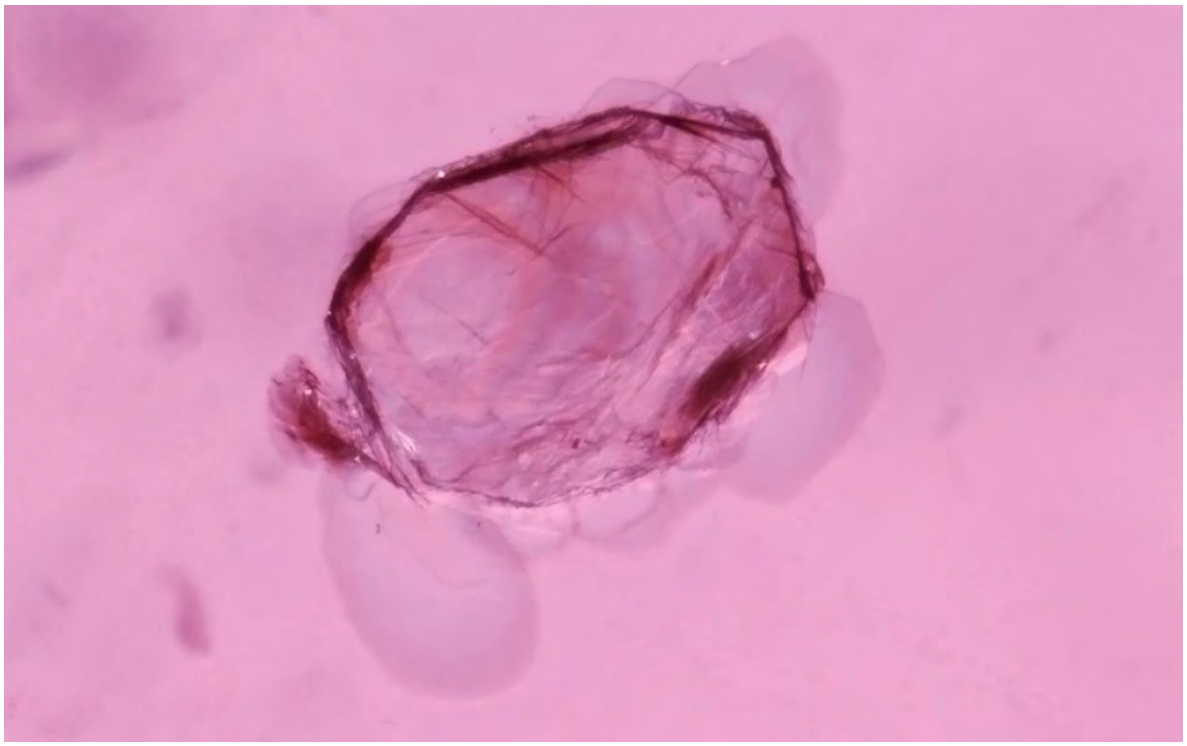

Figure 77: The same margarite crystal seen in figure 76 via diffused lighting in a Ruby from Montepuez. GIA reference sample number 100305163865, an F type sample obtained in Thailand in January 2013 in a parcel of “Bo Nam” rough. Diffused + fiber optic illumination, magnified 80x. Photo: Jonathan Muyal © GIA.

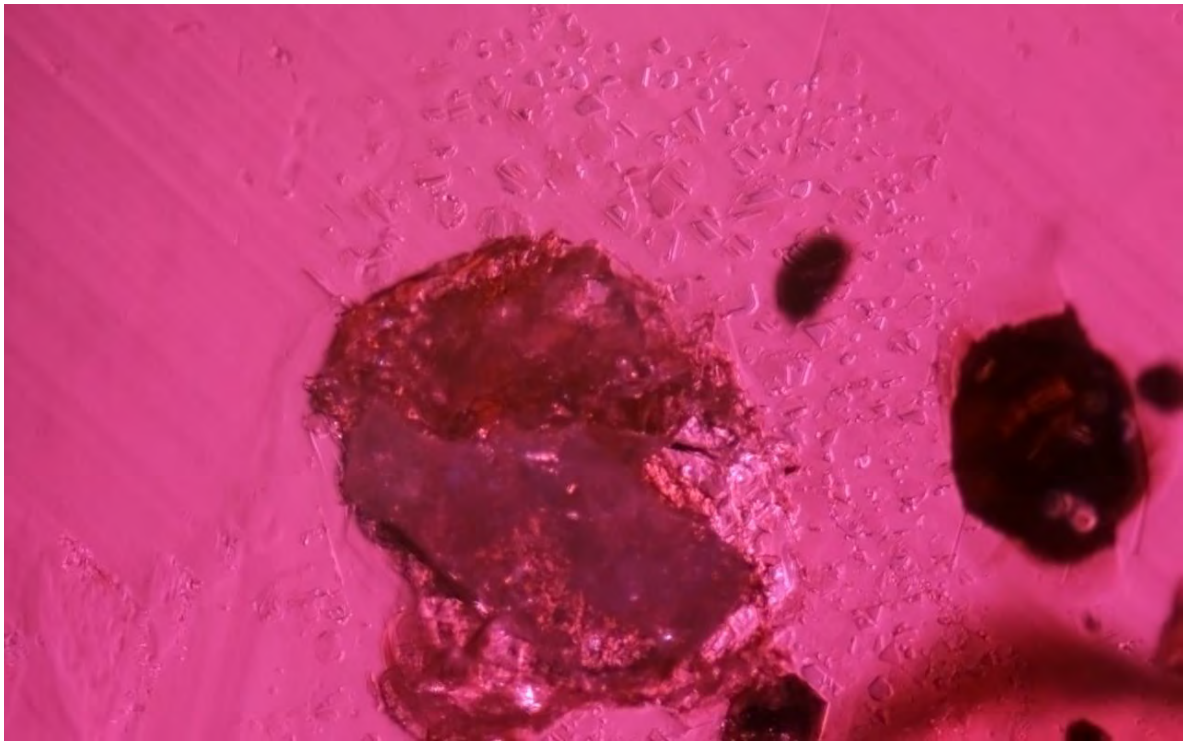

Figure 78: Hexagonal mica crystal (identified by Raman using the RRuff database as a reference) associated with a network of very flat negative crystals resembling thin films surrounding the crystal in a Ruby from Montepuez. GIA reference sample number 100305163836, an F type sample obtained in Thailand in January 2013 in a parcel of "Bo Daeng" rough. Transmitted + fiber optic illumination, magnified 90x. Photo: Jonathan Muyal © GIA.

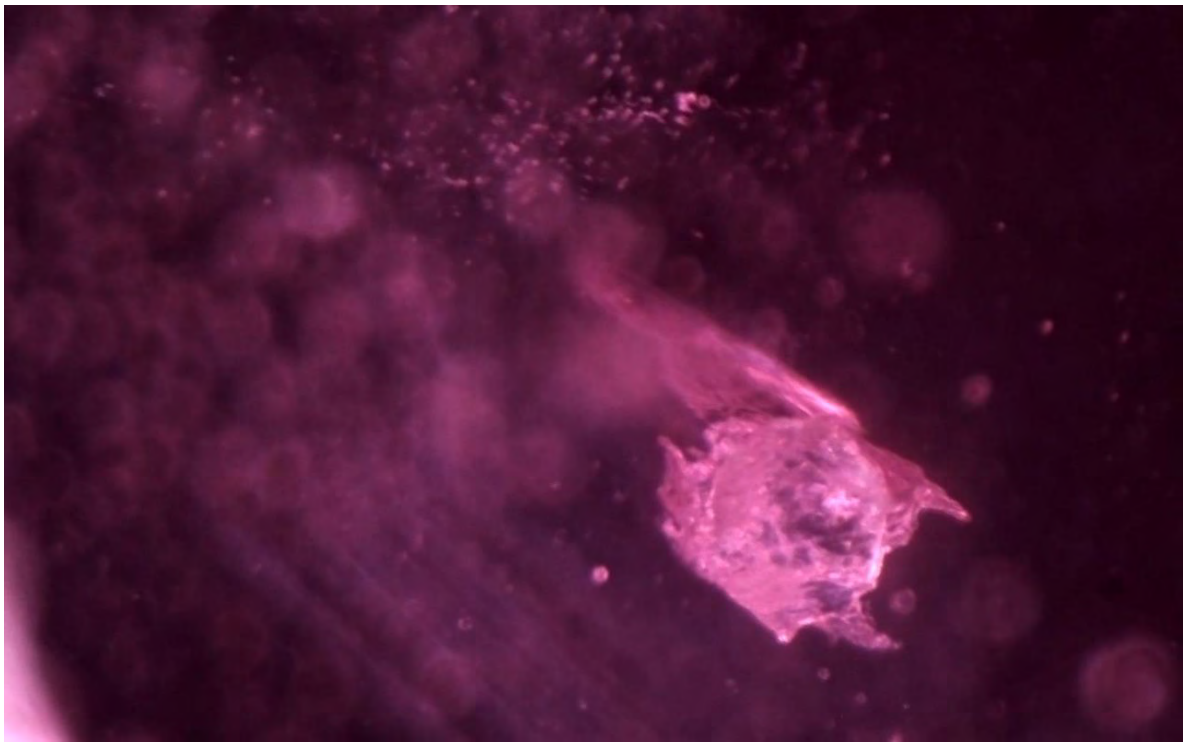

Figure 79: Hexagonal translucent mica crystal (identified by Raman using the RRuff database as a reference) associated with frosty fringes. GIA reference sample 100305163925, an A type samples collected in the "Central" area in September 2012. Diffused + fiber optic illumination, magnified 80x. Photo: Jonathan Muyal © GIA.

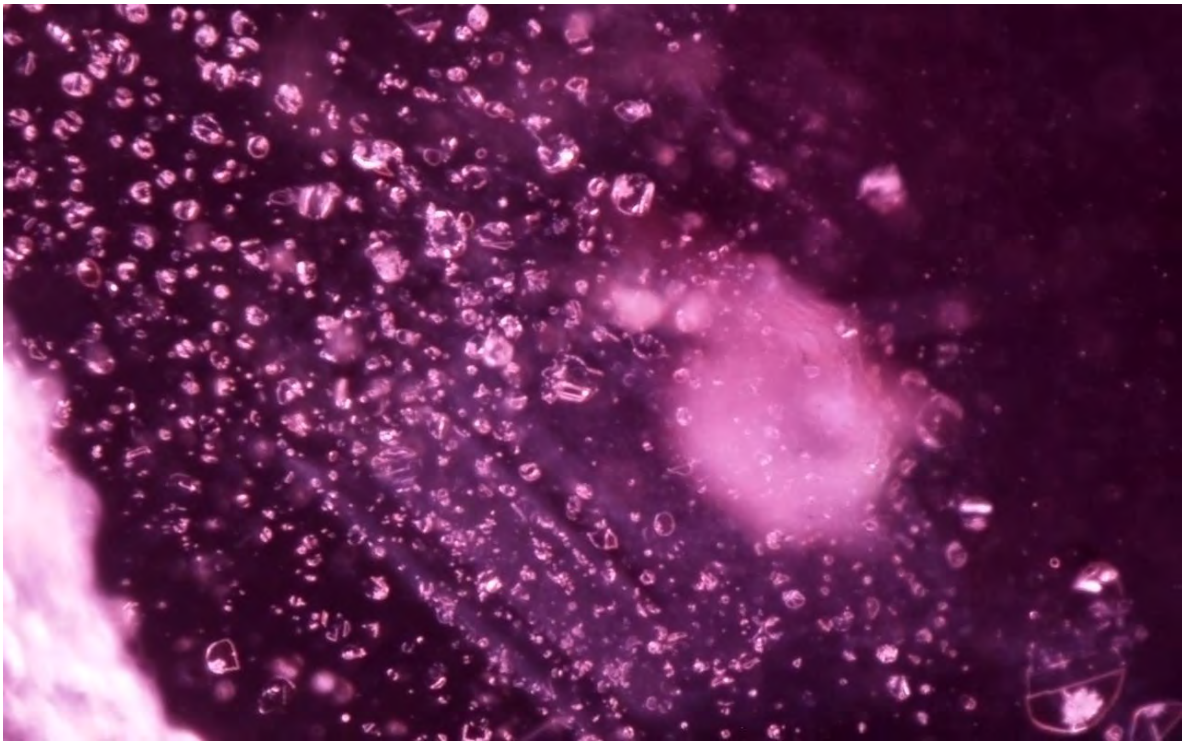

Figure 80: The same “A” type sample shown in the previous photo only focused slightly above the mica crystal to reveal a plane of numerous thin negative crystals/thin films. GIA reference sample 100305163925, an A type sample collected in the “Central” area in September 2012. Darkfield + fiber optic illumination, magnified 80x. Photo: Jonathan Muyal © GIA.

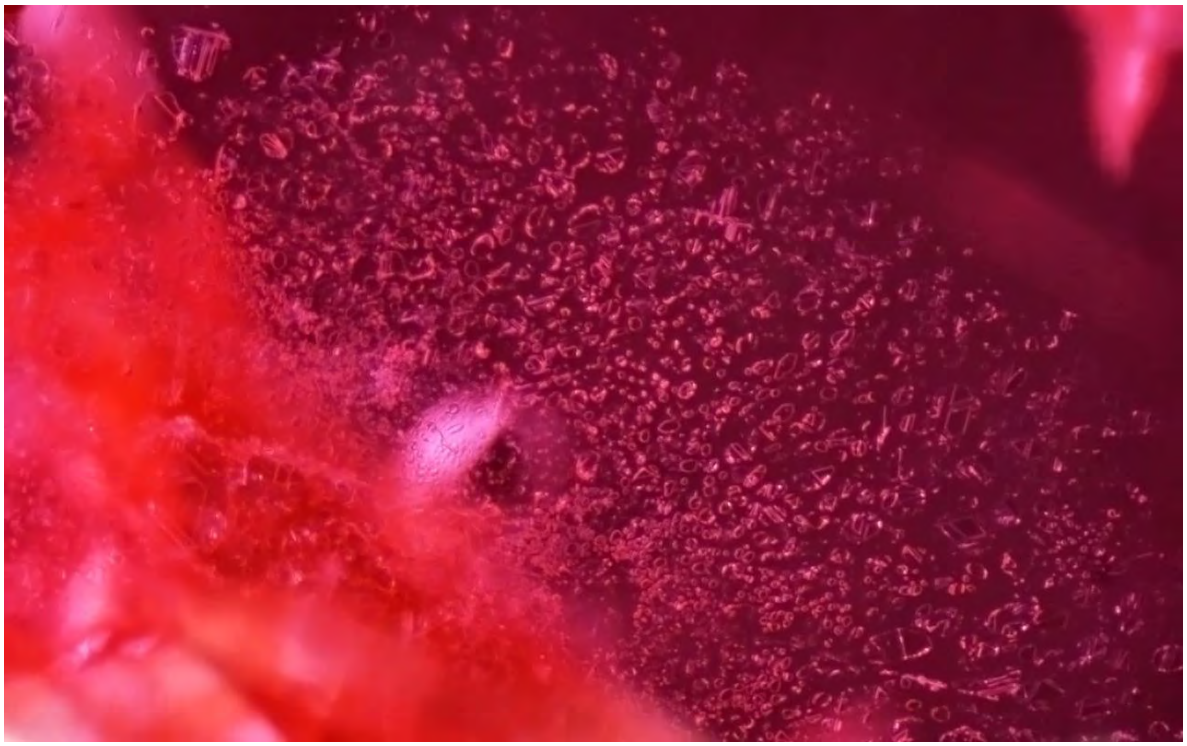

Figure 81: A plane composed of hundreds of small thin film like negative crystals forming a beautiful pattern in a Ruby from Montepuez. GIA reference sample number 100305163864, an F type sample obtained in Thailand in January 2013 in a parcel of “Bo Nam” rough. Transmitted + fiber optic illumination, magnified 100x. Photo: Jonathan Muyal © GIA.

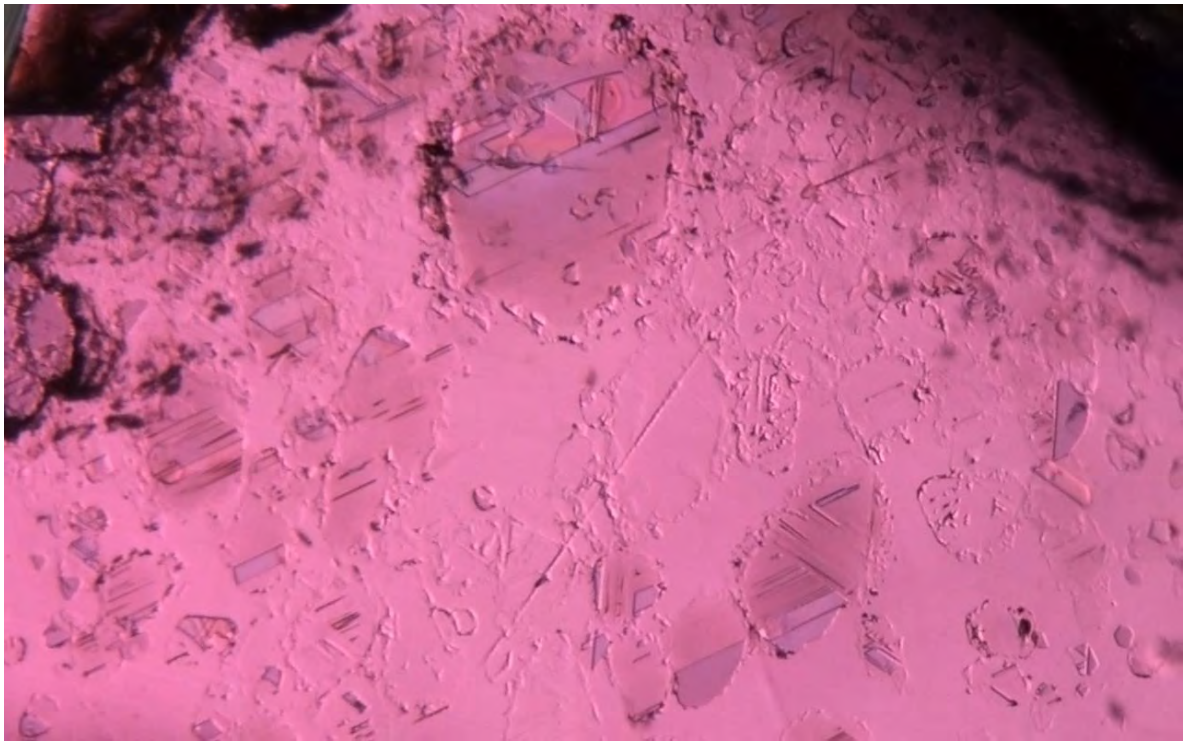

Figure 82: Detailed view of some of the thin film like negative crystals similar to the ones pictured in figure 81 in a Ruby from Montepuez. GIA reference sample number 100305162868, an E type sample obtained in Mozambique in September 2009. Diffused illumination, magnified 112.5x. Photo: Jonathan Muyal © GIA.

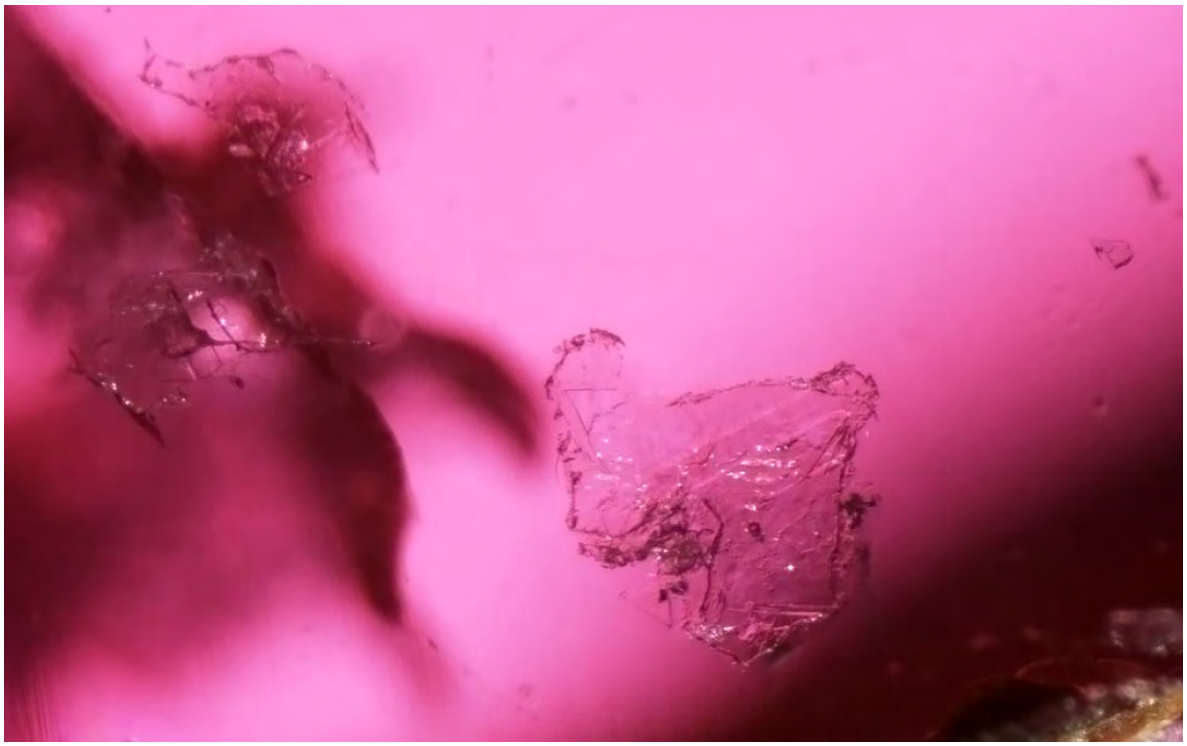

Figure 83: Detailed view of one of the negative crystals associated with a partial fringe like structure in a ruby from Montepuez. GIA reference sample 100305163864, an F type sample obtained in Thailand in January 2013 in a parcel of "Bo Nam" rough. Diffused + fiber optic illumination, magnified 80x. Photo: Jonathan Muyal © GIA.

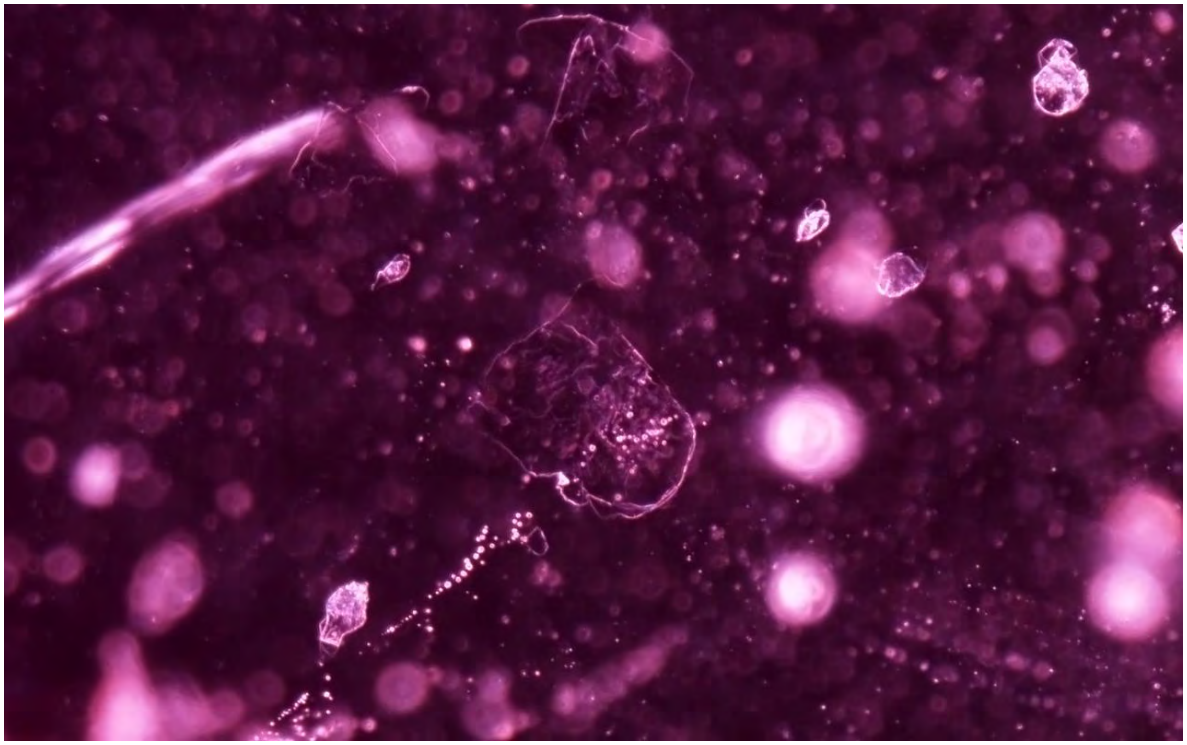

Figure 84: Detailed view of some isolated negative crystals in a Ruby from Montepuez. GIA reference sample 100305163889, an A2 type sample obtained in September 2013 at the "Nova Mina" but probably originating from the "Maninge Nice" area. Diffused illumination magnified 80x. Photo: Jonathan Muyal © GIA.

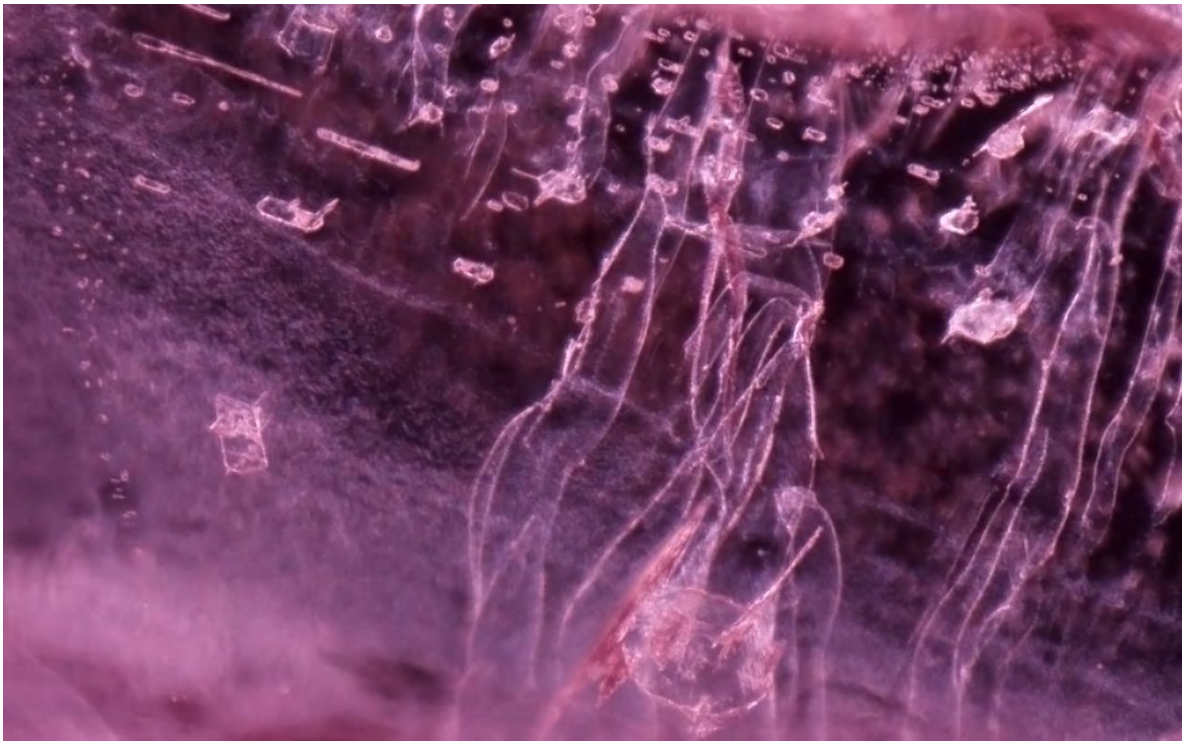

Figure 85: A plane of negative crystals associated with bands of particles (see following photo) and surface reaching fissures in a Ruby from Montepuez. GIA reference sample number 100305163938, an A type sample from the "Central" area collected on site in September 2012. Diffused + fiber optic illumination, magnified 80x. Photo: Jonathan Muyal © GIA.

Figure 86: A plane of flat reflective particles (out of focus in the previous photo) associated with surface reaching fissures and negative crystals in a Ruby from Montepuez. GIA reference sample number 100305163938, an A type sample from the "Central" area collected on site in September 2012. Diffused + fiber optic illumination, magnified 80x. Photo: Jonathan Muyal © GIA.

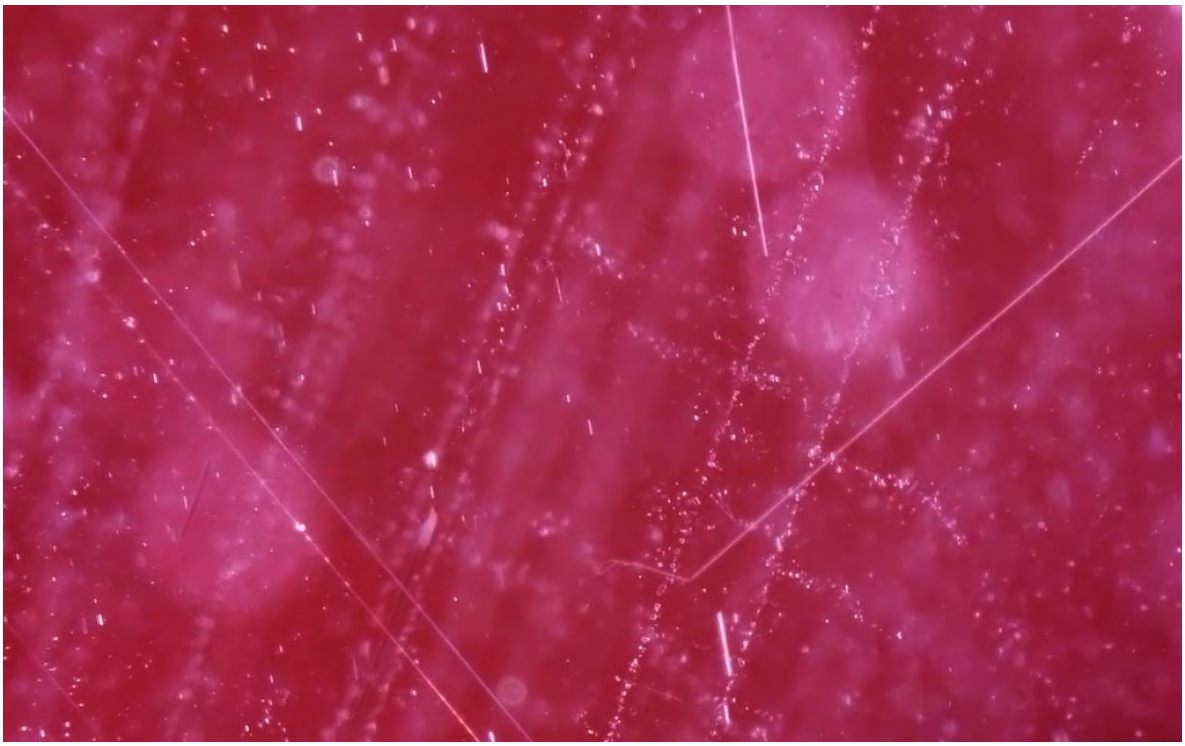

Figure 87: Parallel planes of minute and coarse whitish particles, crossing each other at 90 degrees, associated with long and short thin needles, crossing each other at 60 degrees, in a Ruby from Montepuez. GIA reference sample 0668532602, an "E" type sample (probably from the "Central" area) collected in Pemba in September 2009. Darkfield + fiber optic illumination, magnified 60x. Photo: Jonathan Muyal © GIA.

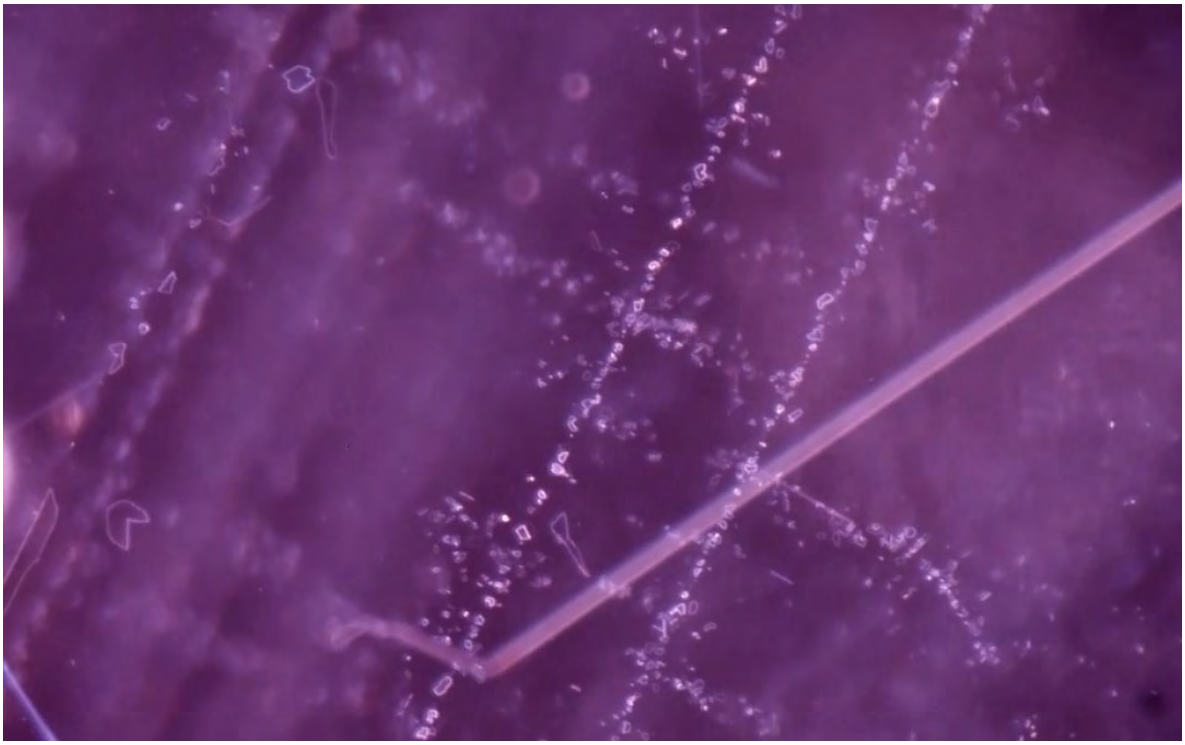

Figure 88: Detailed view of the same parallel planes of minute and coarse whitish particles, crossing each other at 90 degrees. It is clearly evident that the majority of these particles are transparent irregularly shaped orientated particles. GIA reference sample 0668532602, an "E" type sample (probably from the "Central" area) collected in Pemba in September 2009. Darkfield illumination, magnified 112.5x. Photo: Jonathan Muyal © GIA.

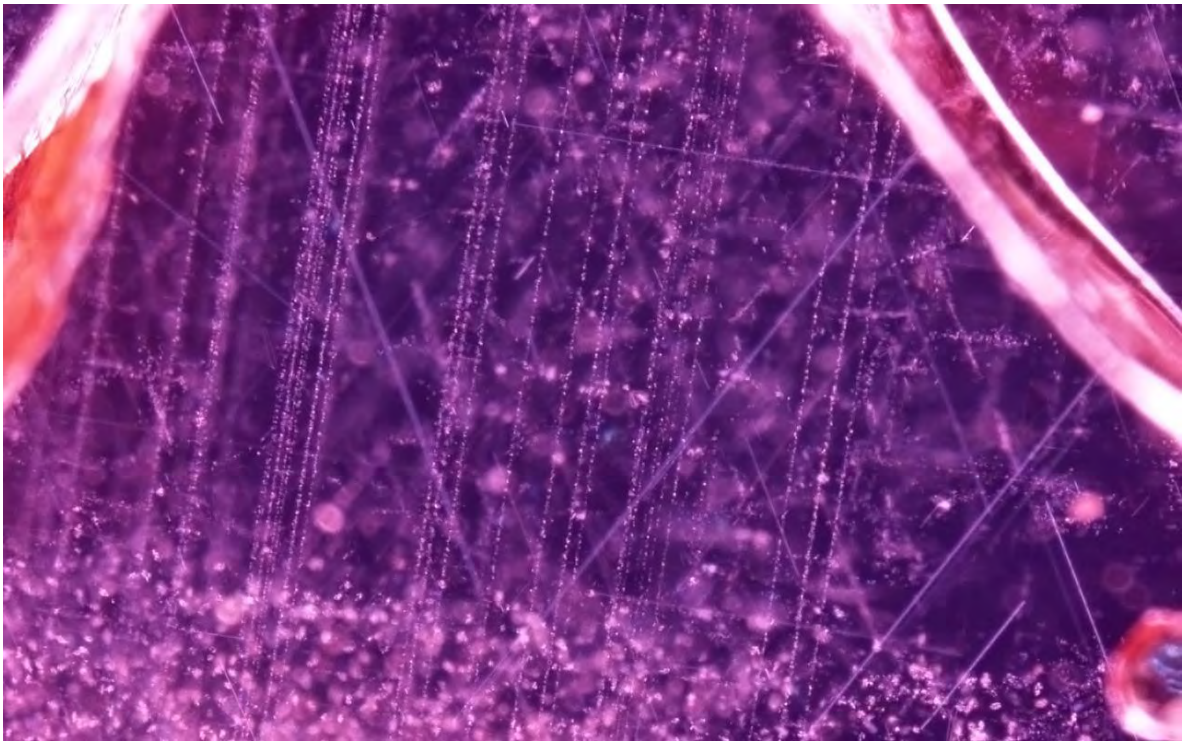

Figure 89: Avery busy inclusion scene showing bands of minute whitish particles arranged parallel, or 90 degrees to each other, associated with long and short rutile like needles aligned at 60 degrees to each other. GIA reference sample 0668538702, an "E" type sample (probably from the "Central" area) collected in Nampula in September 2009. Darkfield + fiber optic illumination, magnified 40x. Photo: Jonathan Muyal © GIA.

Figure 90: Bands of minute whitish particles forming part of a hexagonal pattern associated with long and short thin needles aligned at 60 degrees to each other. GIA reference sample 0668540102, an "E" type sample (probably from the "Central" area) collected in Nampula in September 2009. Darkfield + fiber optic illumination, magnified 40x. Photo: Jonathan Muyal © GIA.

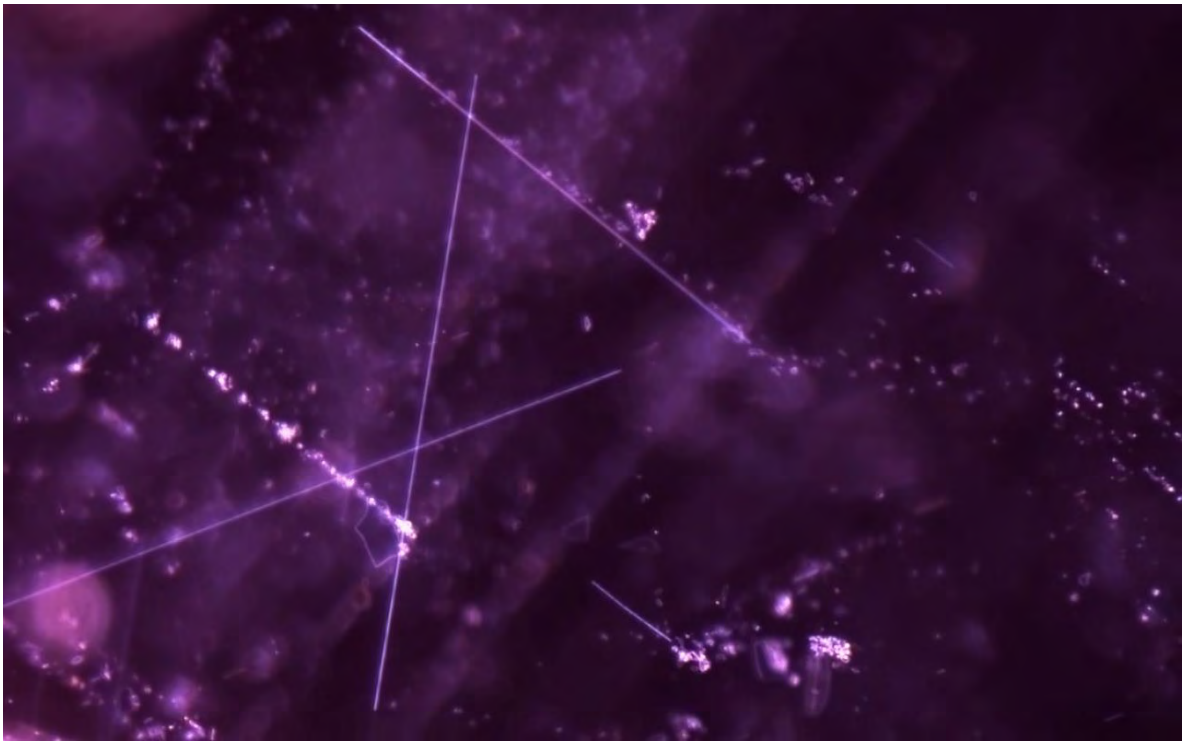

Figure 91: Bands of minute whitish particles arranged 90 degrees to each other associated with long and short rutile like needles aligned at 60 degrees to each other. GIA reference sample 0668539302, an "E" type sample (probably from the "Central" area) collected in Nampula in September 2009. Darkfield + fiber optic illumination, magnified 112.5x. Photo: Jonathan Muyal © GIA.

Figure 92: Bands of minute whitish (?) particles forming part of a hexagonal pattern with additional bands of particles arranged perpendicular to them, together with a low density network of long and short thin needles where the needles are aligned at 60 degrees to each other. GIA reference sample 100305163865, an "F" type sample from parcel of Montepuez rubies of the "Bo Nam" type collected in Thailand in January 2013. Darkfield + fiber optic illumination, magnified 40x. Photo: Jonathan Muyal © GIA.

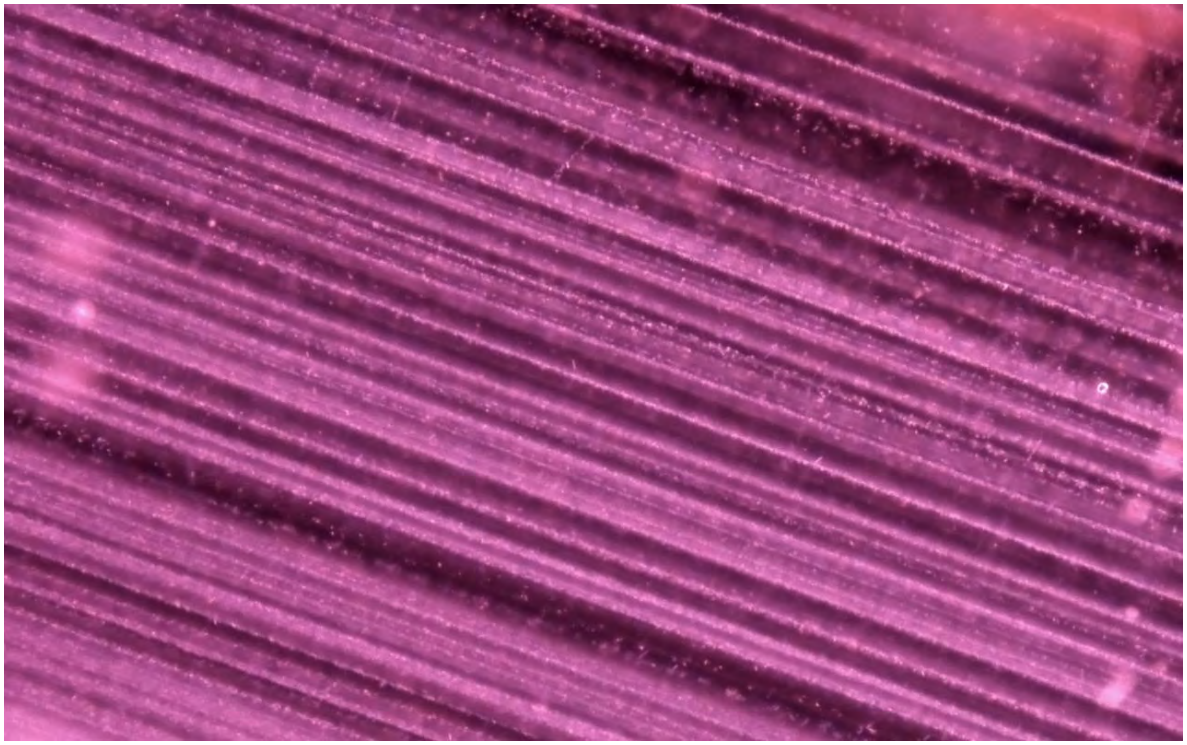

Figure 93: Detailed view of the bands of minute whitish particles in a Ruby from Montepuez. GIA reference sample 100305163944, a "B" type sample collected in the Namujo/Torro area in September 2012. Darkfield + fiber optic illumination, magnified 40x. Photo: Jonathan Muyal © GIA.

Figure 94: Broad and thin bands of minute whitish particles aligned at 60 degrees to each other resulting in very silky appearance to the stone. GIA reference sample 100305163946, a "B" type sample collected in the Namujo/Torro area in September 2012. Darkfield + fiber optic illumination, magnified 40x. Photo: Jonathan Muyal © GIA.

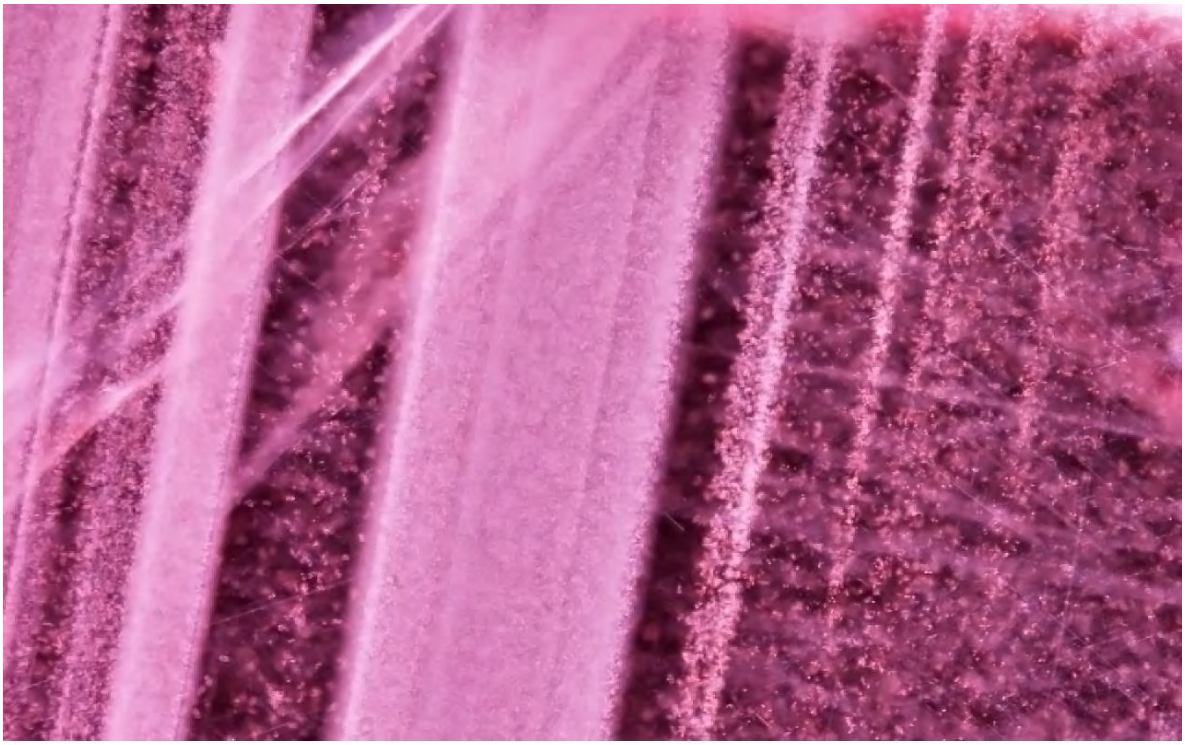

Figure 95: Detailed view of some of the broad and thin bands of minute whitish particles revealing the short thin needles aligned at 60 degrees to each other that form them. GIA reference sample 0668539402, an "E" type sample (probably from the "Central" area) collected in Nampula in September 2009. Darkfield + fiber optic illumination, magnified 40x. Photo: Jonathan Muyal © GIA.

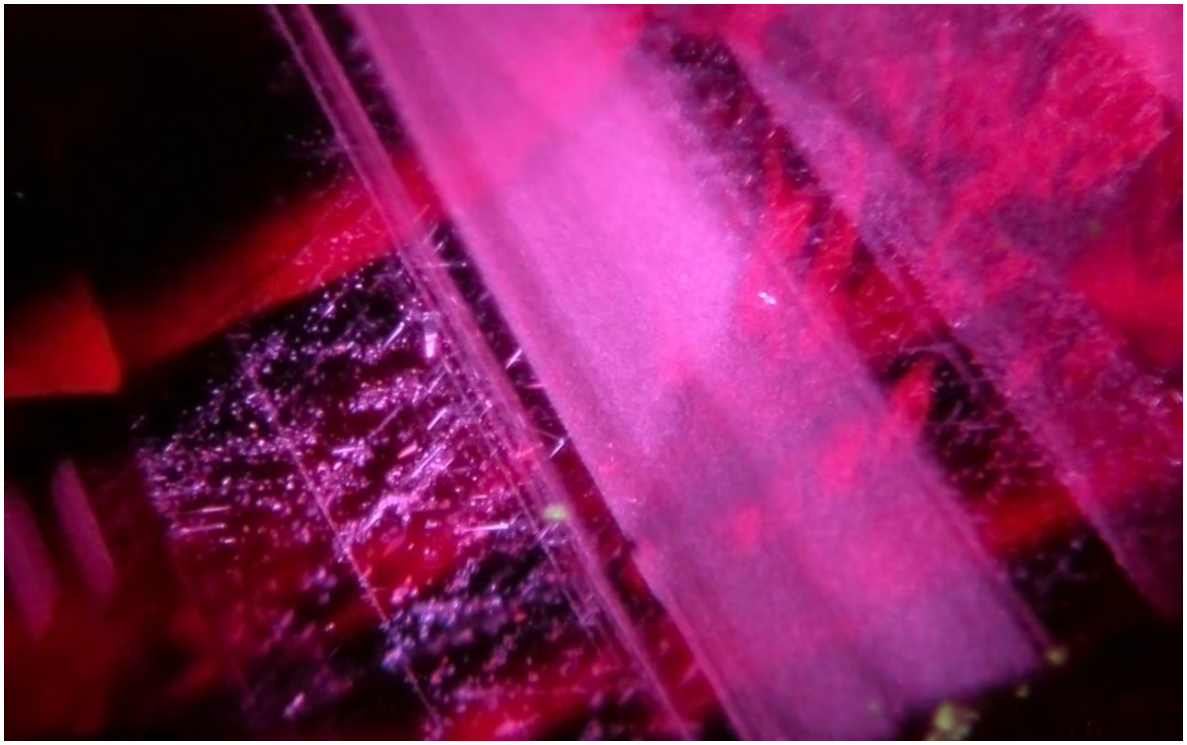

Figure 96: Broad bands of minute particles appearing as white clouds together with “arrow-head” needles aligned at 60 degrees to each other in a Ruby from Montepuez. Darkfield + fiber optic illumination, magnified 30x. Photo: Vincent Pardieu © GIA.

Figure 97: Detailed view of some bands of minute particles showing short and long thin needles within them aligned at 60 degrees to each other. GIA reference sample 100305164538, an “E” type sample (probably from the “Central” area) collected in Nampula in September 2009. Fiber optic illumination, magnified 80x. Photo: Jonathan Muyal © GIA.

Figure 98: A group of parallel planes (thin bands) of minute whitish particles associated with short and long thin needles aligned at 60 degrees to each other. GIA reference sample 100305164542, an "E" type sample (probably from the "Central" area) collected in Nampula in September 2009. Darkfield illumination magnified 60x. Photo: Jonathan Muyal © GIA.

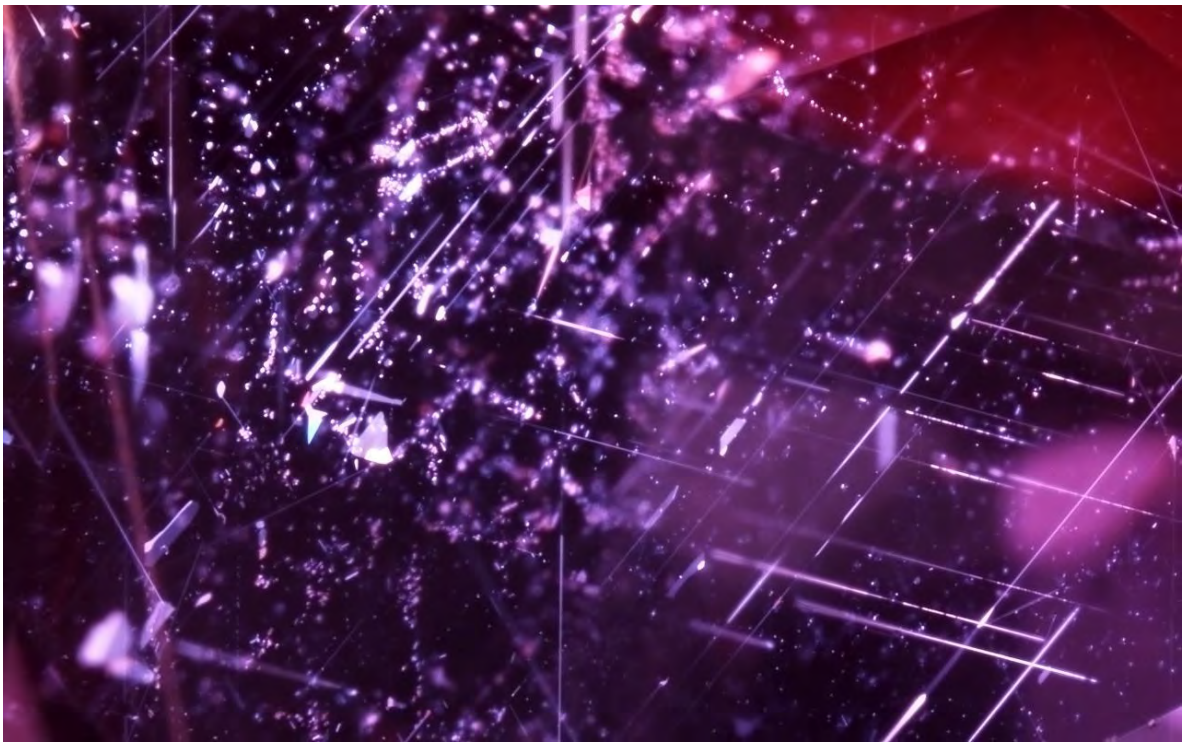

Figure 99: Detailed view of the short and long thin needles associated with broader particles of a mostly irregular shape reminiscent of some thin films. GIA reference sample 100305164544, an "E" type sample (probably from the "Central" area) collected in Nampula in September 2009. Darkfield + fiber optic illumination, magnified 40x. Photo: Jonathan Muyal © GIA.

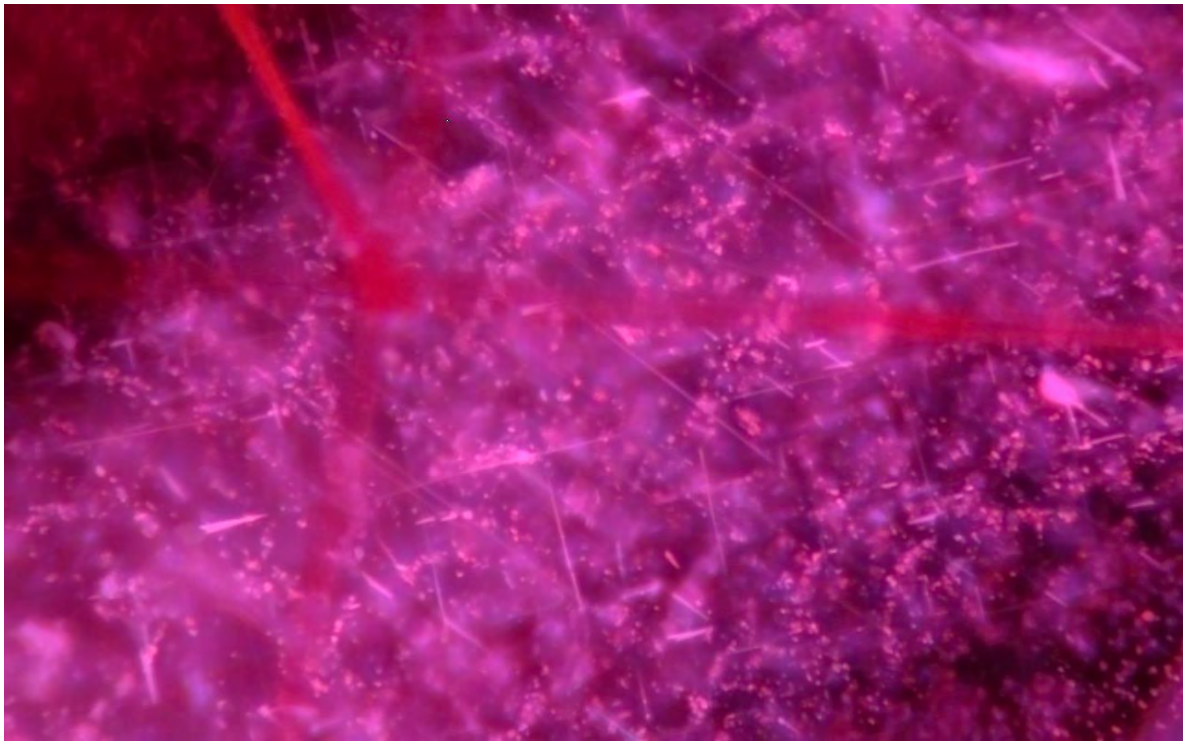

Figure 100: Detailed view within a low density band of minute whitish particles showing that the particles consist of short and long needles of various forms (thin ones, irregular broad ones and a few “arrow-head” ones). The red lines are several out of focus tubes intersecting each other at 90 degrees in a Ruby from Montepuez. Darkfield + fiber optic illumination, magnified 40x. Photo: Vincent Pardieul © GIA.

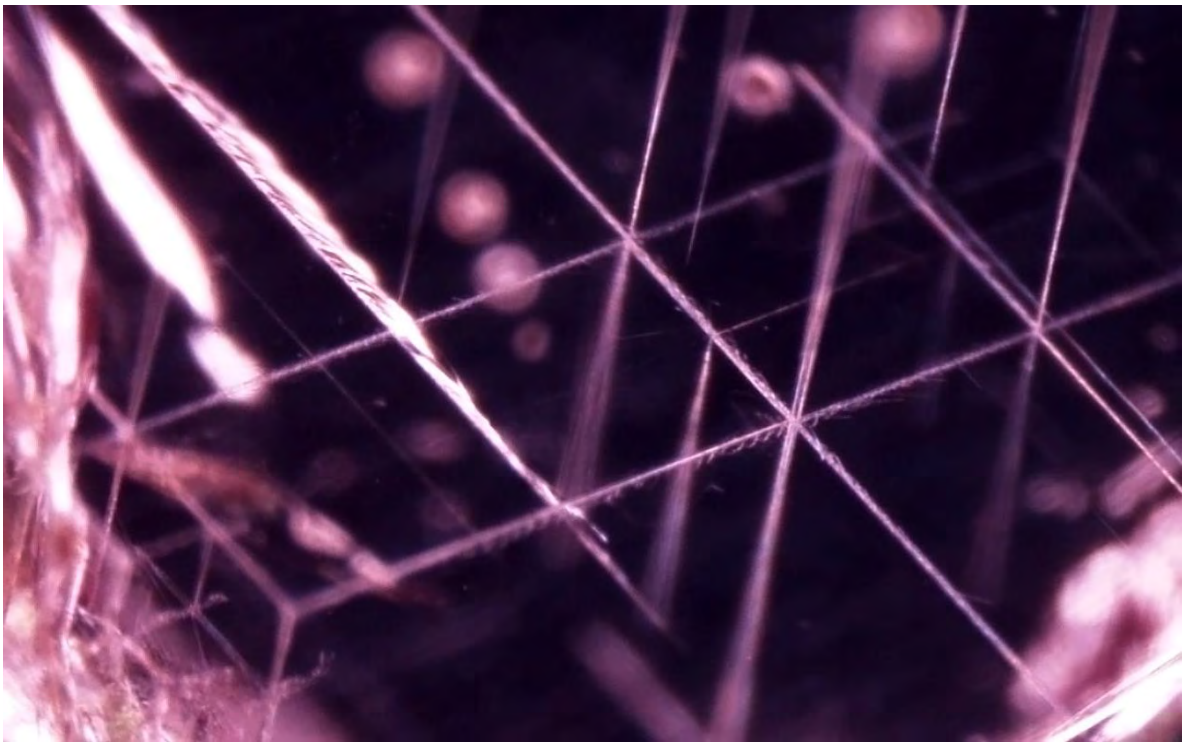

Figure 101: Detailed view of a group of tubes intersecting each other at 90 degrees in a Ruby from Montepuez. GIA reference sample 0668541702, an “E” type sample (probably from the “Central” area) collected in Nampula in September 2009. Darkfield illumination, magnified 80x. Photo: Jonathan Muyal © GIA.

Figure 102: Tubes intersecting each other at 90 degrees associated with a dark, opaque euhedral crystal (probably chalcopyrite) and a few healed tension-like fissures as well as low density bands consisting of minute particles in a Ruby from Montepuez. GIA reference sample 100305163852, an "E" type sample (probably from the "Central" area) collected in Nampula in September 2009. Darkfield + fiber optic illumination, magnified 60x. Photo: Jonathan Muyal © GIA.

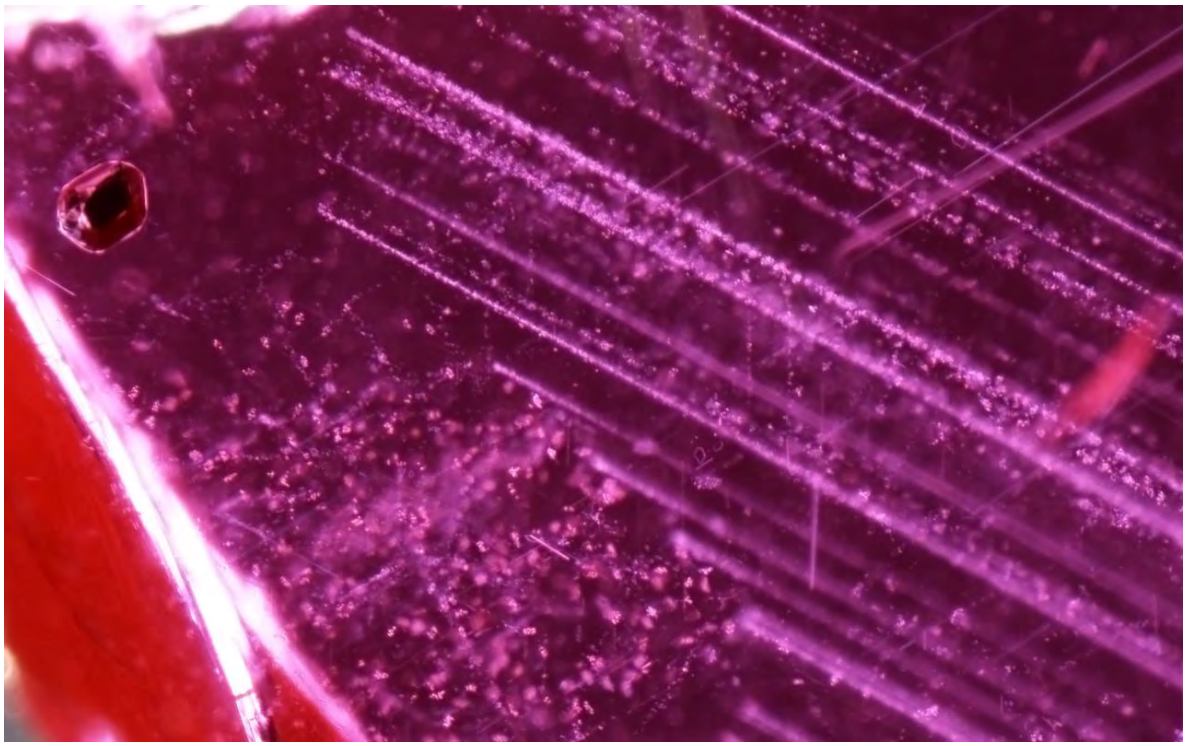

Figure 103: A dark, opaque euhedral crystal (probably chalcopyrite) associated with narrow bands and clouds of whitish particles and short and long thin needles arranged at 60 degrees to each other in a Ruby from Montepuez. GIA reference sample 100305163824, an "E" type sample (probably from the "Central" area) collected in Nampula in September 2009. Darkfield + fiber optic illumination, magnified 60x. Photo: Jonathan Muyal © GIA.

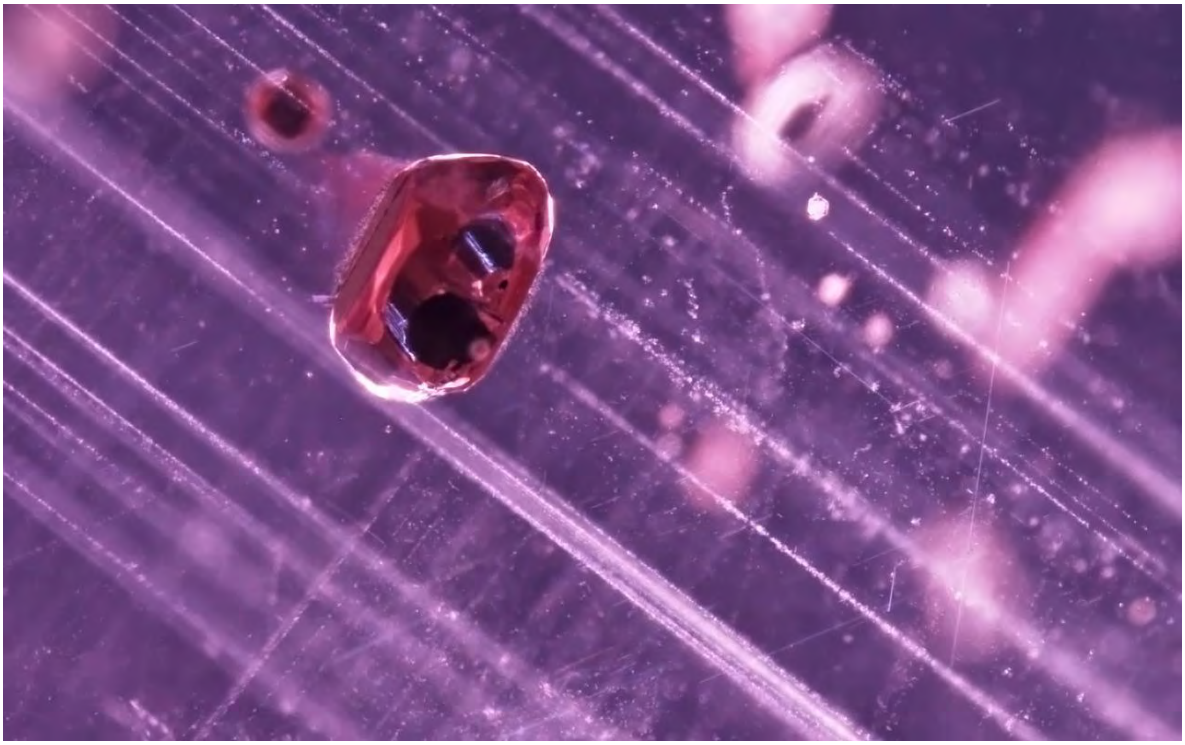

Figure 104: A more detailed view of a highly lustrous, dark, , opaque euhedral crystal (probably chalcopyrite) associated with narrow bands of whitish particles (perpendicular to each other) and long and short thin needles aligned at a60/120 degree orientation. GIA reference sample 0668539302, an "E" type sample (probably from the "Central" area) collected in Nampula in September 2009. Darkfield + fiber optic illumination, magnified 60x. Photo: Jonathan Muyal © GIA.

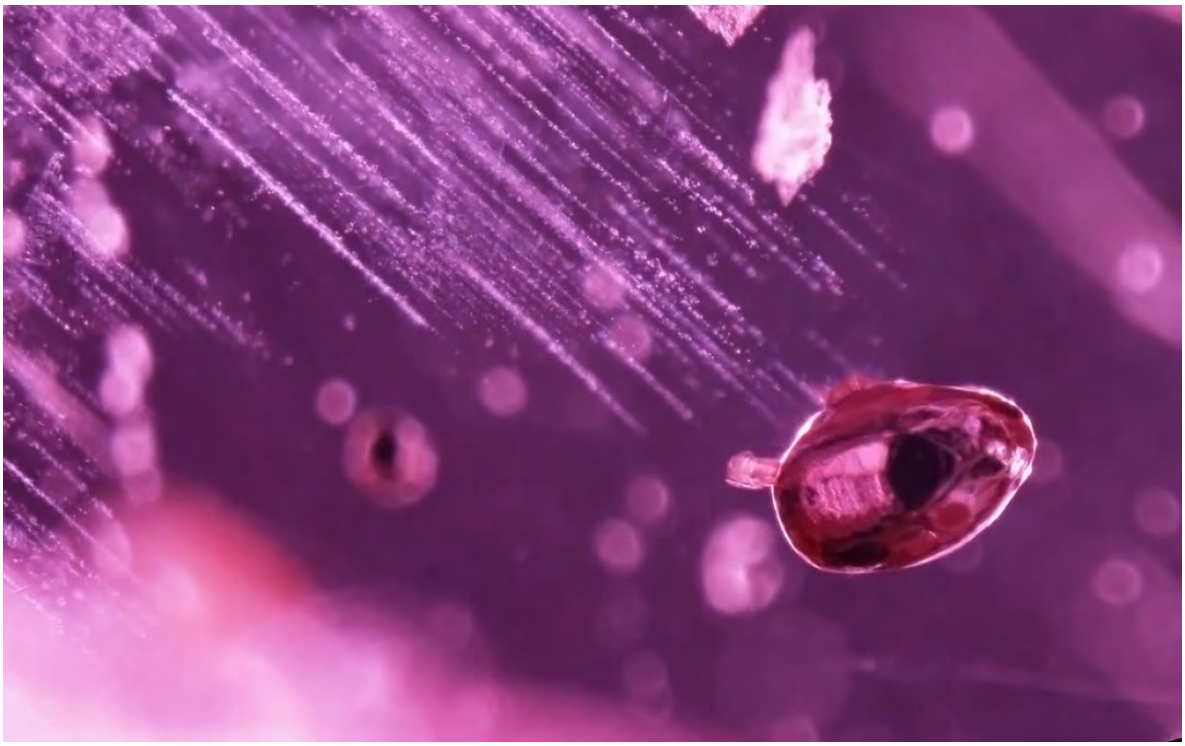

Figure 105: A more detailed view of a highly lustrous, dark, , opaque euhedral crystal (probably chalcopyrite) associated with narrow bands of whitish particles. GIA reference sample 0668542002, an "E" type sample (probably from the "Central" area) collected in Nampula in September 2009. Darkfield + fiber optic illumination, magnified 60x. Photo: Jonathan Muyal © GIA.

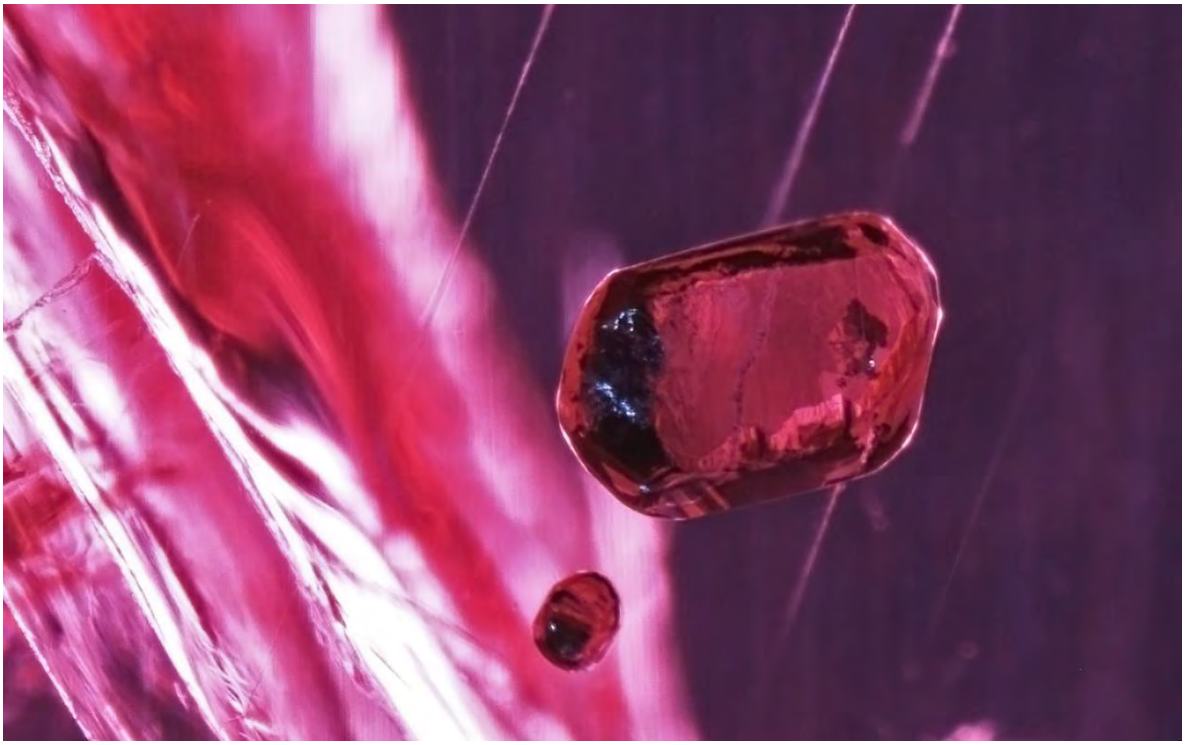

Figure 106: Two highly lustrous, dark, opaque euhedral crystals (probably chalcopyrite) associated with long thin needles and a fissure. GIA reference sample 0668538802, an "E" type sample (probably from the "Central" area) collected in Nampula in September 2009. Darkfield + fiber optic illumination, magnified 50x. Photo: Jonathan Muyal © GIA.

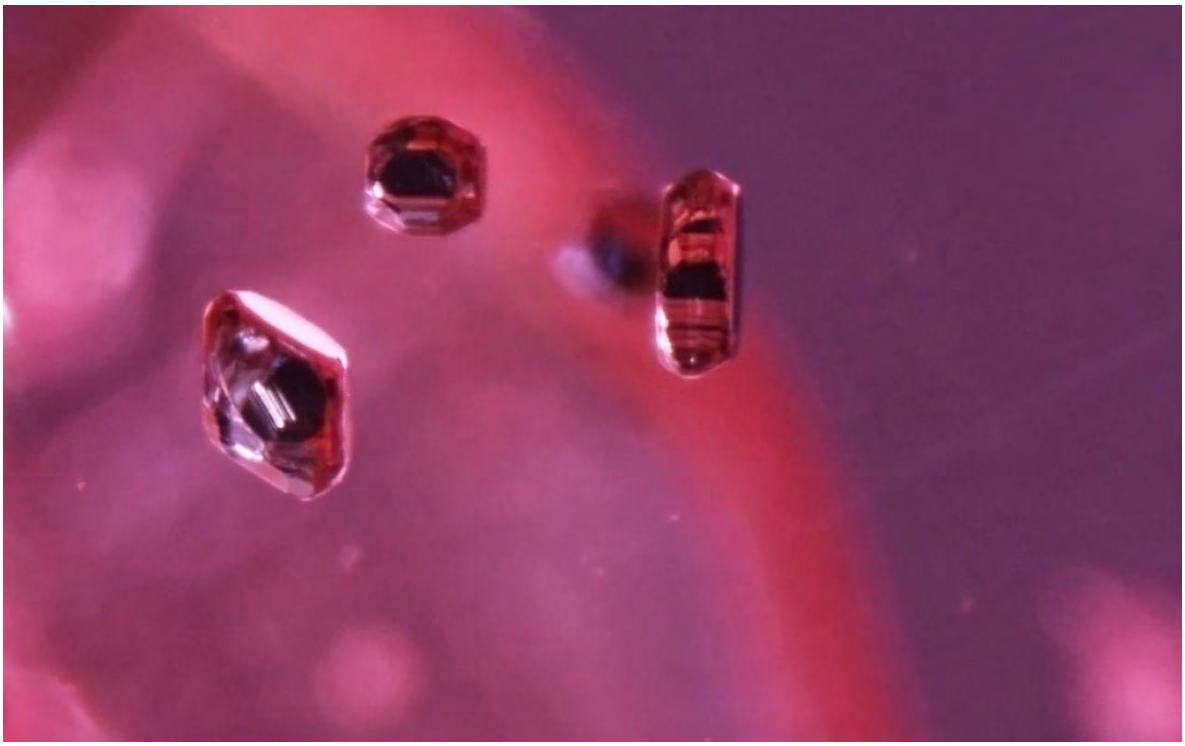

Figure 107: A group of highly lustrous, , dark, opaque euhedral crystals (probably chalcopyrite). GIA reference sample 100305162443, an "E" type sample (probably from the "Central" area) collected in Nampula in September 2009. Darkfield illumination, magnified 160x. Photo: Jonathan Muyal © GIA.

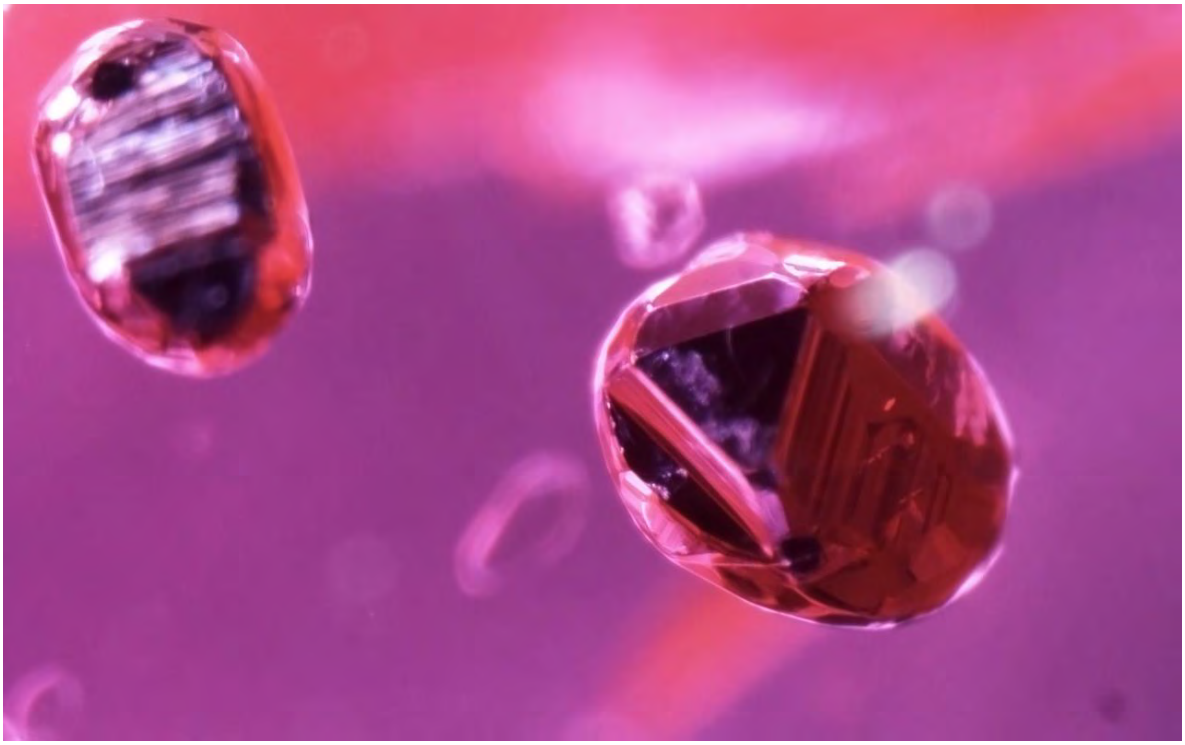

Figure 108: Two highly lustrous, dark, opaque euhedral crystals (identified by Raman as chalcopyrite using the RRuff database as a reference). GIA reference sample 100305163845, an F type ruby from a parcel of "Bo Nam" rubies from Montepuez acquired in Thailand in 2013. Darkfield + fiber optic illumination, magnified 90x. Photo: Jonathan Muyal © GIA.

Figure 109: The same crystals as shown in the previous image seen using bright field and fiber optic illumination revealing growth lines in the ruby. GIA reference sample 100305163845, an F type ruby from a parcel of "Bo Nam" rubies from Montepuez acquired in Thailand in 2013. Bright field + fiber optic illumination, magnified 90x. Photo: Jonathan Muyal © GIA.

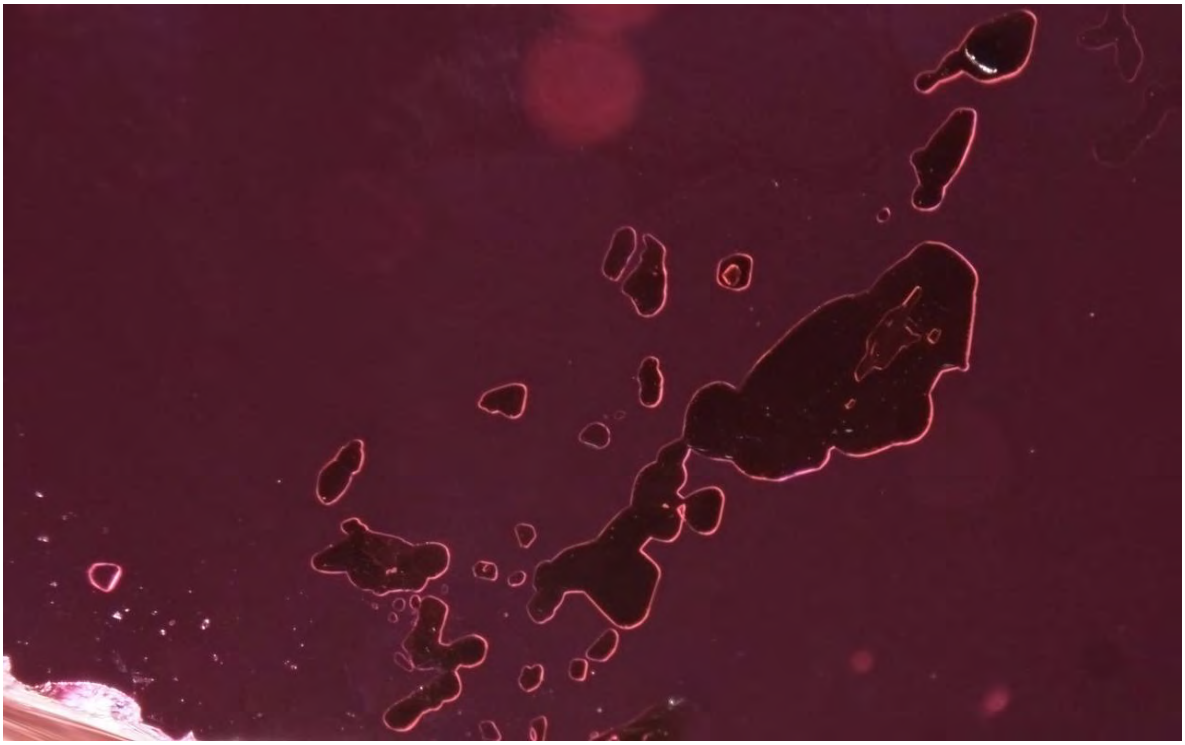

Figure 110: A very unusual group of flat irregularly shaped inclusions arranged in a plane with a dark and opaque appearance. Using Raman a spectrum similar to chromite was collected, but it was not a perfect match, hence the nature of the inclusion is still a bit of a mystery. GIA reference sample 100305163815, an "E" type sample (probably from the "Central" area) collected in Nampula in September 2009. Darkfield + fiber optic illumination, magnified 60x. Photo: Jonathan Muyal © GIA.

Figure 111: The same mysterious inclusions, seen using transmitted light are not opaque but rather a very dark red. Some also seem to host inclusions of their own and when viewed via fiber optic light surface growth lines appear to be visible. Additional treacle-like growth lines are also apparent when using bright field illumination. GIA reference sample 100305163815, an "E" type sample (probably from the "Central" area) collected in Nampula in September 2009. Brightfield + fiber optic illumination, magnified 60x. Photo: Jonathan Muyal © GIA.

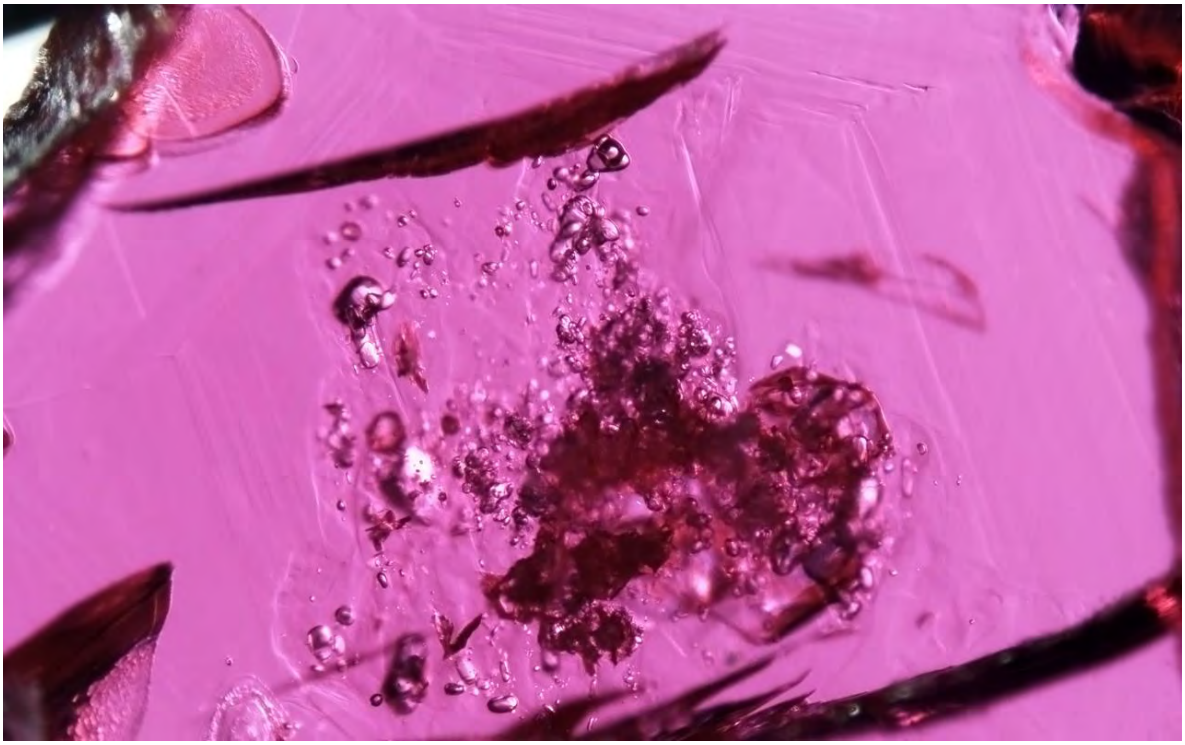

Figure 112: Under bright field illumination a very interesting inclusion scene was revealed consisting of a group of crystal inclusions (probably mostly mica and amphibole) associated with two types of growth lines. Firstly some hexagonal growth lines surrounding all the crystals, and secondly, near the center of the ruby, amongst the crystal inclusions, some flowing growth lines reminiscent of treacle or roiling. GIA reference sample 100305163835, an "E" type sample (probably from the "Central" area) collected in Nampula in September 2009. Brightfield + fiber optic illumination, magnified 40x. Photo: Jonathan Muyal © GIA.

CONCLUSIONS:

Montepuez rubies are particularly interesting because they rapidly dominated the ruby trade in traditional markets like Thailand and Sri Lanka after their discovery during the Spring of 2009.

The new material differs from the rubies traditionally seen in the market such as those from most major commercial deposits, i.e. Myanmar (Burma), Vietnam, Pakistan, Afghanistan, and Tajikistan, but also from some deposits in Kenya and Tanzania where marble type rubies known for their strong fluorescent reactions that are related to their low iron content occur. They also differ markedly from the Thai / Cambodian rubies that are of basalt origin and which are known for their low fluorescent reactions due to a much higher iron content.

In fact the new deposit near Montepuez is not marble or basalt related but rather an amphibole related deposit. This is of interest as up to very recently amphibole related deposits were not known to produce gem quality rubies (Giuliani et al. 2007). However, the discoveries near Winza (Tanzania), M'sawize and Montepuez (Mozambique) and probably Didy (Madagascar) in 2007, 2008, 2009 and 2012, respectively, prove that this is no longer the case, particularly when it is understood that most of the rubies available in the gem markets of Thailand or Sri Lanka today originated from mines in Montepuez.

The new amphibole related rubies from Montepuez are important to the trade because they provide large quantities of small and large stones of different qualities that may be sold untreated (no heat etc...) or treated (usually either flux healed or glass filled) within the trade. The stones usually exhibit an attractive "Burma like" red color when the iron content is low or more "Thai like" when it is high. Some unheated rubies from Montepuez combine a rich color with excellent crystallization qualities producing truly beautiful gems with a deep red color, high transparency and fine luster.

Besides the appearance of the stones, which mainly varies according to their iron content, their internal features are usually very different from those found in gems from more classic marble or basalt related deposits like those of Myanmar (Burma), Thailand, Afghanistan, Vietnam or Tajikistan due to their amphibole type deposit .

Gemologists who are asked to provide origin opinions on stones can use a combination of the inclusion scene, the chemistry and the spectroscopic data collected to identify their African origin without any difficulty, since so far all the known amphibole related deposits producing gem quality stones are found either in Tanzania, Madagascar or Mozambique. Narrowing down the choice to a specific country or even mining area within those countries can be achieved but is more challenging in some cases.

SPECIAL THANKS:

The authors would like to thank:

- The whole team at *Montepuez Ruby Mining* (M.R.M.) and *Gemfields* for the support they provided us in Mozambique.
- Abdul Y. Msellem for the valuable information he shared with us concerning the garimpeiros.
- Karim Guerchouche from *Premacut* in Bangkok, Thailand.
- The people from Chanthaburi who we met and who provided us with some interesting samples and useful market information.
- The whole team at *GIA Laboratory Bangkok*, particularly Khun Sudarat Seasaew and Ken Scarratt for their support and precious advices.

ANNEX A: GIA FIELD GEMOLOGY CATALOGUING SYSTEM

This system was develop at the GIA Field Gemology department to document precisely the way a given research sample was collected.

A conditions: Mined/collected by the field-gemologist.
A1: Collected in situ from primary deposit by the field-gemologist.
A2: Collected on floor/mine waste at mine (primary/secondary) by the field-gemologist.
A3: Collected after digging in a secondary deposit by the field-gemologist.

B conditions: Field-gemologist witnessed the mining.
B1: Collected on site in jig/sieve from mine in secondary type deposit by field-gemologist.
B2: Collected on site in miner's bottle from mine in secondary type deposit by mines by field-gemologist.

C conditions: Field-gemologist collected from miners at the mine but without witnessing the mining process.
C1: Collected at mine from mine owner (not mined that day in front of field-gemologist's eyes).
C2: Collected at mine from miner on site (not mined that day in front of field-gemologist's eyes).

D conditions: Field-gemologist collected the stones from miner but not at the mines.
D1: Collected from mine owner (at HQ near the mines).
D2: Collected from miner (near the mines).
D3: Collected from person telling that he was the miner (mine not visited).
D4: Collected from miner in regional/international market.

E conditions: Field-gemologist collected the stones from a secondary source close to the mines.
E1: Bought from trusted secondary source (gemologist/dealer/broker) at local market (close to source).
E2: Bought from trusted secondary source (gemologist/dealer/broker) at regional market (close to source).
E3: Bought from unknown secondary source at local gem market (close to source).
E4: Bought from unknown secondary source at regional gem market (close to source).

F conditions: Field-gemologist collected the stones from a secondary source in international market.
F1: Bought from unknown dealer at international gem market (gem show…).
F2: Bought from trusted source (gemologist/collector/dealer…) at international market.
F3: Bought from a lab client after the stone was submitted to the GIA Laboratory.

Z conditions: No information about how the stone was collected.
Z1: Lost information.
Z2: No information.

BIBLIOGRAPHY:

Afonso, R. S., Marques, J.M. (1998). Recursos Minerais da Republica de Mocambique [Mineral resources of the Republic of Mozambique]. Maputo, Mozambique, Direcção Nacionalde Geologica,

Bingen, R., Boyd, R., Thomas, R.J., Bjerkgård, T., Feito, P., Henderson, I.H.C., Hollick, L.M., Jacobs, J., Jamal, D., Key, R.M., Lutro, O., Melezhik, V.A., Nordgulen, Ø., Rossi, D., Sandstad, J.S., Skår, Ø., Smethurst, M., Smith, R.A., Solli, A., Tveten E., Viola, G., (2006). "Crustal architecture in Northern Mozambique: results from a regional bedrock mapping project ", Geophysical Research Abstracts, vol. 8.

Boyd, R., Nordgulen, Ø., Thomas, R.J., Bingen, B., Bjerkgård, T., Grenne, T., Henderson, I., Melezhik, V.A., Often, M., Sandstad, J.S., Solli, A., Tveten, E., Viola, G., Key, R.M., Smith, R.A., Gonzalez, E., Hollick, L.J., Jacobs, J., Jamal, D., Motuza, G., Bauer, W., Daudi, E., Feitio, P., Manhica, V., Moniz, A., Rosse, D., (2010). "The geology and geochemistry of the east african orogen in northeastern Mozambique", South African Journal of Geology, vol. 113, pp. 87-129.

Dubinsky, E., Emmett, J.L., (2013). "The colors of corundum", The GemGuide, vol. 32, n°1, pp. 1-11.

Emmett, J. L., Scarratt, K., McClure, S.F., Moses, T., Douthit, T.R., Hughes, R.W., Novak, S., Shigley, J.E., Wang, W., Bordelon, O., Kane, R.E., (2003). "Beryllium diffusion of ruby and sapphire", Gems & Gemology, vol. 39, n° 2, Summer 2003, pp. 84–135.

Ferguson, J., Fielding, P.E., (1971). "The origins of the colors in yellow, green and blue sapphires", Chemical physics letters, vol. 10, n° 3, pp. 262-265.

Giuliani, G., Ohnenstetter, D., Garnier, V., Fallick, A.E., Rakotondrafazy, M., Schwarz, D. (2007). "The geology and genesis of gem corundum deposits", Geology of gem deposits, Mineralogical Association of Canada, vol 37, pp. 23-80.

Koivula, J., Kammerling, R.C., (1991). "Update on corundum", Gems & Gemology, vol.27, n° 1, p 48.

Kröner, A., Muhongo, S., Hegner, E., Wingate, M.T.D., (2003). "Single-zircon geochronology and Nd isotopic systematics of Proterozoic high-grade rocks from the Mozambique Belt of southern Tanzania (Masasi area): implications for Gondwana assembly", Journal of Geological Society, vol. 160, pp. 745–757.

Kröner, A., Stern, R.J., (2004). "Pan-African Orogeny". Encyclopedia of Geology, editions Elsevier, vol. 1

Lächelt, S. (2004). "Geology and Mineral Resources of Mozambique", Direcção Nacional de Geologia Moçambique.

Macey, P. H., Thomas, R.J., Grantham, G.H., Ingram, B.A., Jacobs, J., Armstrong, R.A., Roberts, M.P., Bingen, B., Hollick, L., de Kock, G.S., Viola, G., Bauer, W., Gonzales, E., Bjerkgård, T., Henderson, I.H.C., Sandstad, J.S., Cronwright, M.S., Harley, S., Solli, A., Nordgulen, Ø., Motuza, G., Daudi, E., Manhiça, V., (2010). "Mesoproterozoic geology of the Nampula Block, northern Mozambique : Tracing fragments of Mesoproterozoic crust in the heart of Gondwana ", Precambrian Research, vol. 182, pp. 124-148.

McClure, S., Koivula, J. (2009). "Preliminary observations on new rubies from Mozambique", Gems & Gemology , vol. 45, n°3, pp. 224-225.

Meert, J. G., Van Der Voo, R., (1997). "The assembly of Gondwana 800-550 Ma", Journal of Geodynamics, vol. 23, n° ¾, pp. 223-235.

Melezhik, V. A., Bingen, B., Fallick, A.E., Gorokhov, I.M., Kuznetsov, A.B., Sandstad, J.S., Solli, A., Bjerkgård, T., Henderson, I., Boyd, R., Jamal, D., Moniz, A., (2008). "Isotope chemostratigraphy of marbles in northeastern Mozambique : Apparent depositional ages and tectonostratigraphic implications.", Precambrian Research, vol. 162, pp. 540-558.

Muhongo, S., Kröner, A., Nemchin, A.A., (2001a). "Single zircon evaporation and SHRIMP ages for granulite-facies rocks in the Mozambique Belt of Tanzania." ." Journal of geology vol. 109: pp. 171–189.

Muhongo, S., Kröner, A., Wallbrecher, E., (2001b). "Anatomy of the suture between West and east Gondawana: The case study of the Mozambique Belt of East Africa.", Gondwana Research, vol. 4, n°2, pp. 183.

Pardieu, V. (2009). "The Winza ruby and Sapphire mining area, Mpwapwa district, Dodoma province, Tanzania", from http://www.fieldgemology.org/Gemology%20tanzania%20ruby%20sapphire%20dodoma%20mpwapwa%20winza.php.

Pardieu, V., Thanachakapad, J., Jacquat, S., Senoble, J.B., Bryl, L.P., (2009a). "Rubies from the Niassa and Cabo Delgado regions of Northern Mozambique. A preliminary examination with an updated Field Report Annex", from http://www.giathai.net/pdf/Niassa_Mozambique_Ruby_September13_2009.pdf.

Pardieu, V., Jacquat, S., Senoble, J.B., Bryl, L.P., Hughes, R.W., Smith, M., (2009b). "Expedition report to the Ruby mining sites in Northern Mozambique (Niassa and Cabo Delgado provinces)", from http://www.giathai.net/pdf/Fieldtrip_to_Mozambique_December_16_2009.pdf.

Pardieu, V., Senoble, J.B., Bryl, L.P., Jacquat, S., (2009c). "Update on rubies from Mozambique", Gems & Gemology, vol. 45, n°4, Winter 2009.

Pardieu, V., Sturman, N., Saeseaw, S., Du Toit, G., Thirangoon, K., (2010). "FAPFH/GFF Treated Ruby from Mozambique - a preliminary report -", from http://www.giathai.net/pdf/Flux_heated_and_glass_filled_rubies_from_Mozambique.pdf.

Pardieu, V., Rakotosaona, N., (2012). "Ruby and sapphire rush near Didy, Madagascar (April - June 2012)", from http://www.giathai.net/pdf/Didy_Madagascar_TH.pdf.

Pardieu, V., Chauviré, B., (2012). "Update on ruby mining and trading in northern Mozambique", Gems & Gemology, vol. 48, n°4, Winter 2012, pp. 309-311.

Pardieu, V., Chauvire, B., (2013). "Les rubis du Mozambique", Les cahiers du Regne Mineral, n°2, ("Les gemmes du Gondwana"), pp. 101-108.

Schwarz, D., Pardieu, V., Saul, J.M., Schmetzer, K., Laurs, B., Giuliani, G., Klemm, L., Malsy, A.K., Erel, E., Hauzenberger. C., Du Toit, G., Fallick, A.E., Ohnenstetter, D., (2008). "Rubies and sapphires from Winza, central Tanzania", Gems & Gemology, vol. 44, n° 4, Winter 2008, pp. 322–347.

Snee, L. W., Wu, T., (2010). "More on ruby from Cabo Delgado, Mozambique", Gems & Gemology, Vol. 46, n° 2, pp. 151-152.